NUMERICAL SOLUTION OF A TWO-DIMENSIONAL MULTIGROUP DIFFUSION EQUATION FOR THE ANALYSIS OF THE MINIATURE NEUTRON SOURCE REACTOR (MNSR)

BY

S. ANIM-SAMPONG

A DISSERTATION PRESENTED TO THE

UNIVERSITY OF GHANA, LEGON

FOR THE AWARD OF THE

MASTER OF PHILOSOPHY (M.Phil) DEGREE

IN PHYSICS

SEPTEMBER 1993

TABLE OF CONTENTS

DEDICATION

This work is dedicated by the **AMAZING GRACE OF THE LORD JESUS CHRIST**, to my family for their care and love.

DECLARATION

I declare that, except for references to other people's work, this thesis is the result of my own research and that it has neither in part nor whole been presented elsewhere for another degree.

S. ANIM-SAMPONG
(STUDENT)
DATE : 27 Sept 1993

Dr. E.H.K. AKAHO
(SUPERVISOR)
DATE : 27 Sept. 1993

ACKNOWLEDGEMENTS

I am most grateful to Dr. E.H.K. Akaho, my main supervisor and Head of the Department of Nuclear Engineering, National Nuclear Research Institute, Ghana Atomic Energy Commission (GAEC), for his advice, guidance and suggestions.

My appreciations also go to my co-supervisors Prof. E.K. Agyei and Dr. K.A. Owusu-Ansah, and to all the lecturers of the Physics Department, University of Ghana for their stupendous contributions and concern.

I am also indebted to my senior colleagues Dr. H.O. Boadu and Dr. K.A. Danso and to my fellow graduate students Messrs G.K. Amoh, B.T Maakuu and J. Agbotse for their useful suggestions. I wish to thank my colleagues at the Biotechnology and Nuclear Agriculture Research Institute (BNARI) of GAEC, Dr. H.M. Amoatey, Ms T. Torto, Mr. C Gbedemah and Mrs C. Owusu-Boaitey for their moral support.

I wish to register my profound gratitude to my great brothers and sisters in the Lord, Drs Michael and Emmanuel Osei-Boamah, Mrs Akosua Baah Achamfuor and Ms Mavis Ofori-Boateng for their unflinching support.

A special acknowledgement is due Ms. Josephine A. Parry, a dear sister for her love, encouragement, and concern. I remember also the steady monitoring of this work by Misses C. Antwi-Agyei and Y. Obesebea Asamoah.

Finally, I would like to register my gratitude to the GAEC for permitting me the use of its facilities

ABSTRACT

The lattice code **WIMS** was used to generate a two-group macroscopic cross-section data base for all homogeneous zones of the prototype Miniature Neutron Source Reactor (MNSR) for radial and axial directions. The data base takes into account the effect of increments in burnup, temperature and reactor power. The error analysis has shown that the data base is accurate enough for the purpose intended. The maximum deviation from the actual value is 0.2%.

The two-dimensional two-group neutron diffusion equation was solved numerically using the finite difference technique. A computer code called **KWABEN** is being developed to solve numerically the diffusion equation. The numerical methods and techniques used in the development of the code are presented in this work.

Preliminary calculations with the code using the data base were carried out at 20 kW thermal power and the computed zone average thermal fluxes in the radial direction follow the same trend of results available from experiments. The value of the flux for the annular Be reflector where the inner irradiation sites are located was determined by **KWABEN** to be 7.78×10^{11} n/cm^2-s as compared with the experimental value of 7.69×10^{11} n/cm^2-s.

CHAPTER ONE

INTRODUCTION

The physics design of nuclear reactors requires the determination of the gross statistical behaviour of the neutron population in the reactor system. This in turn calls for the solution of the Boltzmann equation of neutron transport theory which forms the subject matter of reactor theory. It is however not easy to solve this equation by a direct discretization process even on the largest computers because of the presence of too many independent variables, complicated energy variations of the macroscopic cross-sections and the complex geometrical arrangement of the core materials such as fuel, coolant, moderator, reflectors, etc, in a reactor. This thesis describes the mathematical model used to analyze the Miniature Neutron Source Reactor (MNSR) and the method of creation of a data base for the reactor.

In Chapter Two, a brief description of the reactor for which the present analysis is conducted is presented. Basic work in reactor theory which includes the study of the mathematical properties of the relevant equations is discussed. A review of the Boltzmann neutron transport theory and the neutron diffusion approximation to the transport theory, specifically to two-dimensional, two-group theory which is concerned with the dependence of the neutron flux on spatial coordinates (radial and axial) and the direction of neutron motion, are presented. Finally the various methods of solution are also discussed.

Chapter Three discusses different reactor parameters affecting group macroscopic cross-sections such as fuel burnup, coolant density, core temperature variations along the axial direction and xenon concentration. A two-group macroscopic data base is therefore created for the analysis of the MNSR based upon these observations. In Chapter Four, the numerical methods and techniques applied in the solution of the two-dimensional two-group diffusion analysis is presented. Based upon this, a computer code called KWABEN is being developed for the analysis of the MNSR. The chapter also deals with preliminary results which are compared with those obtained experimentally.

The main conclusions and recommendations for future work are finally presented in Chapter Five.

CHAPTER TWO

LITERATURE REVIEW

A nuclear reactor is a device in which materials are arranged so that a self-sustained nuclear chain reaction can proceed in a controlled manner.

Nuclear reactors in which most of the fissions are induced by thermal neutrons (neutrons with energies in thermal equilibrium with the thermal motion of matter, i.e, less than 1eV) are called thermal reactors. Low power operating thermal reactors used mainly for research and training purposes in nuclear establishments and other allied institutes are called research reactors.

A brief description of an example of a low power research reactor called the Miniature Neutron Source Reactor (MNSR) for which the present investigation is conducted is presented in the next section. The Ghana Atomic Energy Commission (GAEC) through the technical assistance of the International Atomic Energy Agency has planned to install this reactor at the National Nuclear Research Institute (NNRI), Kwabenya in the near future. In this chapter, the various mathematical models which describe the neutron flux distributions in a nuclear reactor shall be considered. The different methods of solutions will also be discussed.

2.1 THE MINIATURE NEUTRON SOURCE REACTOR

The prototype Miniature Neutron Source Reactor (MNSR) is a thermal light water under-moderated and cooled (by natural convection), pool-tank type low power research reactor built by the China Institute of Atomic Energy, Beijing. It has a low power rating of 27kW, low critical mass, low radioactive impact on the environment but a high stable thermal neutron flux (of order 10^{12}n/cm^{3}s maximum) [1]. These parameters, together with its inherent safety feature of a large negative temperature coefficient are important physical characteristics of the MNSR.

Primarily, the MNSR is designed for neutron activation analysis (NAA) in a large number of fields like geology, medicine, agriculture, environment, food and industry. It also finds use in other areas such as short-lived radioisotope production, research, teaching and training.

2.1.1 Structural Design of the Miniature Neutron Source Reactor

The MNSR facility consists of a reactor vessel, the reactor core and its supporting structures, beryllium reflectors, a control rod with an associated drive mechanism, irradiation tubes, water temperature and neutron detectors. Fig 2.1 is a schematic illustration of the vertical cross-section of the reactor.

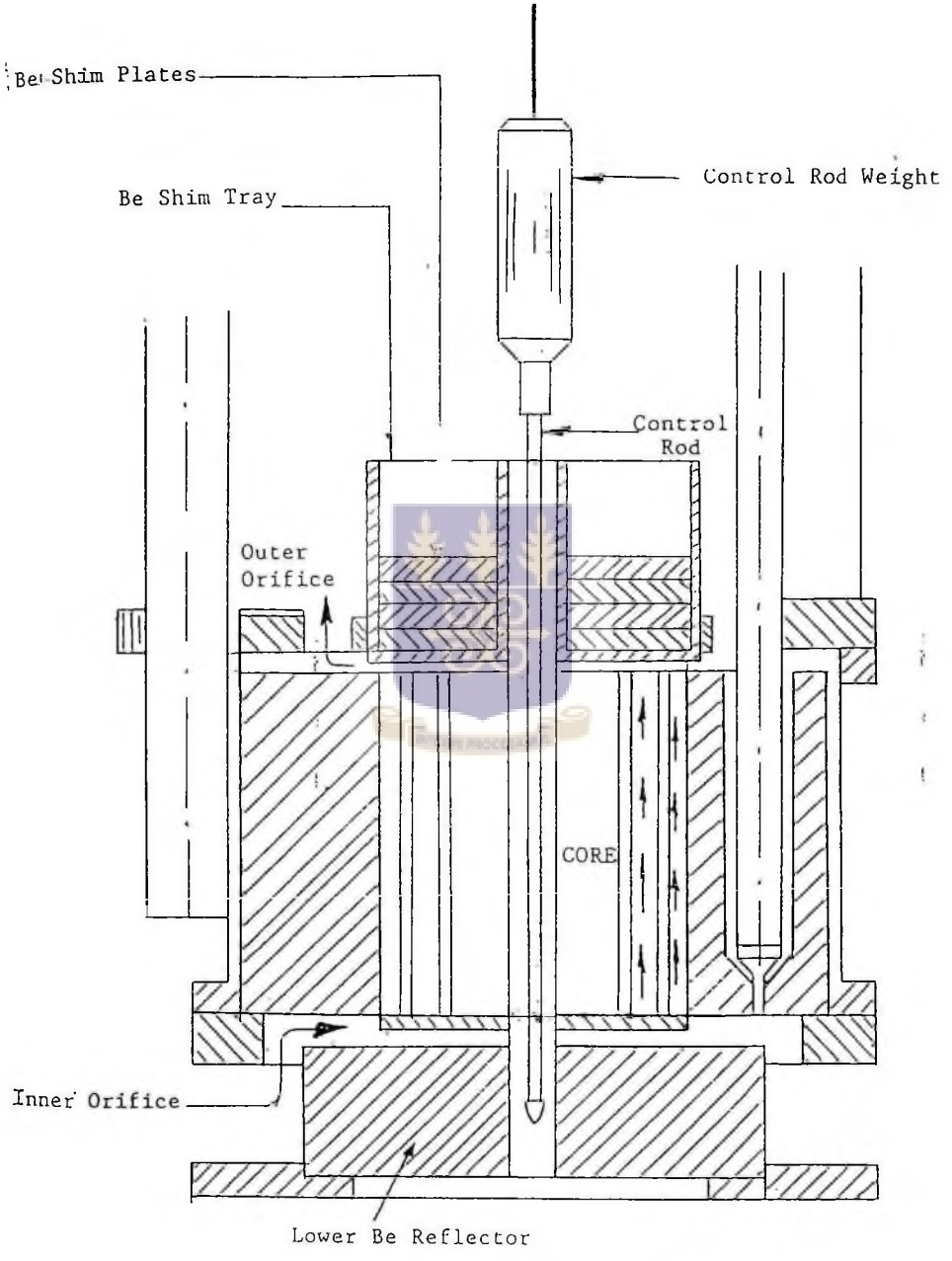

Fig.2.1 Cross-section of MNSR

The long cylindrical reactor vessel made of aluminum (Al) alloy houses the reactor core. It is divided into two sections to ease reactor core installation and refuelling processes. Table 2.1 shows the elemental composition of the Al alloy material used in the MNSR vessel fabrication. The main geometrical design parameters of the MNSR vessel and the reactor pool are depicted in Tables 2.2 and 2.3 respectively.

Element	Composition (%)
Mg	0.45 - 0.90
Si	0.60 - 1.20
Fe	0.20
Cu	0.01
Mn	0.01
Ti	0.01
Zn	0.03
Ni	0.03
Cd	0.0001
B	0.0001

Table 2.1: Elemental Composition of MNSR Al Alloy vessel and Control Guide Tube.

Parameter	Dimension (mm)
Total height	5.60
Total diameter	0.60
Cylinder wall thickness	10.00
Upper section	4.70
Lower section	0.90

Table 2.2: Geometrical Dimensions of MNSR Reactor vessel.

Parameter	Dimension (mm)
Inner diameter	2.70
Depth	6.50
Wall thickness	0.40
Pool base thickness	0.40

Table 2.3: Geometrical Dimensions of MNSR reactor Pool.

The region adjacent to the core is called the reflector. In general reflectors significantly reduce the quantity of nuclear fuel required for reactor criticality. The MNSR core is heavily reflected on both sides, top and bottom by metal beryllium (Be) alloy material as shown in Fig 2.1. The top Be plates are added to the shim tray to increase the excess reactivity after every 1.5 - 2 years and thus extend the lifetime of each fuel cycle [2]. Beryllium is a good reflector with a small thermal neutron absorption cross-section of 7.0 barn. Tables 2.4 and 2.5 show respectively the geometrical dimensions and elemental composition of the MNSR Be alloy reflectors.

Parameter	Dimension (mm)
Outside diameter (side)	435.00
Inner diameter (side)	231.00
Height (side)	238.50
Bottom plate diameter	290.00
Bottom plate thickness	50.00

Table 2.4: Geometrical Dimensions of MNSR Be Reflectors.

Element	ppm	Element	ppm
Fe	4000	Cu	200
Si	800	Eu	0.1
Mg	1000	Ni	100
BeO	25000	Co	10
Pb	3000	Sm	0.5
N	200	Mn	20
B	2.0	Al	3000
Ag	15	Cd	0.5
Li	1.0	Zn	150
Dy	1.0	Cr	20
C	0.1	Be	962298

Table 2.5: Elemental Composition of MNSR Be Alloy Reflectors.

The MNSR is equipped with ten irradiation tube facilities made of Al alloy. Five of these are located in the side Be annuli with the remaining five located outside the side Be reflectors.

To detect and test the reactor characteristics and its associated instrumentation, the MNSR is further equipped with several different detectors such as BF_3 and gamma fission chambers for the detection and measurement of neutron flux and gamma radiation. The inlet and outlet temperatures are detected and measured by four thermocouples housed in the outer irradiation sites.

An important structural component of a nuclear reactor is the control rod. The MNSR has only one central control rod. It is made of cadmium and cladded with stainless steel (type SS-304). The use of only one control rod in the operation of the MNSR is due to its inherent safety features and simplified drive mechanism. The control rod serves as a shim, safety and regulatory rod. A cold excess reactivity of 3.5mk at 20° C and a control rod worth of 6.8mk is reported [2]. The design parameters of the MNSR control rod are shown in Table 2.6 . The elemental composition of the control rod guide tube is illustrated in Table 2.1.

Parameter	Dimension
Clad thickness	0.50mm
Total length	290mm
Total travelling length	250mm
Total diameter	5.00mm
Cd diameter	3.90mm
Control rod worth	7mk
Normal speed	11.4mm/s

Table 2.6: Design Parameters of the MNSR Control Rod.

2.1.1.1 MNSR Fuel Element Design

The MNSR fuel element is a thin-rodded element consisting of an Al cladding tube, a highly enriched (90.12%) uranium-aluminum (U-Al) alloy with a low neutron absorption cross-section employed as fuel with two end plugs as shown schematically in Fig 2.2. Tables 2.7 and 2.8 show the geometrical dimensions and elemental composition of the MNSR fuel element and its cladding respectively.

Parameter	Dimension (mm)
Active length	250
Total length	270
Outer diameter	5
Fuel meat diameter	4

Table 2.7: Geometrical Dimensions of MNSR Fuel Element.

Element	Composition (%)
Si	0.16
Fe	0.24 - 0.40
Cu	0.012
Mn	0.01
Ti	0.01
Mg	0.01
Zn	0.03
Ni	0.03
Cd	0.0001
B	0.001
Li	0.0006

Table 2.8: Elemental Composition of MNSR Fuel Element Cladding.

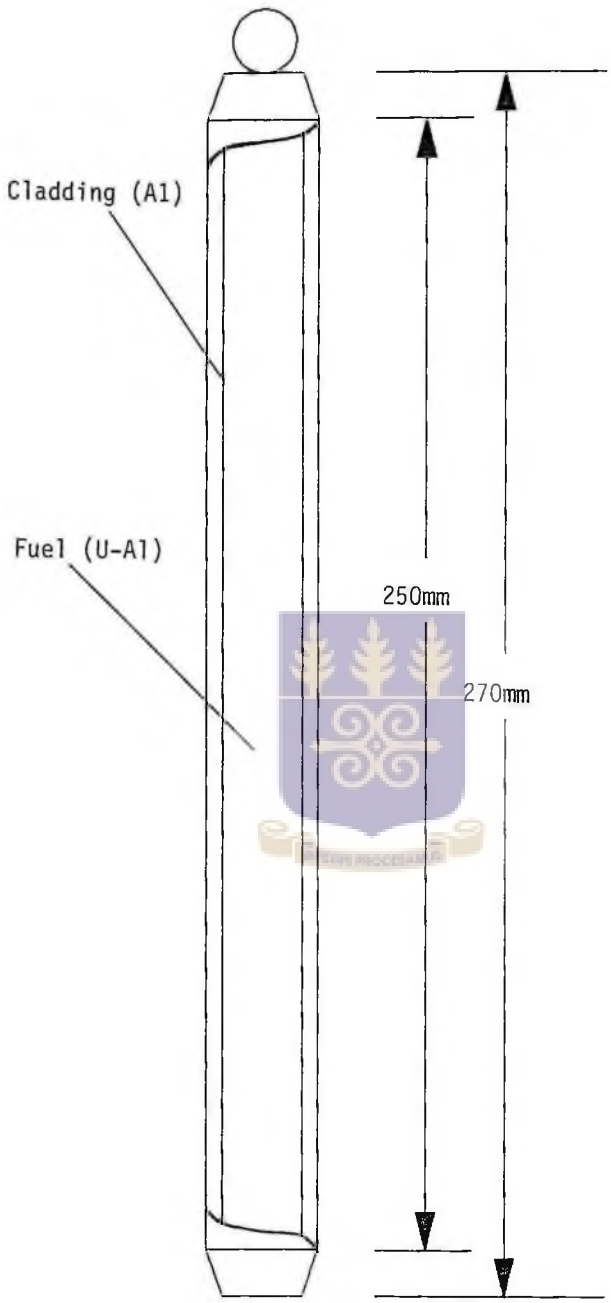

Fig 2.2: MNSR Fuel Element

Below are the main design parameters of the prototype MNSR fuel element:

Reactor thermal power	27kW
Maximum heat flux at Fuel element surface	3.06E+06 kcal/m.hr
Inlet/Outlet coolant temperature	30°C/45°C
Coolant velocity	15 - 30 mm/s
U-235 content/fuel element	2.75g
Enrichment factor	90.12%
Uranium weight fraction	26.1%
Fuel density	3.305g/cm
Volume porosity	3%

2.1.1.2 Core Configuration of the MNSR

The core of a nuclear reactor is the central part or heart of the reactor. The MNSR core is located at the bottom of the lower section of the cylindrical reactor vessel. It comprises the fuel cage, the fuel elements and a central control rod guide tube as illustrated in Fig 2.1. There are ten lattice rows concentrically arranged about the control rod guide tube. The arrangement of the control rod in its guide tube surrounded by the first ring of six fuel rods can be seen in Fig 2.3.

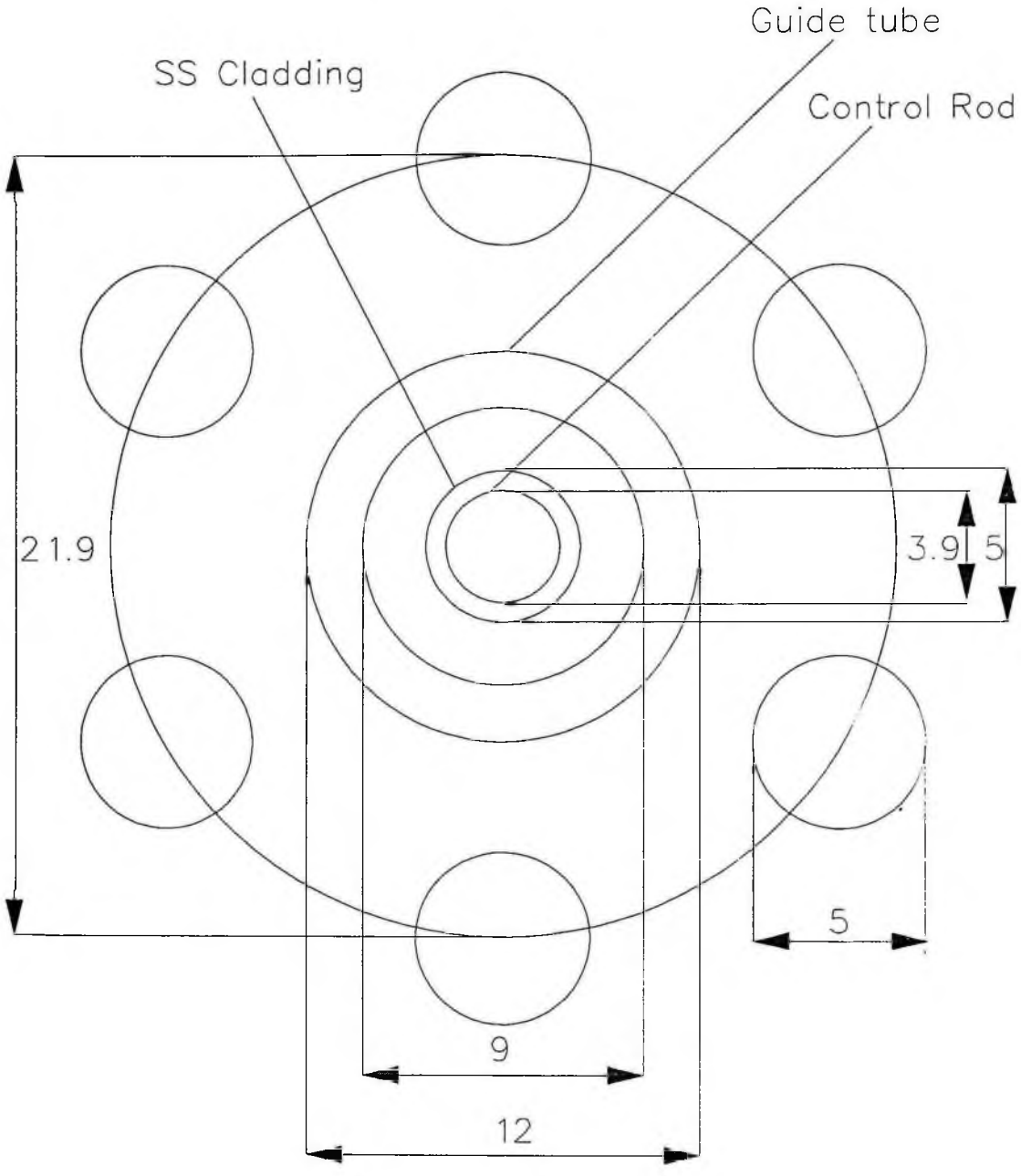

Fig.2.3 Layout of Control Rod with 6 neighbouring fuel rods

The core assembly of the prototype MNSR consists of 355 fuel lattices in the fuel cage with an average radial pitch of 10.95mm between adjacent rows. There are four tie and six dummy rods uniformly located at the 8th and 10th rows respectively. The other lattices are used as fuel elements. Table 2.9 describes the geometrical parameters of the MNSR core configuration [1].

Ring No.	Diameter (mm)	No of Elements	Radial pitch(mm)
A	0.0	1	0.00
B	21.9	6	11.47
C	43.8	12	11.47
D	65.7	19	10.86
E	87.7	26	10.98
F	109.5	32	10.78
G	131.4	39	10.58
H	153.5	45	10.70
I	175.2	52	10.58
J	197.1	58	10.68
K	219.0	65	10.58

Table 2.9: Geometrical Parameters of MNSR Core Configuration.

Fig 2.4 is a schematic diagram of the MNSR core configuration.

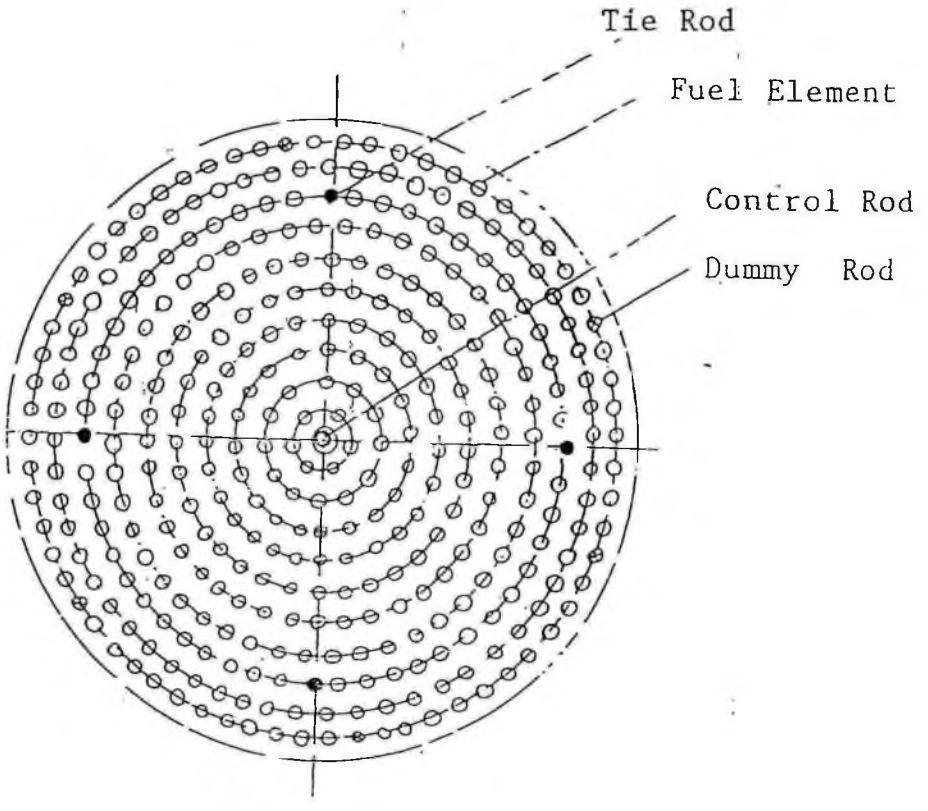

Fig.2.4 Core Configuration of MNSR

2.2 NUCLEAR REACTOR THEORY

Basic reactor physics is a broad field of physics covering cross-sections, transport and diffusion theory, reactor kinetics and multigroup theory [3]. In this work, the basic reactor physics will be restricted to light water reactors (LWRs).

The operation of a nuclear reactor depends fundamentally on the mode of neutron interactions with the atomic nuclei. Neutrons interact with nuclei in various ways such as fission, scattering, absorption and radiative capture. These nuclear reactions must be carefully accounted for in the design of nuclear reactors. It is convenient to describe each type of nuclear reaction in terms of a characteristic cross-section which defines the probability of occurrence of such reactions. A detailed knowledge of all the nuclear reactions or events taking place throughout a reactor can be attained provided the nuclear data base for constructing the various macroscopic cross-sections and the scalar flux density are available.

The neutron flux is a measure of the combined effects of the motion of neutrons, as evidenced by the interaction rates to which they give [4]. When the neutron flux (which is of central importance in this work and to which much attention will be given to finding this function) is known throughout a reactor, the total interaction rate can be computed. The problem of the computation of the scalar neutron flux is thus of prime importance in nuclear reactor design and analysis.

In nuclear reactor design, it is therefore necessary for a prediction to be made about the neutron flux distribution in the reactor system. To make an effective prediction of this function, the motion of the neutrons at different positions or locations will have to be followed or analyzed. The analysis of the neutron motion is best described by mathematical or physical models. Two such models which provide solutions to the above problem shall be examined the next sections.

2.2.1 Transport Theory

A treatment of the neutron flux distribution problem in a reactor is generally difficult. This is due to the complicated random trajectories executed by the neutrons as a result of their repeated nuclear collisions. As a consequence of this motion, neutrons of some energy travelling in a certain direction in the reactor are transported to some other part of the reactor system, moving in another direction with some other energy . The mathematical or physical model which studies this transport phenomena and rigorously treats the problems of neutron conservation and their interactions with their environment is the neutron transport theory.

The exact equation governing transport phenomena is called the transport equation. This theory considers as a variable, the angular distribution of the neutron velocity vectors which is equal to

the number of neutrons at a given position per unit volume travelling at a specified speed per unit velocity, in a given direction per unit solid angle. The transport equation which is credited to the German mathematical physicist Boltzmann, illustrates the fundamental property of neutron transport. In particular, the Boltzmann transport equation is an integro-partial differential equation embodying the physics of neutron particle transport [5]. It is a neutron balance equation in which the sum of the reaction rates inducing loss and the net neutron surface leakage is balanced by the source rate for a discrete volume, i.e sources(gains) = losses.

The one-speed Boltzmann transport formulation or equation is

$$\frac{\partial n}{\partial t} + v\boldsymbol{\Omega}.\nabla n + v\Sigma_t n(\mathbf{r},E,\boldsymbol{\Omega},t) =$$

$$\int_{4\pi}\int_{0}^{\infty} v'\Sigma_s(E'\rightarrow E,\ \boldsymbol{\Omega}'\rightarrow\boldsymbol{\Omega})\,d\Omega'\,dE'\ n(\mathbf{r},E,\boldsymbol{\Omega},t) + S(\mathbf{r},E,\boldsymbol{\Omega},t) \qquad (2.1)$$

where $n(\mathbf{r},E,\boldsymbol{\Omega},t)$ is the angular neutron density with energy E in dE in a direction $\boldsymbol{\Omega}$ in $d\Omega$, v is the velocity of the neutrons and Σ_s and Σ_t are the scattering and total cross-sections respectively. In constructing the multigroup transport equation from the above one-speed time dependent Boltzmann formulation, our purpose shall be to reduce the energy dependence of the Boltzmann equation to a set of transport equations which are applicable to

each group. It is assumed in this treatment that the angular neutron density is time independent.

The energy dependent linearized Boltzmann transport equation can be written in the form

$$\Omega.\nabla\phi(\mathbf{r},E,\Omega) + \Sigma_t\phi(\mathbf{r},E,\Omega) =$$

$$\int_{E'}\int_{\Omega'}\Sigma_s(\mathbf{r},E'\rightarrow E,\Omega'\rightarrow\Omega)\phi(\mathbf{r},E',\Omega')\,d\Omega'\,dE' + S(\mathbf{r},E,\Omega) \qquad (2.2)$$

where the quantity $\phi(\mathbf{r},E,\Omega)$ connotes the number of neutrons with energy E per unit energy crossing a unit surface at position $\mathbf{r}$ per unit time travelling in a unit solid angle centered in the direction Ω. $\Sigma_s(\mathbf{r},E'\rightarrow E,\Omega'\rightarrow\Omega)$ is the scattering probability per unit path length that a neutron at $\mathbf{r}$ and travelling in a direction Ω' with energy E' is scattered into a unit solid angle centered at Ω with energy E. $\Sigma_t(\mathbf{r},E,\Omega)$ is the total cross-section at $\mathbf{r}$ with energy E and centered at Ω and $S(\mathbf{r},E,\Omega)$ is the source term which defines the number of neutrons with energy E created per unit volume at $\mathbf{r}$ going in a unit solid angle centered at Ω.

In developing the multigroup equation, the neutron energy spectrum is divided into a number of groups (say G) and Eq.(2.2) is integrated over the energy limits E_{g-1} to E_g to obtain the elegant expression

$$\Omega.\nabla\phi_g(r,\Omega) + \Sigma_{tg}(r,\Omega)\phi_g(r,\Omega) = Q_g(r,\Omega) + S_g(r,\Omega) \qquad (2.3)$$

where

$$Q_g = \int\int \Sigma_s(r,E'\rightarrow E,\Omega'\rightarrow\Omega)\,\phi(r,E,\Omega)\,d\Omega'\,dE' \qquad (2.4)$$

and the energy dependence has been eliminated. The group cross-sections are averaged over the appropriate flux. Since the total cross-section Σ_{tg} is nearly independent of Ω, the angular dependence of Σ_{tg} is dropped arriving at the desired multigroup transport equation

$$\Omega.\nabla\phi_g(r,\Omega) + \Sigma_{tg}(r)\phi_g(r,\Omega) = Q_g(r,\Omega) + S_g(r,\Omega) \qquad (2.5)$$

Although calculations based on the transport theory gives more nearly exact results, its rigorous approach to the neutron flux distribution is however computationally expensive, tedious and long, leading to severe mathematical difficulties and to equations that are cumbersome to solve for most reactor systems. An approximate mathematical theory which leads to expressions for the neutron flux distribution variations with the geometrical coordinates is called the neutron diffusion theory. This theory is examined below in the next sub-section.

2.2.2 Multigroup Diffusion Theory

The diffusion theory approximation to neutron transport is the most useful primary technique for performing neutronic reactor core analysis. This approximation theory, if successively corrected for transport effects, is computationally less expensive to solve than the transport equation. The diffusion theory has two basic requirements. Firstly, it relies on the absence of large gradients of the neutron density or flux in any spatial region of the problem. Large gradients are implications of highly directional neutron migration and the diffusion theory does not include the direction-of-motion variables. Secondly for an accurate definition of the diffusion coefficient for the material, this theory demands that the migration process be scattering collision dominated [6].

The two conditions both relate to neutron leakage and it is in this description that the diffusion theory suffers most relative to the transport theory. The diffusion theory is thus inaccurate at certain locations such as near a reactor boundary or near strong neutron absorbers, e.g. control rods where large gradients exist, or sources. In such cases, the more rigorous transport theory is resorted to. Indeed, the diffusion theory and the neutron diffusion equation which is a mathematical formulation transformed by Ficks' law for neutron conservation, are reduced or simplified forms of the transport theory which can be adopted and used in the development of analytical models for reactor analysis and design [4].

The one-speed diffusion model can be used on occasions to provide useful qualitative information such as in preliminary reactor design studies. The model however, has a principal drawback. It assumes that all neutrons can be characterized by only one speed or energy. This assumption is quite untrue since the spectrum of neutron energies in a nuclear reactor spans the range from an upper limit of 10MeV to a lower limit less than 0.01eV. Furthermore it is also known that the neutron-nuclear cross-sections are dependent on the energies of the incident neutrons. The one-speed diffusion model is therefore inadequate for treating practical reactor design and computation problems. For such purposes, a rather more realistic multigroup treatment of the neutron energy dependence is required. A development of the multigroup diffusion model is thus presented in this section.

Multigroup diffusion equations are the most frequently solved equations in reactor design and analysis [7]. In developing this model and taking into account the behavior of neutrons in LWRs, the total neutron energy spectrum is divided or discretized into a number of energy groups (say G) as shown below.

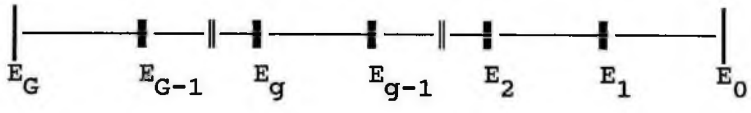

In this treatment any one group of neutrons with energy between E_g and E_{g-1} are identified as being in one energy group g. The neutrons in each energy group are then lumped together and the various group interaction processes such as diffusion, absorption, scattering etc, are described in terms of averaged diffusion coefficients and cross-sections known as group constants. Fig. 2.5 shows a typical neutron energy spectrum for LWRs extending from 0 to 10MeV.

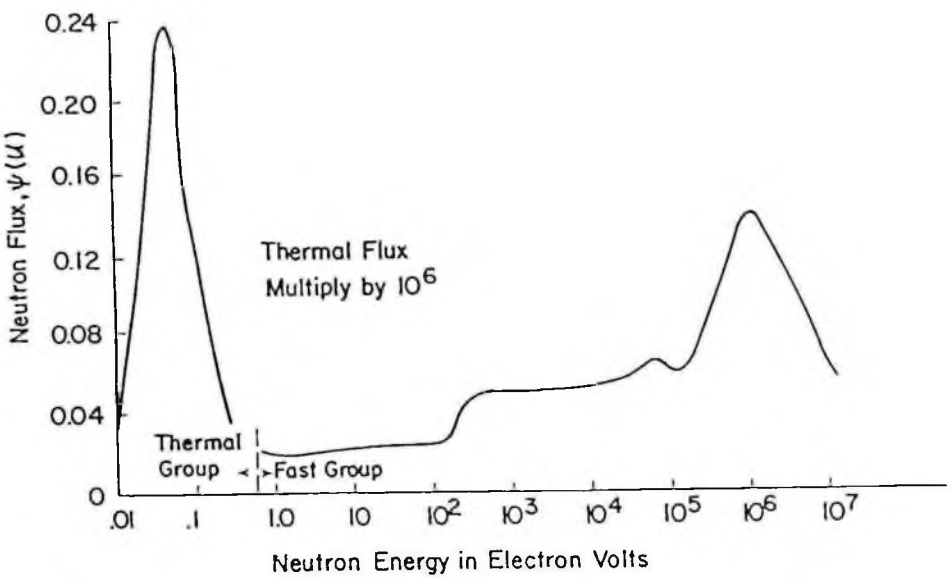

Fig.2.5: Typical Neutron Spectrum for a LWR

The form of the multigroup diffusion equation can be arrived at by applying the concept of neutron balance to a given energy group by balancing the ways in which the neutrons can enter or leave this group. The balance of neutrons reads as:

$$\begin{bmatrix}\text{Time rate change of neutrons in group g}\end{bmatrix} = -\begin{bmatrix}\text{change due to leakage}\end{bmatrix} + \begin{bmatrix}\text{absorption in group g}\end{bmatrix} + \begin{bmatrix}\text{Source neutrons appearing in group g}\end{bmatrix}$$

$$- \begin{bmatrix}\text{neutrons scattering out of group g}\end{bmatrix} + \begin{bmatrix}\text{neutrons scattering into group g}\end{bmatrix} \qquad (2.6)$$

An alternative and more satisfying way of arriving at this equation is to integrate or average the diffusion equation for the energy-dependent neutron flux $\phi(r,E,t)$ over a given group interval $E_g < E < E_{g-1}$. It is assumed that the flux can be adequately described by the energy-dependent equation:

$$\frac{1}{v}\frac{\partial\phi}{\partial t} - \nabla.D\nabla\phi + \Sigma_t\phi(r,E,t) = \int_0^\infty \Sigma_s(E'\rightarrow E)\phi(r,E,t)dE' +$$

$$\chi(E)\int_0^\infty \nu(E')\Sigma_f(E')\phi(r,E',t)dE' + S_{ext}(r,E,t) \qquad (2.7)$$

Eliminating the energy variable from the above equation over the gth energy group characterized by $E_g < E < E_{g-1}$ gives

$$\frac{\partial}{\partial t}\int_{E_g}^{E_{g-1}} \frac{1}{v}\phi dE - \nabla.\int_{E_g}^{E_{g-1}} D\nabla\phi dE + \int_{E_g}^{E_{g-1}} \Sigma_t \phi dE$$

$$= \int_{E_g}^{E_{g-1}} \int_{0}^{\infty} \Sigma_s(E'\rightarrow E)\phi(r,E,t)dE'dE + \int_{E_g}^{E_{g-1}} SdE \qquad (2.8)$$

It is more convenient to discretize the energy group fluxes to be integrals of $\phi(r,E,t)$ over the energies of each group. The multigroup fluxes $\phi_g(r,t)$ will then represent the total flux of all neutrons with energy E in the group interval $E_g < E < E_{g-1}$. The group neutron flux is then defined as

$$\phi_g(r,t) = \int_{E_g}^{E_{g-1}} \phi_g(r,E,t)\, dE \qquad (2.9)$$

A cross-section for the energy group g is similarly defined as

$$\Sigma_g = \frac{\int_{E_g}^{E_{g-1}} \Sigma(E)\phi(r,E,t)\,dE}{\int_{E_g}^{E_{g-1}} \phi(r,E,t)\,dE} \qquad (2.10)$$

The total cross-section for group g is then

$$\Sigma_{tg} = \frac{\int_{E_g}^{E_{g-1}} \Sigma_t(E)\phi(r,E,t)\,dE}{\int_{E_g}^{E_{g-1}} \phi(r,E,t)\,dE} \qquad (2.11)$$

The diffusion coefficient for group g is

$$D_g = \frac{\int_{E_g}^{E_{g-1}} D(E)\nabla_i\phi(r,E,t)\,dE}{\int_{E_g}^{E_{g-1}} \nabla_i\phi(r,E,t)\,dE} \qquad (2.12)$$

and the neutron speed characterizing group g as

$$\frac{1}{v} = \frac{1}{\phi_g}\int_{E_g}^{E_{g-1}} \frac{1}{v}\,\phi(r,E,t)\,dE \qquad (2.13)$$

The group transfer scattering cross-section is given as

$$\Sigma_{sgg'} = \frac{1}{\phi_g}\int_{E_g}^{E_{g-1}}\int_{E_g}^{E_{g-1}} \Sigma_s(E'\rightarrow E)\,\phi(r,E,t)\,dE'dE \qquad (2.14)$$

and the fission cross-section for group g is

$$\nu_g \Sigma_{fg'} = \frac{1}{\phi_g} \int_{E_g}^{E_{g-1}} \nu(E') \Sigma_f(E') \phi(r,E',t) dE' \qquad (2.15)$$

while defining the group fission spectrum χ_g as

$$\chi_g = \int_{E_g}^{E_{g-1}} \chi(E) dE \qquad (2.16)$$

Assembling these purely formal definitions [Eqs.(2.9) - (2.16)] into Eq.(2.8) yields the multigroup diffusion equation:

$$\frac{1}{v} \frac{\partial \phi_g}{\partial t} - \nabla . D \nabla \phi + \Sigma_{tg} \phi(r,t) = \sum_{g'=1}^{G} \Sigma_{sg' g} \phi_{g'} + \chi_g \sum_{g'=1}^{G} \nu_{g'} \Sigma_{fg'} \phi_{g'} + S_g$$

$$g = 1,2,\ldots,G \qquad (2.17)$$

The scattering term can be re-written as

$$\sum_{g'=1}^{G} \Sigma_{sg'g}\phi_{g'} = \sum_{g'=1}^{G-1} \Sigma_{sg'g}\phi_{g} + \Sigma_{sgg}\phi_{g} \qquad (2.18)$$

where the in-group scattering term Σ_{sgg} characterizes the probability that a neutron can suffer a scattering collision, lose energy and remain in the group. Transferring this term to the left hand side of Eq.(2.17) a removal cross-section can be defined as

$$\Sigma_{Rg} = \Sigma_{tg} - \Sigma_{sgg} \qquad (2.19)$$

which also characterizes the probability that a neutron will be removed from group g by a collision process. The assumption of no upscattering greatly simplifies the solution of the multigroup diffusion equation. In particular, further simplification can be achieved by choosing the group spacing such that the neutrons will scatter from a higher energy to the next lower energy group, i.e

$$\sum \Sigma_{sg'g}\phi_{g'} = \Sigma_{sg-1}\phi_{g-1} + \Sigma_{sgg}\phi_{g} \qquad (2.20)$$

In this case, the multigroup equation is said to be directly coupled, as illustrated below:

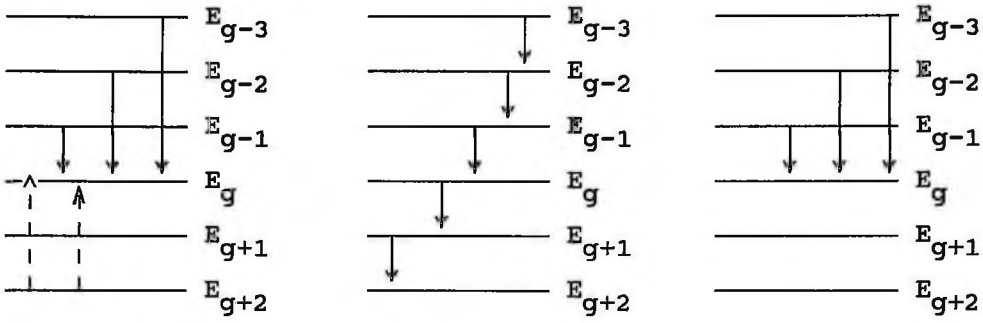

No upscatter Direct coupling Non-direct coupling

Ignoring the time dependence of the neutron flux and the presence of an external source (e.g. in criticality calculations), the multigroup equation reduces to

$$-\nabla . D_g \nabla \phi_g + \Sigma_{Rg} \phi_g = \sum_{g'=1}^{G} \Sigma_{sg' \to g} \phi_{g'} + \frac{1}{k} \chi_g \sum_{g'=1}^{G} \nu_{g'} \Sigma_{fg'} \phi_{g'} \qquad (2.21)$$

where the criticality eigenvalue k has been inserted.

In practice, the choice of the number of energy groups for reactor calculations depends on the problem under consideration. Normally one works with 2 - 20 energy groups. Such few group calculations can only be effective with reasonably accurate estimates of the group constants [3]. In general it is sufficient to use two-group (fast and thermal) diffusion theory to analyze thermal LWRs since it is the simplest case of multigroup equations while retaining most of its mathematical properties. For such analysis the group constants in each group are calculated separately. Below is a brief review of this model.

2.2.2.1 The Two-Group Diffusion Theory

In two-group diffusion studies, one neutron energy group characterizes fast neutrons and the other thermal neutrons. In ignoring upscattering of the thermal neutrons, the energy cut-off for the thermal group is usually chosen high, e.g. 0.5 - 1.0eV for water moderated reactors. Consider below the schematic of a two-group energy structure.

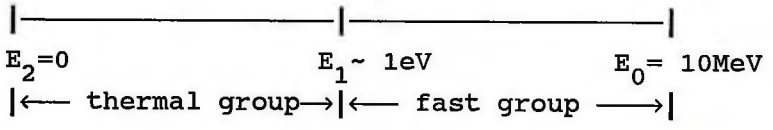

The group fluxes are identified as

$$\phi_1(r,t) = \int_{E_1}^{E_0} \phi(r,E,t)dE \qquad \text{(fast flux)} \qquad (2.22)$$

$$\phi_2(r,t) = \int_{E_2}^{E_1} \phi(r,E,t)dE \qquad \text{(thermal flux)} \qquad (2.23)$$

where ϕ_1 and ϕ_2 are the fast and thermal neutron flux distributions. The group constants for this model can be simplified. In particular since all fission neutrons are born as fast neutrons (fast group), the group fission spectra can be writen as:

$$\chi_1 = \int_{E_1}^{E_0} \chi(E)dE = 1 \quad \text{and} \quad \chi_2 = \int_{E_2}^{E_1} \chi(E)dE = 0 \qquad (2.24)$$

By this the fission source will only appear in the fast energy group equation as

$$S_{f1} = \nu_1\Sigma_{f1}\phi_1 + \nu_2\Sigma_{f2}\phi_2 \qquad \text{(fast group)} \qquad (2.25)$$

$$S_{f2} = 0 \qquad \text{(thermal group)} \qquad (2.26)$$

Assuming no upscattering for the thermal group, we have

$$\int_{E_2=0}^{E_1\sim 1eV} \Sigma_s(E'\rightarrow E)\,dE = \Sigma_s(E'), \qquad E_2 \leq E' \leq E_1 \qquad (2.27)$$

Hence the thermal in-group scattering cross-section is obtained as

$$\Sigma_{s22} = \frac{1}{\phi_2}\int_{E_2}^{E_1}\int_{E_2}^{E_1}\Sigma_s(E'\rightarrow E)\phi(r,E')\,dE'\,dE$$

$$= \frac{1}{\phi_2}\int_{E_2}^{E_1}\Sigma_s(E')\phi(r,E)\,dE' = \Sigma_{s2} \qquad (2.28)$$

Thus the group removal cross-section is just

$$\Sigma_{R2} = \Sigma_{t2} - \Sigma_{s22} = \Sigma_{t2} - \Sigma_{s2} = \Sigma_{a2} \tag{2.29}$$

If both the time derivatives and the external source terms are set to zero, the two-group diffusion equation is finally obtained as

$$-\nabla.D_1\nabla\phi_1 + \Sigma_{R1}\phi_1 = \frac{1}{k}\left[\nu_1\Sigma_{f1}\phi_1 + \nu_2\Sigma_{f2}\phi_2\right] \tag{2.30}$$

$$-\nabla.D_2\nabla\phi_2 + \Sigma_{a2}\phi_2 = \Sigma_{s12}\phi_1 \tag{2.31}$$

where the multiplication factor k has been inserted in Eq.(2.30) for criticality determinations. The source term in the fast group corresponds to the fission neutrons, whereas the source term in the thermal group is due to slowing down of fast neutrons. The various methods of solutions available in the literature for reactor physics calculations shall be discussed in the next section.

2.3 METHOD OF SOLUTION

In the previous section, the important problem of the neutron flux distribution in a nuclear reactor was first identified. Secondly, for a prediction of this function, different mathematical theories that effectively describe and offer solutions to this problem were discussed. The multigroup diffusion theory approximation to the Boltzmann transport theory was formulated and found to be the most appropriate model commonly used for reactor analysis. Two different methods of solving the multigroup diffusion equation shall be considered in the next section.

2.3.1 Analytical Method

The analytical method for solving the multigroup neutron diffusion equation for the analysis of reactor cores exists and is available for multidimensional and transient cases. However in cases with complicated geometries or boundary conditions, such exact analytical solutions are either complex or non-existent. In practice many diffusion problems cannot be solved analytically and other appropriate methods are invoked. One such method of solution is numerical analysis. This review shall therefore be restricted to numerical methods only.

2.3.2 Numerical Methods

Numerical methods is concerned with the mathematical derivation, description and analysis of obtaining numerical solutions of mathematical problems. Numerical computations can also be used even where the analytical solution is known simply because it may be less time consuming to solve the diffusion equation directly by numerical methods than to evaluate a complicated, albeit elegant analytical expression. This is particularly true when the calculations must be repeated many times in connection with parametric studies of reactors [8]. Numerical methods may fall into two different approaches:

(i) Probabilistic Monte Carlo Method

(ii) Numerical integration

2.3.2.1 Monte Carlo Technique

The Monte Carlo technique is a statistical method employed for special purposes. It is usually used as a means of checking appropriate procedures in reactor analysis. It is the most accurate way of computing the Dancoff correction. Indeed, the Monte Carlo model also finds use in 3-dimensional (3-D) reactor computations and complicated reactor geometries. However, it suffers a major drawback in that it requires long computation

times. It is therefore not widely used in reactor calculations. Details of the technique applicable to reactor analysis are available in references [7-9].

2.3.2.2 Numerical Integration

Numerical integration consists of the finite element and finite difference techniques. The finite element method (FEM) was originally developed as a numerical technique for structural analysis [8,9]. It is based on the variational principle as a physical law and has become successful and is almost exclusively used in some fields such as mechanical stress and structural analysis.

The FEM is very versatile and powerful in dealing with domains of irregular shapes usually associated with structural analysis. This is due to the freedom of selecting an arbitrary distribution of mesh points. Recent developments have witnessed a rapid growth in the use of this technique. Reasons accounting for this are:

(i) the finite element approach is versatile in dealing with irregular geometries

(ii) it has a higher degree of accuracy over the finite difference method (FDM)

(iii) higher order approximations can be easily obtained

(iv) treatment of boundary conditions with FEM is easier than with the FDM [7].

The FEM has drawbacks, however. It does not compete well with others such as the FDM when the reactor core is to be modelled adequately with a regular mesh points array or discrete elemental volume of simple shape. Further the lower order form of the finite element formulation that must be used due to computation cost constraints can generate results inferior to those obtained with other methods. However, it could be attractive if large regions of the uniform properties or demands for improved modelling of mixed geometries or of deformations existed [10].

The finite difference form of discretization is the most common method of approximating differential and integral equations. It is widely employed as a powerful numerical tool in solving multigroup equations and in reactor core analysis. However, a difficulty in the use of the FDM occurs when the shape of the domain is irregular because the mesh points based on the cartesian coordinate system cannot fit boundaries of irregular shapes. In general the FDM proves to be a more economical and convenient numerical technique in reactor analysis. It may therefore be used in such analytical problems even though the exact analytical solutions exist.

In the Safety Analysis Report on the prototype MNSR [2] reactor submitted to the NNRI, Kwabenya, no detailed information is available concerning the nuclear design of the reactor. Few experimental measurements of the fluxes at 2kW were reported for some sections of the core. Experimental results were not compared with those available from theoretical analysis. It is important that an

appropriate computational model is established for the analysis of the MNSR core to provide neutron fluxes at any point within the core. This information will be useful for the safe operational methodology for the MNSR and its maximum utilization for neutron activation analysis, reactor physics experiments and for radio-isotope production.

2.4 DISCUSSIONS AND SUGGESTIONS

A brief description of the prototype MNSR has been presented in this chapter. In particular, attention was paid to its fuel element and structural designs and also to the core configuration. This was followed by mathematical theories, namely the Boltzmann transport theory and the multigroup diffusion theory approximation which are used to provide solutions to the problem of the neutron flux distribution in nuclear reactors.

It is expected that fluxes will vary radially along the core. Since the temperature distributions along the axial direction of the core varies, one would expect that the group constants along the axis will be affected. As already stated in Section 2.1, the small core of the MNSR is enclosed with Be reflectors in order to minimize neutron leakages from the core. In the light of this discussion, the neutron flux will vary along the radial and axial directions of the reactor. A multigroup two-dimensional (2-group, 2-D,in r-z geometry) analysis of the MNSR core is preferred to the

one-group diffusion model which is inadequate in performing more accurate reactor analysis.

With this in mind, the objectives set for this work are as follows:

(1) creation of a two-group, two-dimensional (r,z) data base for the MNSR. This will require an appropriate model taking into consideration all the known parameters which influence group constants

(2) development of a computer package to solve the two-group, two-dimensional neutron diffusion equation using the created data base. The values obtained using the model will be checked against experimental values obtained using the prototype MNSR.

TWO-GROUP MACROSCOPIC DATA BASE

In general changes in certain nuclear parameters such as fuel burnup, U-238 temperature which in turn causes Doppler broadening of the U-238 neutron absorption resonances and in the concentrations of boron(B) and xenon (Xe) can induce changes in macroscopic group constants.

Thermal-hydraulics calculations performed by Akaho et al [11] on the MNSR core show significant changes in the coolant and fuel temperatures along the flow channel as graphically depicted in Fig 3.1. This plot suggests that changes in coolant density and temperature will affect group macroscopic cross-sections. An investigation of the variation of the neutron spectrum with burnup of the U-Al fuel elements reveals no significant change up to 10,000 MWd/tU (1.1%) burnup as shown in Fig 3.2. However, the fuel burnup curve illustrated in Fig 3.3 shows that the infinite multiplication factor k_∞ is strongly burnup dependent. The k_∞ value can be computed using the correlation equation fitted to the data:

$$k_\infty(\tau) = 1.8019 - 2.4114E\text{-}06\tau - 7.2635E\text{-}11\tau^2 \qquad (3.1)$$

where τ is burnup(MWd/tU)

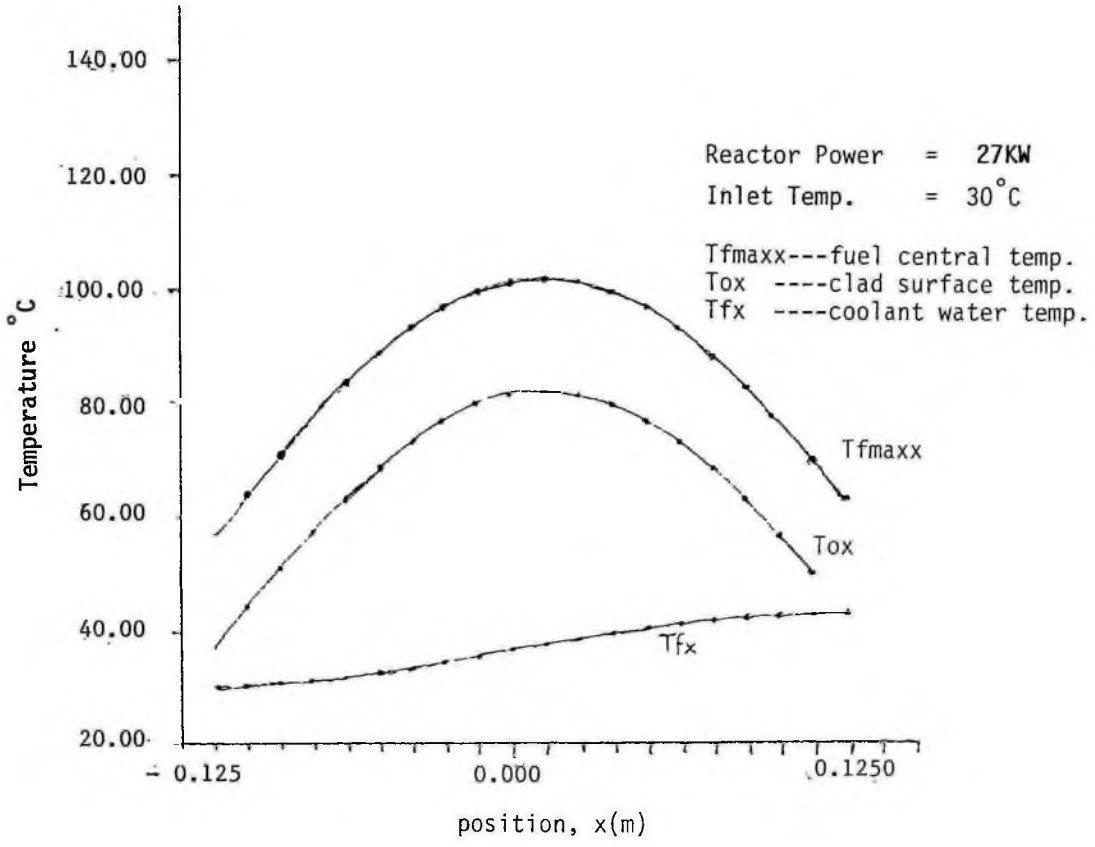

Fig 3.1: Temperatures in Fuel, Clad, Coolant along the Flow Channel

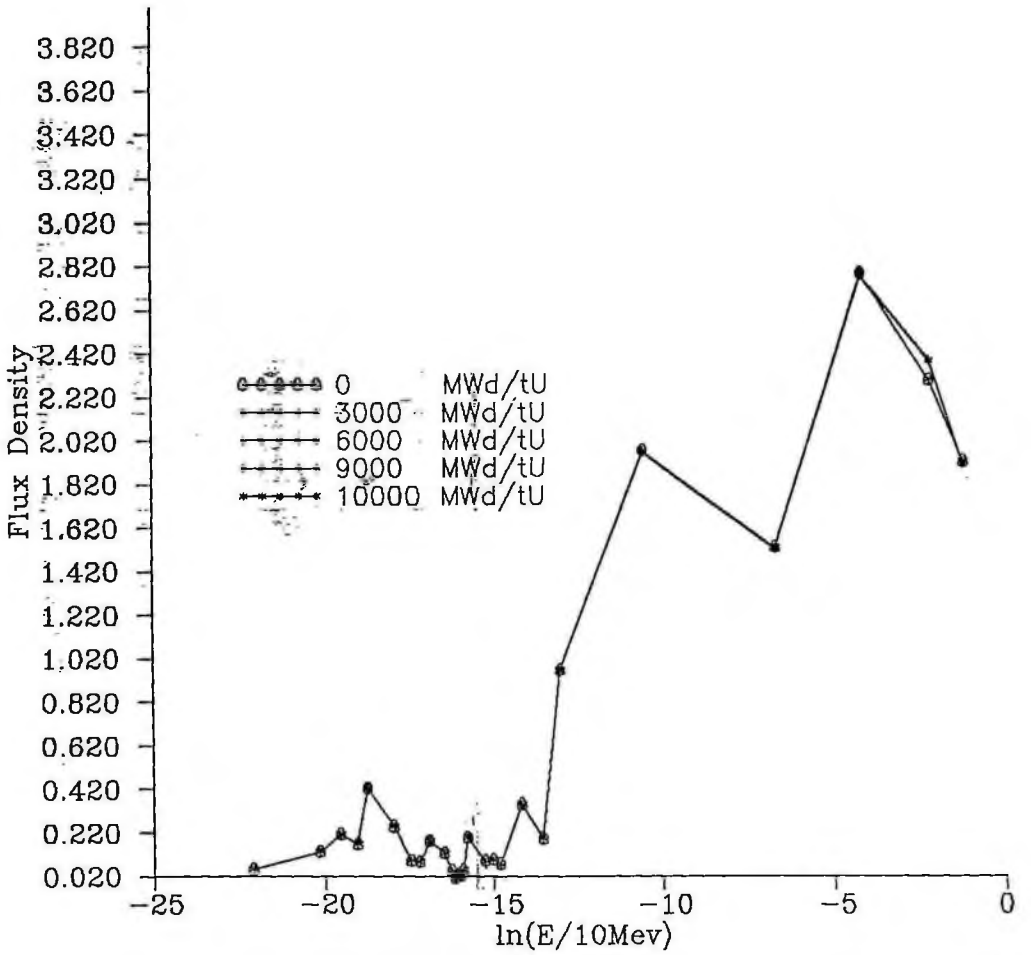

Fig 3.2: Variation of Neutron Spectrum with Burnup in MNSR Fuel Element

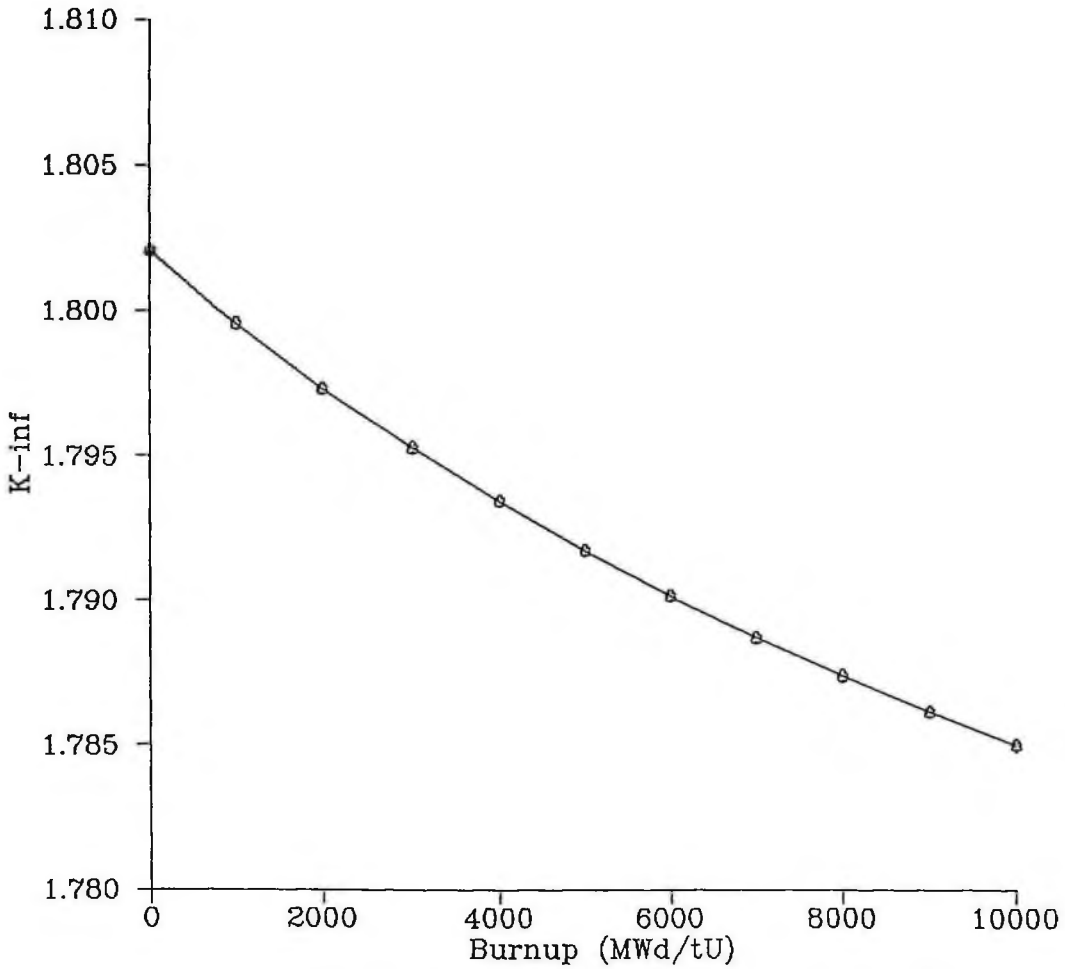

Fig.3.3: Burnup Curve for MNSR Fuel Element

Based on the above observations, it has been decided to examine the effects of these parameters on the group constants which will lead to the creation of an appropriate two-group macroscopic data base for the prototype MNSR. This data library will be helpful in the analysis of the reactor and will in particular, be used in performing reactor physics calculations for fast and thermal neutron fluxes at any point in the reactor core. In general, the complex problem of generating group constants is performed with sophisticated transport codes which take into consideration the influence of neutron spectrum, geometry and material composition.

In this presentation, a brief description of the lattice code for generating the two-group constants (D_1, D_2, Σ_{a1},Σ_{a2}, $\nu_1\Sigma_{f1}$, $\nu_2\Sigma_{f2}$,$\Sigma_{s1\rightarrow 2}$) is given. Macroscopic cross-sections referred to as basic will be calculated for the various homogeneous zones of the MNSR reactor at a reference level and their dependence on burnup correlated. Correction terms to these cross-sections which account for the spatially varying thermal hydraulic effects and operating power of the reactor will be discussed.

3.1 Mathematical Model

In the analysis of nuclear reactors, the basic portion of the reactor that is studied is the fuel unit cell. It consists of a single fuel rod, its cladding, the coolant and moderator. The overall behaviour of a reactor is the result of an interaction between the neutronic and thermal hydraulic properties relating to the fuel unit cell or assemblies.

A mathematical model for generating macroscopic group constants for a lattice cell of the MNSR [12] can be represented in terms of certain physical parameters as:

$$\Sigma_l^{xg} = \Sigma_l^{xg}\left[\tau,\ \rho_z,\ T_{fz},\ T_{mz},\ T_{clz},\ P,\ Xe\right] \qquad (3.2)$$

where Σ_l^{xg} = group macroscopic constant of reaction type x at energy g for zone l

τ, P, Xe = burnup, reactor power and Xe-135 concentration respectively

ρ_z = coolant and moderator density at axial position z

T_{fz}, T_{mz}, T_{clz} = fuel, moderator and cladding temperatures respectively at axial position z.

Considering a lattice cell of the MNSR core as shown in Fig 3.4, the group constants can be classified into two groups:

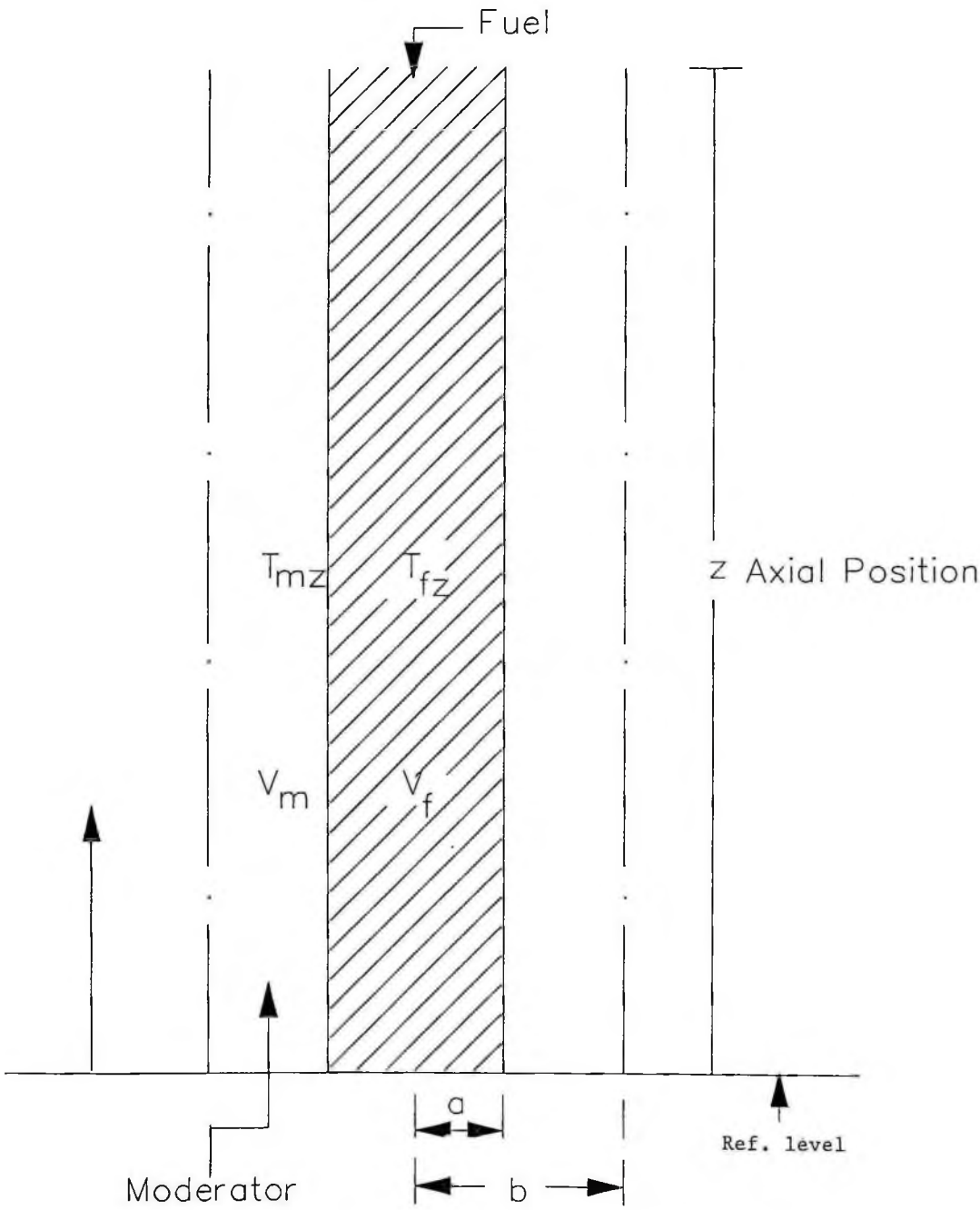

Fig 3.4: Lattice Cell for Macroscopic Crossections

(1) basic cross-sections determined at a chosen reference level at nominal power (27kW). For this work, the reference level was fixed at the middle of the core.

(2) the correction terms to the basic cross-sections due to the axial temperature variations along the flow channel, operating power and xenon effect.

Basic macroscopic cross-sections (BMCs) were determined for a fresh core at nominal power P_ϕ. It was assumed here that the group constants for the various homogeneous zones of the reactor at the reference level are functions of burnup only. These cross-sections will change from the reference level as the fuel and moderator temperatures change along the axis. In the precalculation of the cross-sections, it is assumed Xe-135 is absent and that only the thermal absorption cross-section would be affected. A further assumption is that the fuel, cladding and coolant temperatures will vary linearly with reactor power as stated by Mele et al[13].

On the basis of these assumptions, Eq.(3.2) can be expressed as

$$\Sigma_l^{xg}\left[\tau,\ z,\ P\right] = \left[\Sigma_{r,l}^{xg}(\tau) + \Delta\Sigma_l^{xg}(z)\right]\left[\frac{P}{P_\phi}\right] \qquad (3.3)$$

where

$\Sigma_{r,1}^{xg}(\tau)$ = burnup dependent cross-section at the reference level

$\Delta\Sigma_1^{xg}(z)$ = axial incremental change caused by changes in the coolant density, the fuel, cladding and moderator temperatures from reference level conditions and expressed as a function of z.

The thermal absorption group constant Σ_1^{xg}, is corrected for Xe-135 effect by the relation:

$$\Sigma_1^{xg}\left[\tau,\ z,\ P\right] = \left[\Sigma_{r,1}^{a2}(\tau) + \Delta\Sigma_1^{a2}(z)\right]\left[\frac{P}{P_\phi}\right] + \Delta\Sigma_1^{a2}(Xe) \qquad (3.4)$$

where $\Delta\Sigma_1^{a2}(Xe)$ defines the incremental change due to Xe-135 concentration. In the next section, the methods of computing the BMCs and the correction terms needed for the evaluation of Eqs.(3.3) and (3.4) shall be presented.

3.1.1 Basic Macroscopic Cross-sections

In determining the burnup dependent macroscopic cross-sections $\Sigma_l^{xg}(\tau)$ at the reference level conditions, it is assumed that the burnup term can be separated from the other variables and its influence described by the function $b(\tau)$ as

$$\Sigma_l^{xg}(\tau) = \Sigma_{r,l,o}^{xg}\left(1 + b^{xg}(\tau)\right) \tag{3.5}$$

where $\Sigma_{r,l,o}^{xg}$ connotes the group constant at the reference level for zero burnup. The parameterized cross-section for Eq.(3.3) can be written in the form:

$$\Sigma_l^{xg}\left[\tau, z, P\right] = \left[\Sigma_{r,l,o}^{xg}\left(1 + b^{xg}(\tau)\right) + a_l^{xg}(z)\right] \tag{3.6}$$

The functions $b^{xg}(\tau)$ and $a_l^{xg}(z)$, considered as polynomials of second order are defined as:

$$b^{xg}(\tau) = \sum_{n=1}^{2} b_n^{xg}\tau^n = b_1^{xg}\tau + b_2^{xg}\tau^2 \tag{3.7}$$

and

$$a_l^{xg}(z) = \sum_{n=0}^{2} a_{l,n}^{xg} z^n = a_{l,0}^{xg} + a_{l,1}^{xg} z + a_{l,2}^{xg} z^2 \qquad (3.8)$$

respectively.

3.1.2 Correction to the Xenon Effect

The basic cross-section for computing the thermal absorption cross-section is affected by the presence of xenon. This effect is taken into account by first calculating the correction term $\Delta\Sigma_l^{xg}(Xe)$ in Eq.(3.4). The term is calculated using the relationship [12]

$$\Delta\Sigma_l^{xg}(Xe) = \Sigma_{l,\phi}^{a2} \left[\frac{1-P/P_\phi}{1 + \left(P/P_\phi\right)\left[\sigma_{Xe}^{a2}\,\phi_2/\lambda_{Xe}\right]} \right] \qquad (3.9)$$

where $\Sigma_{l,\phi}^{a2}$ depicts the thermal macroscopic correction corresponding to the equilibrium poison buildup which can be expressed as

$$\Sigma_{l,\phi}^{xg} = \frac{\chi\gamma_{Xe}\left(P/P_\phi\right)}{1 + \lambda_{Xe}/\left(\sigma_{Xe}^{a2}\,\phi_2\right)} \qquad (3.10)$$

where

χ = fission/watt-sec(3.1×10^{10})

γ_{Xe} = total chain yield of Xe-135(0.066)

P, P_ϕ = operating and nominal power densities (kW/cm^3) respectively

λ_{Xe} = Xe-135 decay constant ($2.1 \times 10^{-5} s^{-1}$)

σ_{Xe}^{a2} = macroscopic thermal absorption correction for Xe-135 (1.7×10^6 barns).

A method of computing the group constants from the parameterized functions $b^{xg}(\tau)$ and $a_1^{xg}(z)$ is addressed below.

3.2 METHOD OF ANALYSIS

In this section, a description of the method of computing the group constants from the parameterized functions for variations in burnup and axial effects shall be considered. Emphasis will be laid on the theory of the WIMS lattice code. We shall then look at a method of preparing input data for the MNSR by using transport calculations based on the WIMS lattice code.

3.2.1 Theory of the WIMS Lattice Code

WIMS is an acronym for Winfrith Improved Multigroup Scheme. It is a general lattice cell program which uses transport theory to calculate neutron flux as a function of energy and position in the lattice cell. It also provides solution to the linear transport equation in multigroup (69 groups) for arbitrary cell or multicell geometry.

The WIMS program involves two major steps in the calculation of the neutron flux. It first calculates neutron spectra for few spatial regions in the full number of energy groups of its library and uses these spectra to condense the basic cross-sections into few groups. A few group calculation is then finally carried out using a much more detailed representation. The resulting fluxes are then expanded using the previous calculation so that the reaction rates at each spatial point can be calculated in the library group structure [14]. The group structure required by the WIMS code from the library tape is arbitrary. However, basic libraries are available in 58- and 69-energy groups. The 69-energy group has an increased number of fast and resonance groups and is generally recommended.

The WIMS program treats a number of basic geometries namely;

(1) homogeneous

(2) slab array including plate bundles

(3) regular rod arrays

(4) rod clusters in cylindrical (r,z) geometry

In addition to basic cell calculations the code may be used in point fuel burnup analysis and solution of multicell problems. The multigroup integral transport equation is written in the form

$$\phi(r) = \int \frac{\exp[-\rho(\bar{r} - \bar{r}')]}{4\pi(\bar{r} - \bar{r}')^2} \left\{\Sigma_s(r')\phi(r') + Q(r')\right\} dV' \qquad (3.11)$$

where ρ is the optical distance or the mean free path. The term $\exp[-\rho(\bar{r} - \bar{r}')]$ defines the probability of a neutron starting from a unit isotropic source at position $\bar{r}'$ to reach $\bar{r}$ uncollided. The source term $Q(r')$ accounts for contributions from fission and scattering from other groups. Assuming a flat flux approximation and that the cross-sections $\left(D_g,\ \nu_g\Sigma_{fg},\ \Sigma_{ag},\ \Sigma_{sg'\to g}\right)$ are constants in a homogeneous zone, the following equations can be derived from Eq.(3.11) for energy group g in region i as:

$$\phi_i^g = \sum \frac{V_j}{V_i} M_{ij}^g \left(\Sigma_{sj}^g \phi_j^g + Q_i^g\right) \qquad (3.12)$$

with

$$M_{ij}^g = \int_{V_i} \int_{V_j} \frac{\exp[-\rho(\bar{r} - \bar{r}')]}{4\pi|\bar{r} - \bar{r}'|^2} dV'dV \qquad (3.13)$$

and the total source in region i

$$Q_j^g = \sum_{g'} \left\{ \Sigma_{si}^{g' \to g} \phi_i^{g'} + \chi^g \frac{\left(\nu\Sigma_f\right)_i^{g'} \phi_i^{g'}}{k_{eff}} \right\}$$

$$= \sum S_i^{g' \to g} \phi_i^{g'} + F_i^{g' \to g} \qquad (3.14)$$

with the scattering and fission terms written explicitly. The fission fraction is χ^g and the fission yield is denoted by $\left(\nu\Sigma_f\right)_i^{g'}$. The effective multiplication constant is k_{eff}. Eq.(3.12) is multiplied by the total cross-section in region Σ_i and the collision probability or probability density P_{ij} is then introduced to give the number of collisions in region i caused by the source in the jth region:

$$P_{ij} = P_{ji} = \Sigma_j^g \Sigma_i^g M_{ij} \qquad (3.15)$$

yielding the set of equations for the neutron flux

$$\Sigma_i^g v_i \phi_i^g = \sum c_j^g P_{ji}^g \phi_i^g + \sum \frac{P_{ji}^g Q_j}{\Sigma_j^g} \qquad (3.16)$$

The factor c_j^g connotes the number of secondaries per collision. In solving Eq.(3.16), one needs to determine the one-group probabilities P_{ij} which define the probability that a neutron appearing uniformly and isotropically in region i will have its first collision in region j. Methods for calculating the macroscopic cross-sections which are described in the literature [15] are used in solving Eq.(3.15) for each group g. The equation is written in matrix notation as:

$$\phi = \bar{\bar{P}}\bar{\Psi} \qquad (3.17)$$

$$\Psi = \bar{\bar{S}}\bar{\phi} + \bar{\bar{\lambda}}\bar{\bar{F}} \qquad (3.18)$$

or alternatively as:

$$\begin{bmatrix} \phi \\ \Psi \end{bmatrix} = \begin{bmatrix} 0 & P \\ S & 0 \end{bmatrix} \begin{bmatrix} \phi \\ \Psi \end{bmatrix} + \begin{bmatrix} 0 \\ \lambda F \end{bmatrix} \qquad (3.19)$$

where ϕ and Ψ are the column flux and emission rate vectors of NxG elements (i= 1,2,...,N, region index; g= 1,2,...,G, group index). P is the probability block diagonal matrix with matrices P^g defining the probabilities inside each energy group g. The scattering matrix of NGxNG elements in $\bar{S}$ and $\bar{F}$ is the fission factor and λ is an eigenvalue.

The solution is provided for the fuel and the coolant regions with a special correction applied to obtain a solution for the can region. An approximate technique based on the diffusion theory is used to determine the fluxes in the bulk moderator region where the equation for the neutron current is

$$J_{net} = J_{in} - J_{out} = Q_m \tag{3.20}$$

where

$$J_{out} = J_{in}(1 - P_{iN}) + \sum \Sigma_{si} V_i \phi_i + Q_i \Big) P_{iN} \tag{3.21}$$

leading to

$$J_{in} = Q_m / P_{iN} + (1 / P_{iN}) \Big\{ \sum \Sigma_{si} V_i \phi_i P_{iN} + Q_i P_{iN} \Big) \Big\} \tag{3.22}$$

where the total collision probability on entry to the moderator region is denoted by P_{iN}. The matrix equation Eq.(3.18) is solved to determine the average flux in the moderator using the diffusion boundary condition at the internal boundary of the moderator $r = r_N$:

$$J_{net} = 2\pi r_N D_m \frac{\partial \phi(r_N, E)}{\partial r} \tag{3.23}$$

where the flux derivative is performed at the inner moderator boundary r_N and the diffusion coefficient in the moderator is D_m.

Using the one-group asymptotic diffusion theory, the neutron flux is related to the energy as:

$$\phi(r,E) = \phi(a,E) + \frac{\partial \phi(a,E)}{\partial r}\left[\frac{b^2}{b^2 - a^2}\ln\left(\frac{r}{a}\right) - \frac{r^2 - a^2}{2(b^2 - a^2)}\right] \tag{3.24}$$

where $a=r_N$, and $b=r_m$ are boundaries of the diffusion equation. Integrating Eq.(3.23) across the moderator and dividing by the moderator volume and using Eq.(3.22), the mean flux is obtained in the region as:

$$\phi_m = \left[\phi_N + 3\Sigma_{tr} J_{net} \frac{h(y)}{2\pi}\right] \tag{3.25}$$

where

$$\phi_N = \phi(r_N); \qquad y = \frac{r_m}{r_N}$$

and

$$h(y) = \frac{y^4 \ln(y)}{2(y^2 - 1)} - \frac{3y^2 - 1}{4(y^2 - 1)} \tag{3.26}$$

The neutron current J_{net} is calculated using Eqs.(3.20) - (3.22) A formula is thus obtained which gives the mean flux in the moderator as a function of the solution for the internal regions.

3.2.2. Transport Calculations for Group Constants

The effective group constants needed for diffusion calculations were computed using WIMSPC [16], the PC version of the WIMS lattice code. This version is adapted to IBM 286/386 AT PC from WIMS-D/4 [17]. The present analysis is restricted to two-group theory. Hence only the cross-sections D_1, D_2, $\nu_1\Sigma_{f1}$, $\nu_2\Sigma_{f2}$, $\Sigma_{s1\,2}$ were computed for the various homogeneous zones of the core.

The 69-energy group structure of the WIMS library consists of fourteen fast groups (10MeV - 9.118KeV), thirteen resonance groups (9.118KeV - 4eV) and forty-two thermal energy groups (4eV - 0eV). These group divisions are sufficient to analyze a wide range of nuclear reactors. However, the 28-group structure recommended by

Fayers et al [15] for LWRs was selected for this analysis because core calculations for the MNSR using this group structure yielded a control rod worth of 7.1mk [18] which compared favourably with the measured value of 6.8mk [2].

The unit cell types that were considered in the analysis are:

(1) fuel element + water
(2) Al dummy/tie rod + water
(3) control rod guide tube + water
(4) Be reflectors

Instructions for the preparation of standard input data for WIMS-D/4 were followed. Material compositions for the unit cells of the core listed above and the physical properties such as density and temperature form part of the WIMS input data.

The material card of the WIMS code requires the densities and temperatures of the fuel, its cladding material, the coolant and the moderator at the position of interest (reference level or axial position z). This is followed by weight fractions of the various elements comprising the material. The prevailing conditions at the middle of the MNSR core is shown in Fig 3.5. The physical quantities ρ_0 = 0.99329g/cc, T_{f0} = 374°K, T_{cl0} = 355.2°K, and T_{m0} = 309.77°K were used in the computation of the reference level macroscopic cross-section $\Sigma^{xg}_{r,l,0}$ for zero burnup condition. The operating conditions corresponding to the axial position z from the reference point (ρ_z, T_{fz}, T_{clz}, T_{mz}) were also invoked in

the determination of the group constants. In particular, the densities of the coolant and moderator were computed as functions of the coolant temperature at the position z by using the correlating equation:

$$\rho_z(T_{mz}) = \frac{\sum_i \alpha_i T_{mz}^i}{\sum_j \beta_j T_{mz}^j} \qquad (3.27)$$

The coefficients are listed in reference [18].

The U-235 content(g_{U-235} in grams) in a fuel rod is calculated from the equation:

$$g_{U-235} = \rho_U V(1 - e\%)Xf_m \qquad (3.28)$$

where ρ_U is the fuel density, X is the weight fraction of uranium, e% is the volume porosity and f_m is the weight enrichment of uranium in the U-Al alloy. The volume V of the fuel is given by

$$V = (\pi d_0/4)h \qquad (3.29)$$

where h is the active height of the fuel rod. The weight enrichment of uranium is given by

$$f_m = \frac{m_{U-235}\,\varepsilon}{m_{U-235}\varepsilon + m_{U-238}(1-\varepsilon)} \tag{3.30}$$

where ε is the enrichment factor. The density of the fuel is calculated using the expression:

$$\rho_U = \frac{3.3596(1-e\%)}{1.2443 - X} \tag{3.31}$$

In the determination of the polynomial for $b^{xg}(\tau)$, burnup values were determined using the POWERC card in the WIMS input data. The card is specified by specific power, P_s and the residence time t_r. The specific power, sometimes called power rating is defined as the thermal power produced per unit of the fuel loading:

$$P_s = \frac{10^3 P}{n_f g_U} \tag{3.32}$$

where P is the reactor power, n_f is the total number of fuel

elements and g_U defines the fuel loading (U-235 + U-238).

The burnup of the core, B MWd/tU is needed for residence time t_r computation. The maximum burnup according to the neutronic design calculations of the core is 1% [20]. From burnup physics calculations

$$1 \text{ MWd/tU} \equiv 1 \text{ g U-235} \tag{3.33}$$

thus, an estimation of the maximum burnup of the MNSR fuel element can be made. By using Eqs.(3.28) - (3.31), an amount of 2.5g of U-235 out of the total weight of 2.75g which is equivalent to a burnup of 9090.9MWd/tU corresponding to the maximum value of 1% was computed for the fresh fuel. The core was then depleted from 0 to 9090.9MWd/tU in n_s steps. The residence time of the fuel was determined using the relationship

$$t_r = \frac{B/n_s}{P_s} \text{ days} \tag{3.34}$$

where B is specific burnup (MWd/tU) and n_s is the number of burnup steps. With the various specifications for the WIMS input cards, cross-sections were obtained from which the parameterized equations are derived.

3.2.3. Parameterized Polynomials

In order to evaluate Eq.(3.6), the parameterized polynomials $a_l^{xg}(z)$ for the axial effects and $b^{xg}(\tau)$ for burnup variations at the reference condition must be determined. For nominal power of 27kW, the conditions at position z were used to obtain the group constants. The difference between values at the reference level and position z yields

$$\Delta\Sigma_l^{xg}(z) = \Sigma_{l,z,o}^{xg} - \Sigma_{l,r,o}^{xg} \qquad (3.35)$$

where $\Sigma_{l,z,o}^{xg}$ is the cross-section at position z for zero burnup.

A curve fitting program called DEM4 was used to fit the computed values to obtain the coefficients $a_{l,0}$, $a_{l,1}$ and $a_{l,2}$ of Eq.(3.8). For the burnup variation, the polynomial $b^{xg}(\tau)$ was correlated using data within the range 0 -10,000 MWd/tU comprising ten burnup steps. The percentage burnup is within the range of 0 - 1.1%. The two-group constants were also fitted with the DEM4 program for the burnup coefficients b_1^{xg} and b_2^{xg} for the evaluation of Eq.(3.7).

3.3 DISCUSSIONS AND CONCLUSIONS

The results of the evaluation of the various equations of the mathematical model are used to create a library which can be used to solve either a two-dimensional, two-group transport or diffusion equation in radial-axial (r-z) geometry. The BMC $\Sigma^{xg}_{r,l,0}$ for the various zones at the reference position and zero burnup and coefficients b^{xg}_1 and b^{xg}_2 are contained in a file called **BMC.LIB**. Data for the coefficients $a^{xg}_{l,0}$, $a^{xg}_{l,1}$, and $a^{xg}_{l,2}$ accounting for axial effects are also contained in a file called **AXIS.INP**. A listing for the two files can be found in the Appendix.

The computed values of the macroscopic cross-sections under conditions prevailing at the nominal power for different burnup values at fixed positions along the flow channel are plotted in Figs. 3.5 - 3.11. Graphical representations of the variations of the various group constants with positions of the flow channel are also depicted in Figs. 3.12 - 3.17.

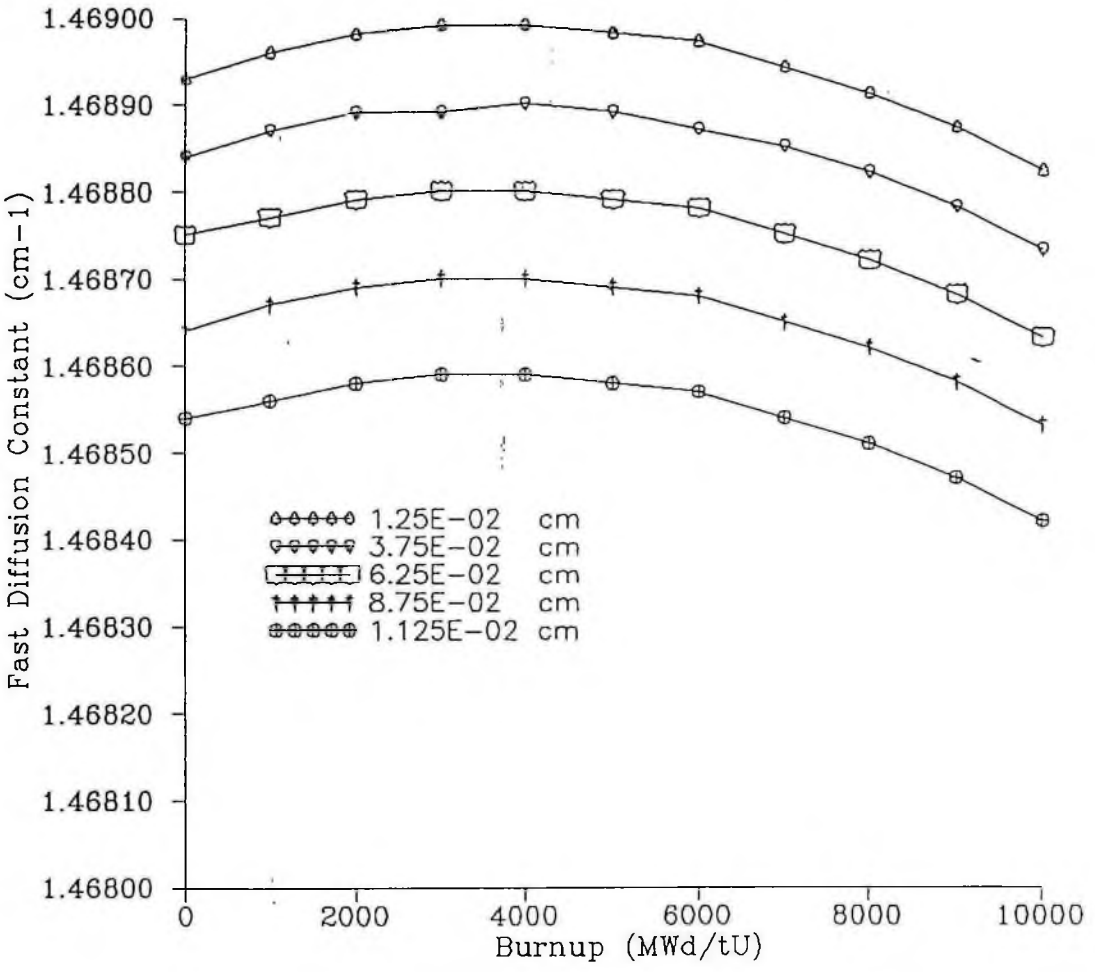

Fig 3.5: Fast Diffusion Constant vrs Burnup

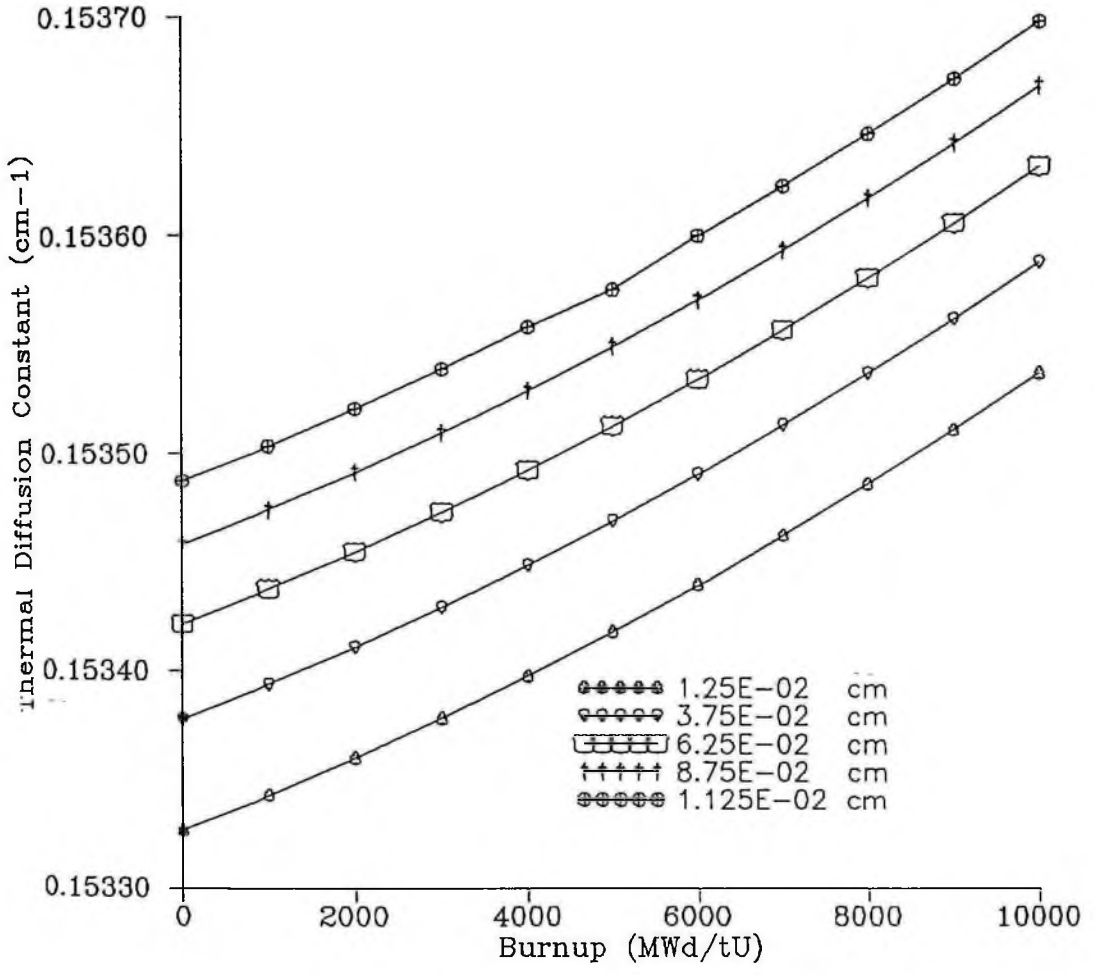

Fig 3.6: Thermal Diffusion Constant vrs Burnup

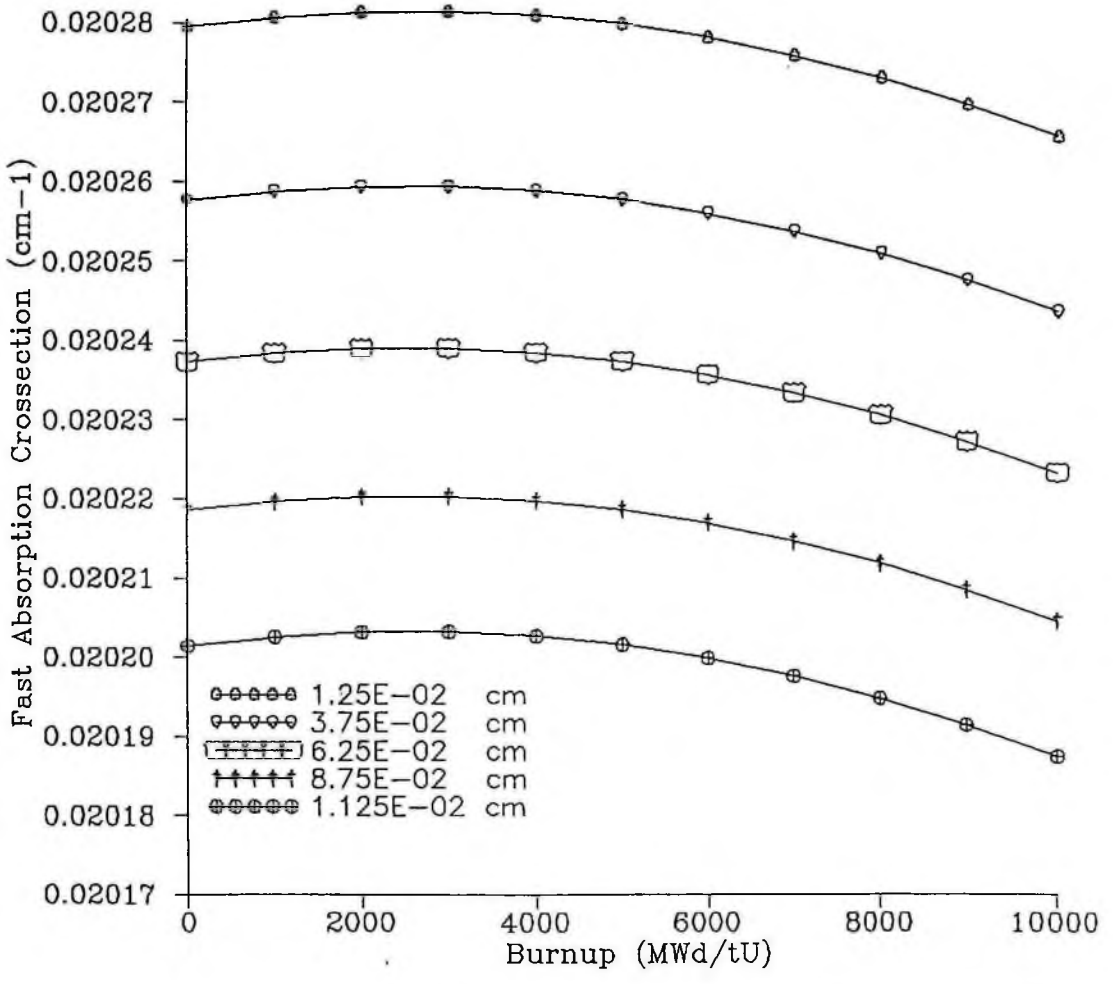

Fig.3.7: Fast Absorption Crossection vrs Burnup

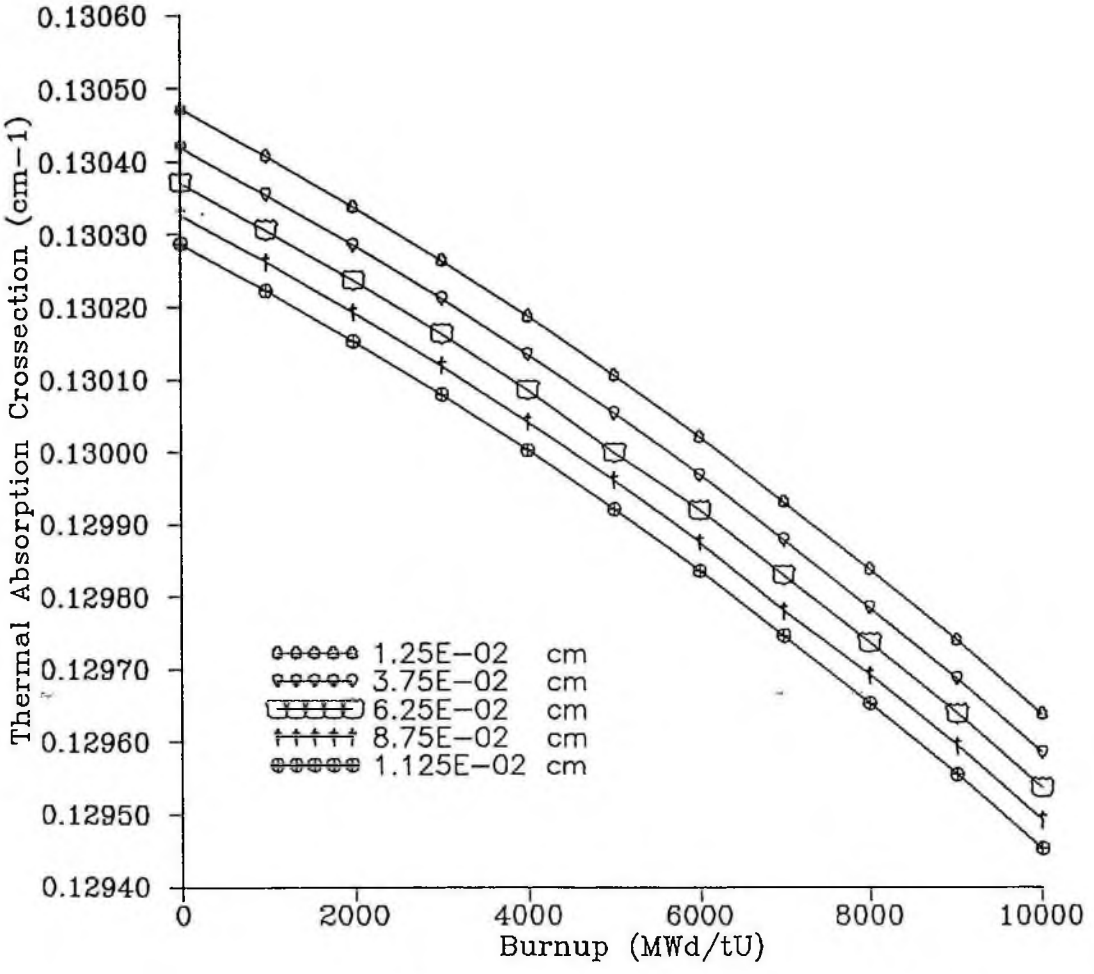

Fig.3.8: Thermal Absorption Crossection vrs Burnup

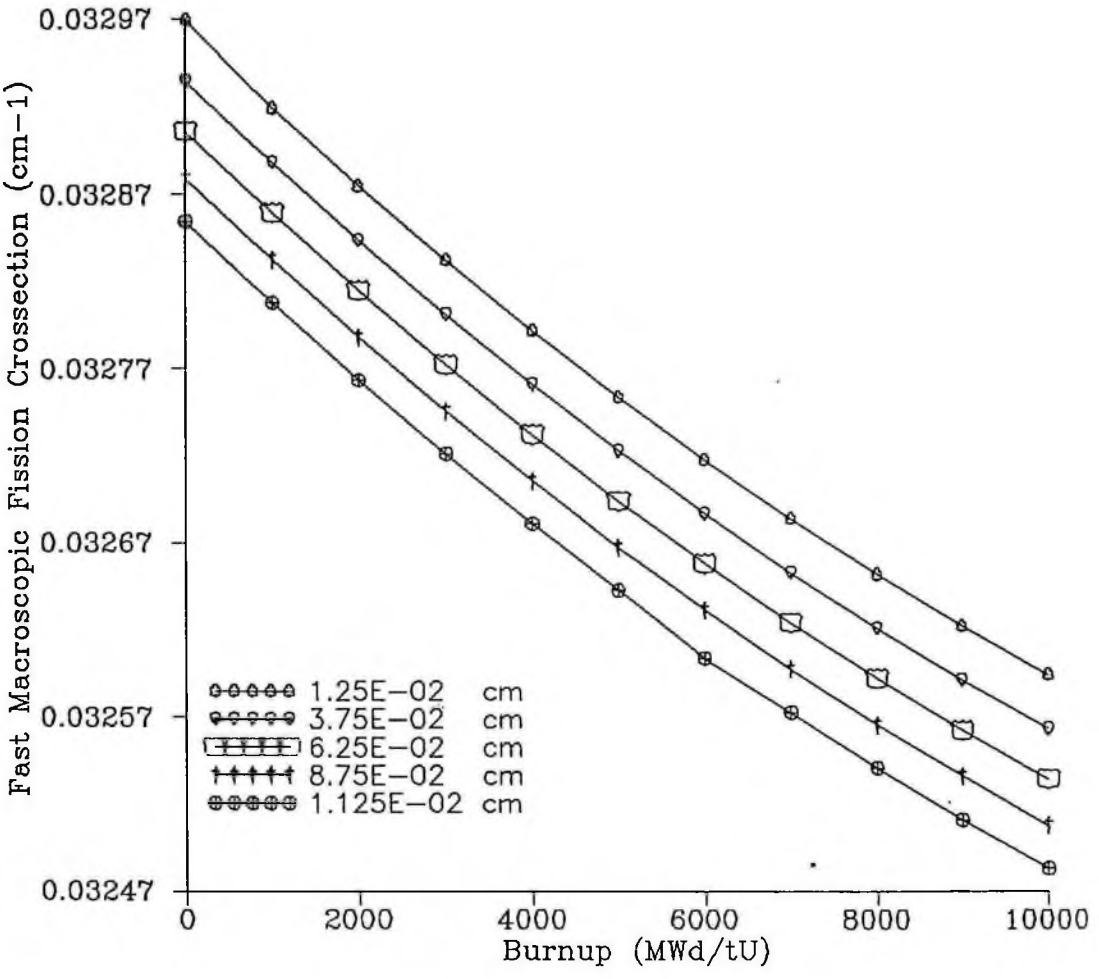

Fig.3.9: Fast Macroscopic Fission Crossection vrs. Burnup

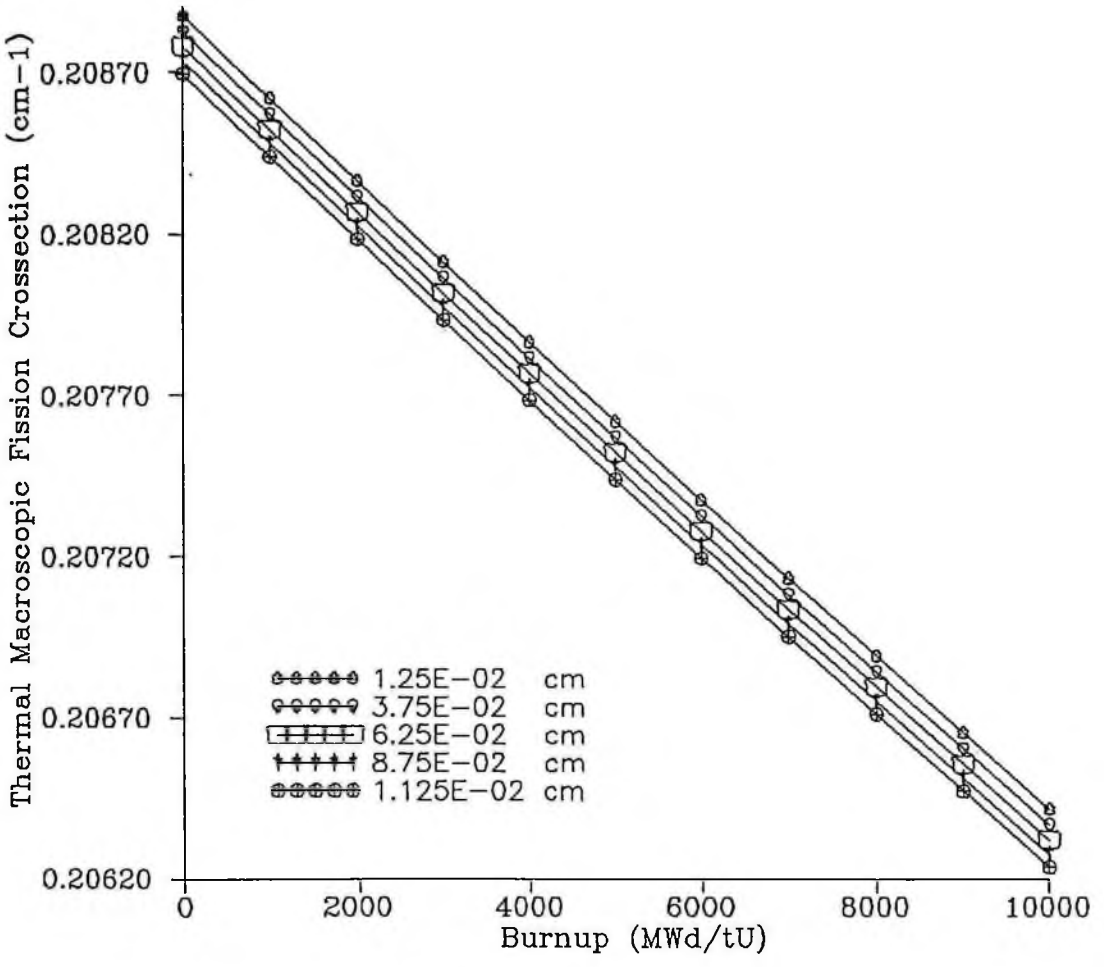

Fig 3.10: Thermal Macroscopic Fission Crossection vrs. Burnup

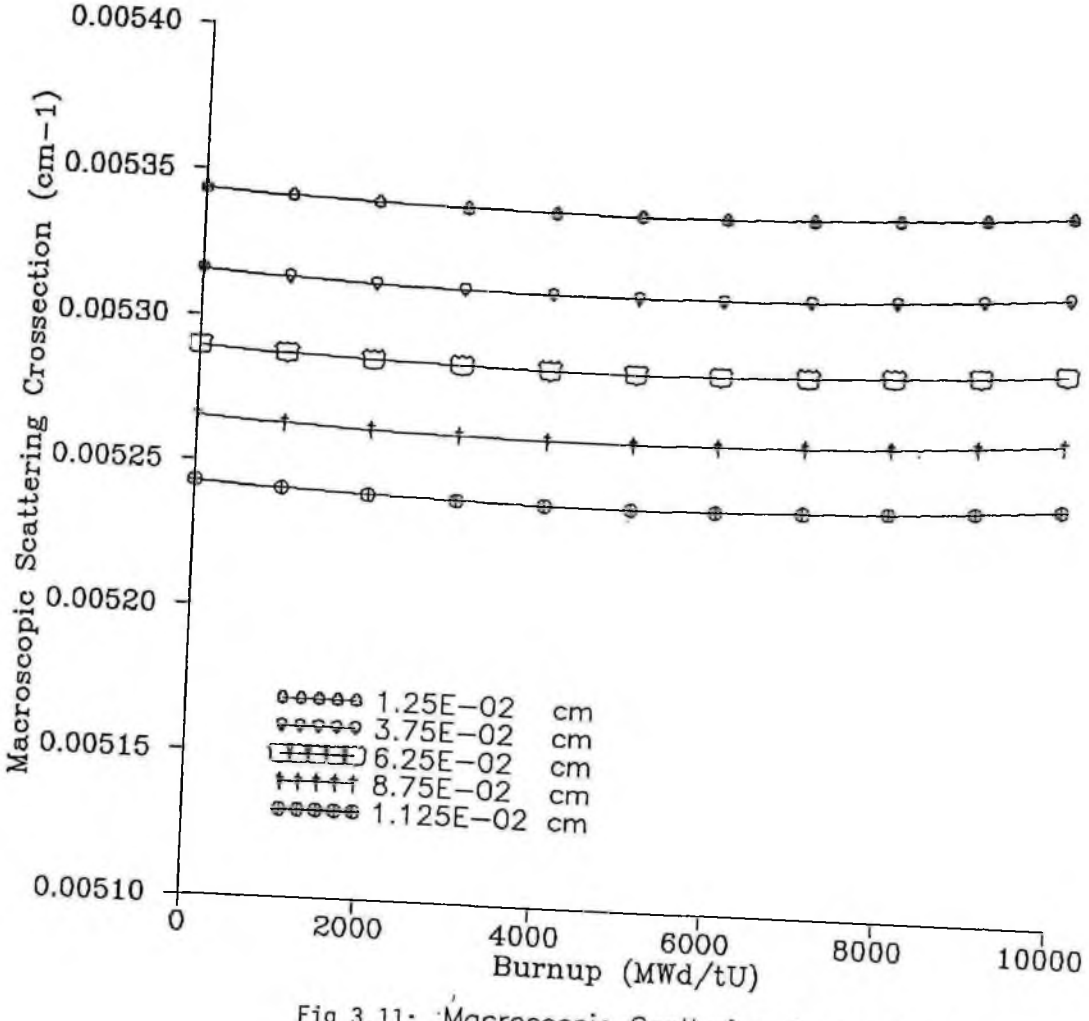

Fig 3.11: Macroscopic Scattering Crossection vrs Burnup

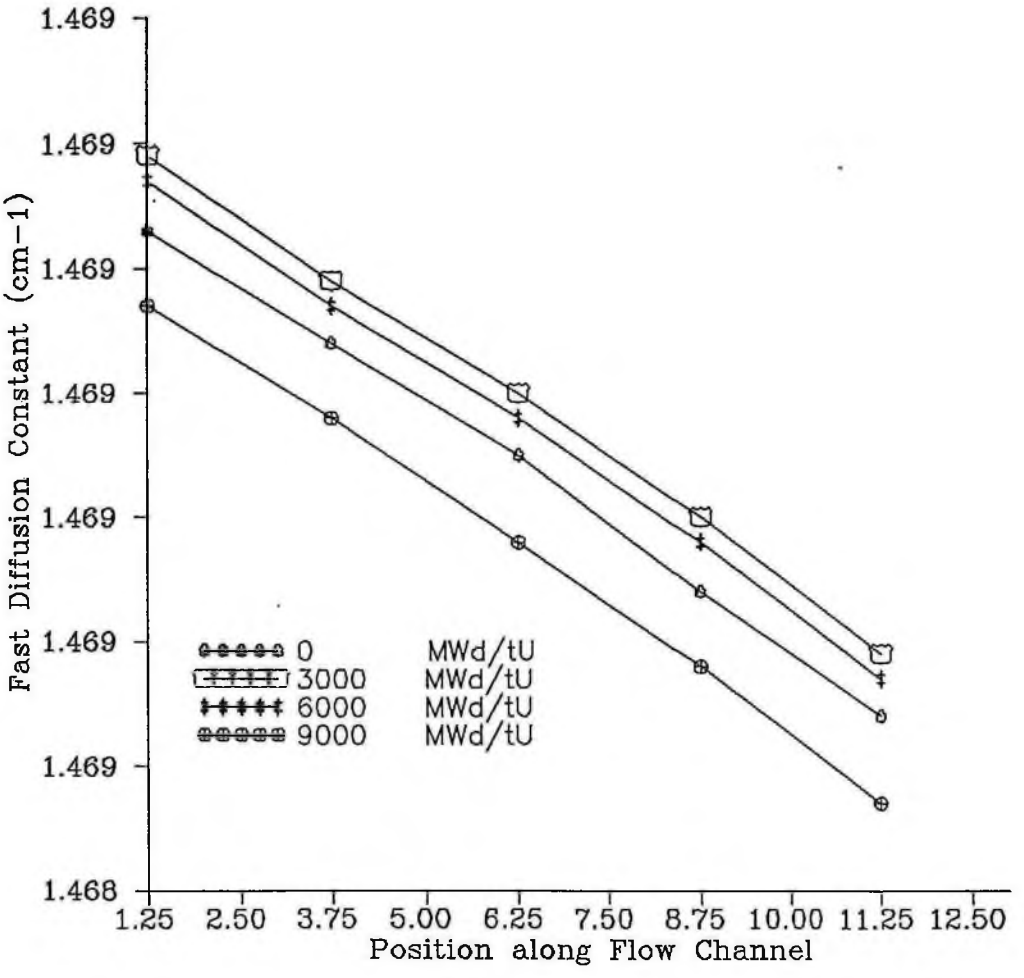

Fig 3.12: Fast Diffusion Constant vrs Position of Flow Channel

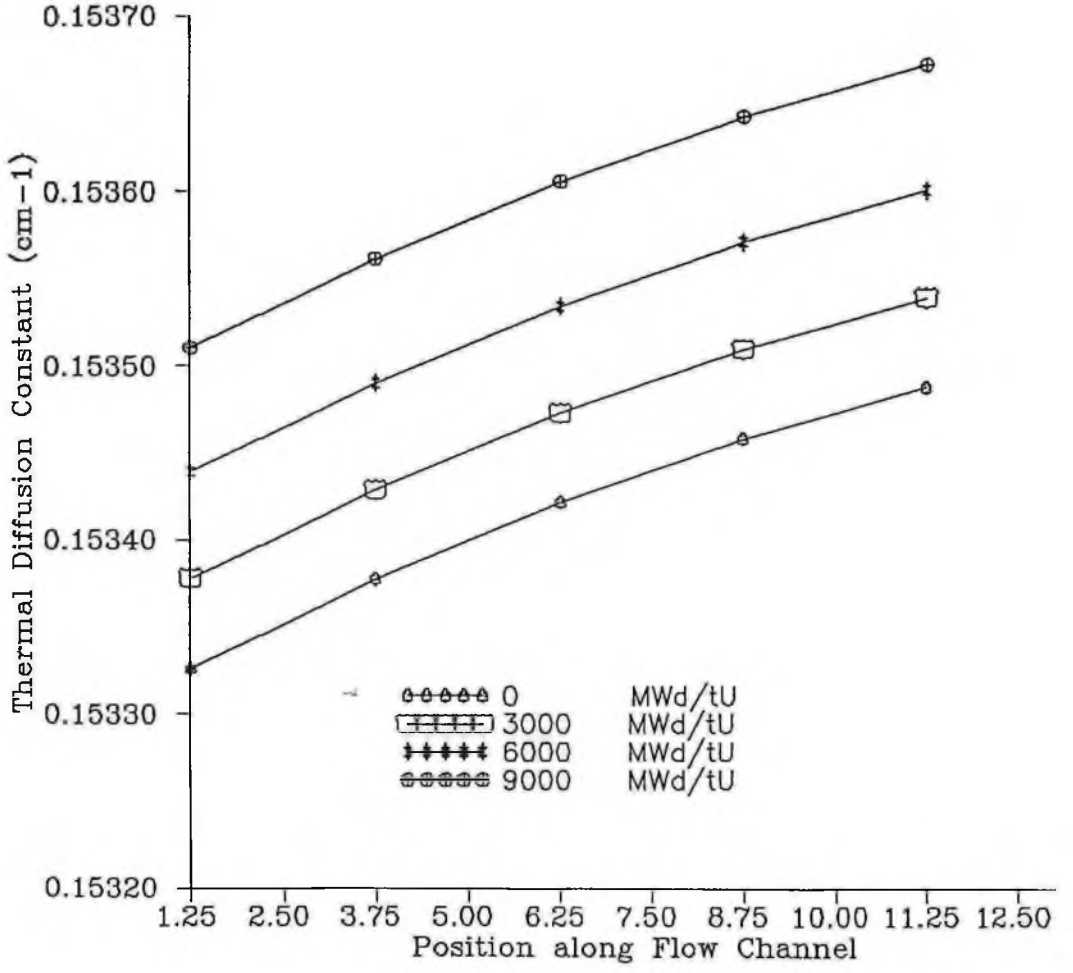

Fig 3.13: Thermal Diffusion Constant vrs Position of Flow Channel

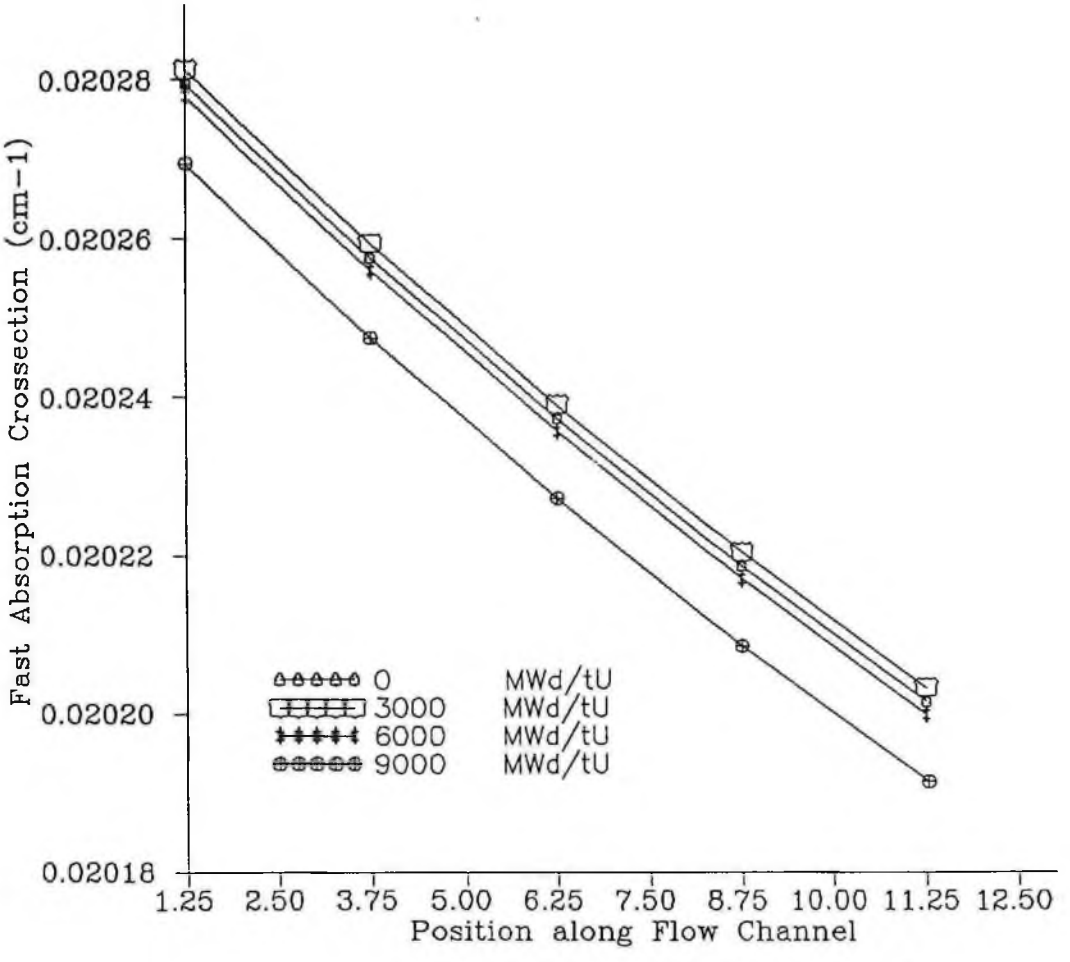

Fig 3.14: Fast Absorption Crossection vrs Position of Flow Channel

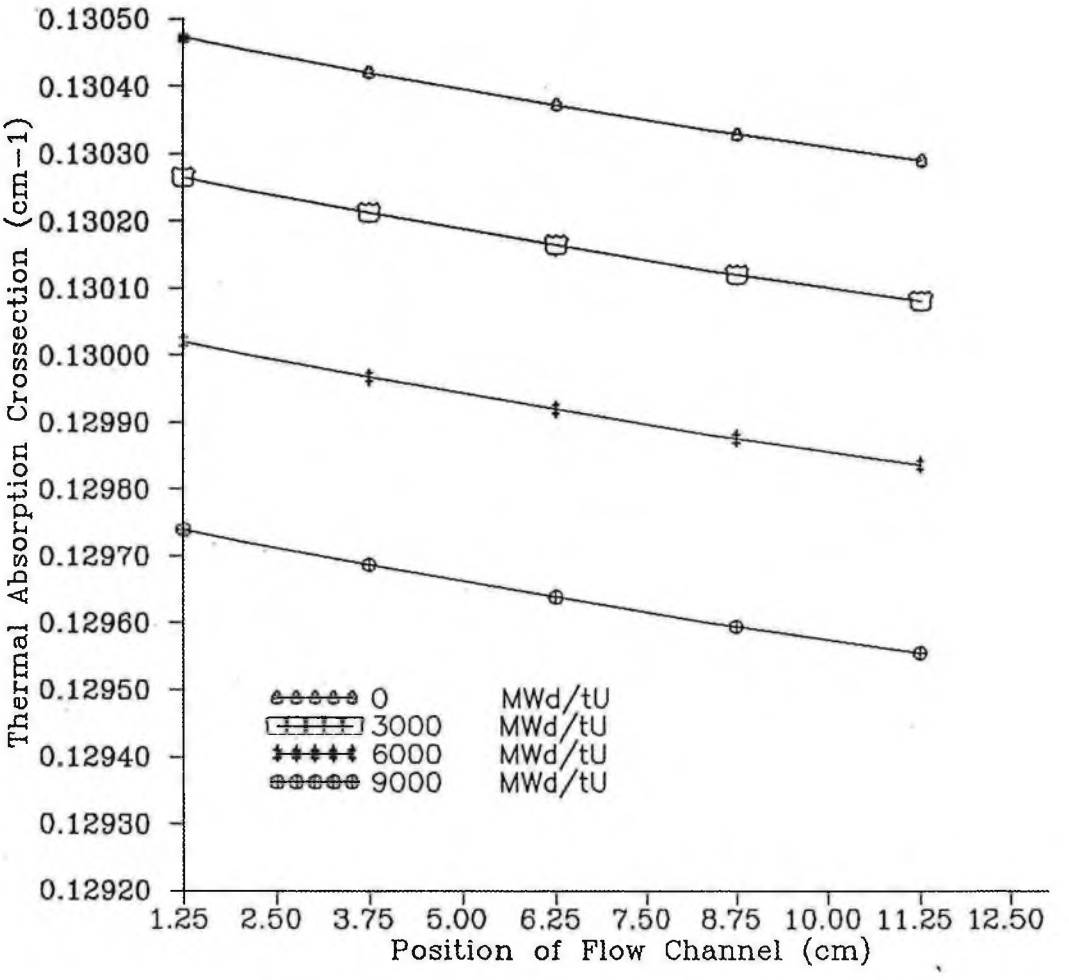

Fig 3.15: Thermal Absorption Crossection vrs Position of Flow Channel

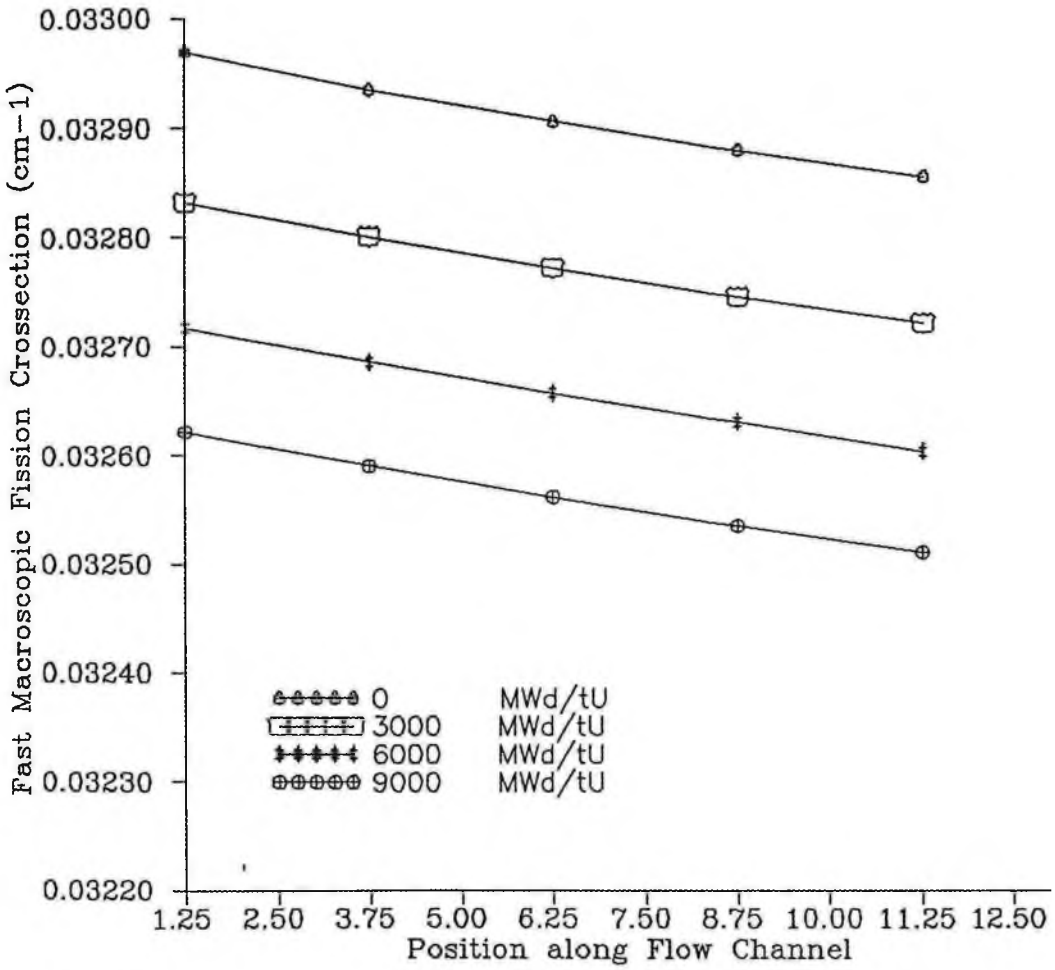

Fig 3.16: Fast Macroscopic Fission Crossection vrs Position of Flow Channel

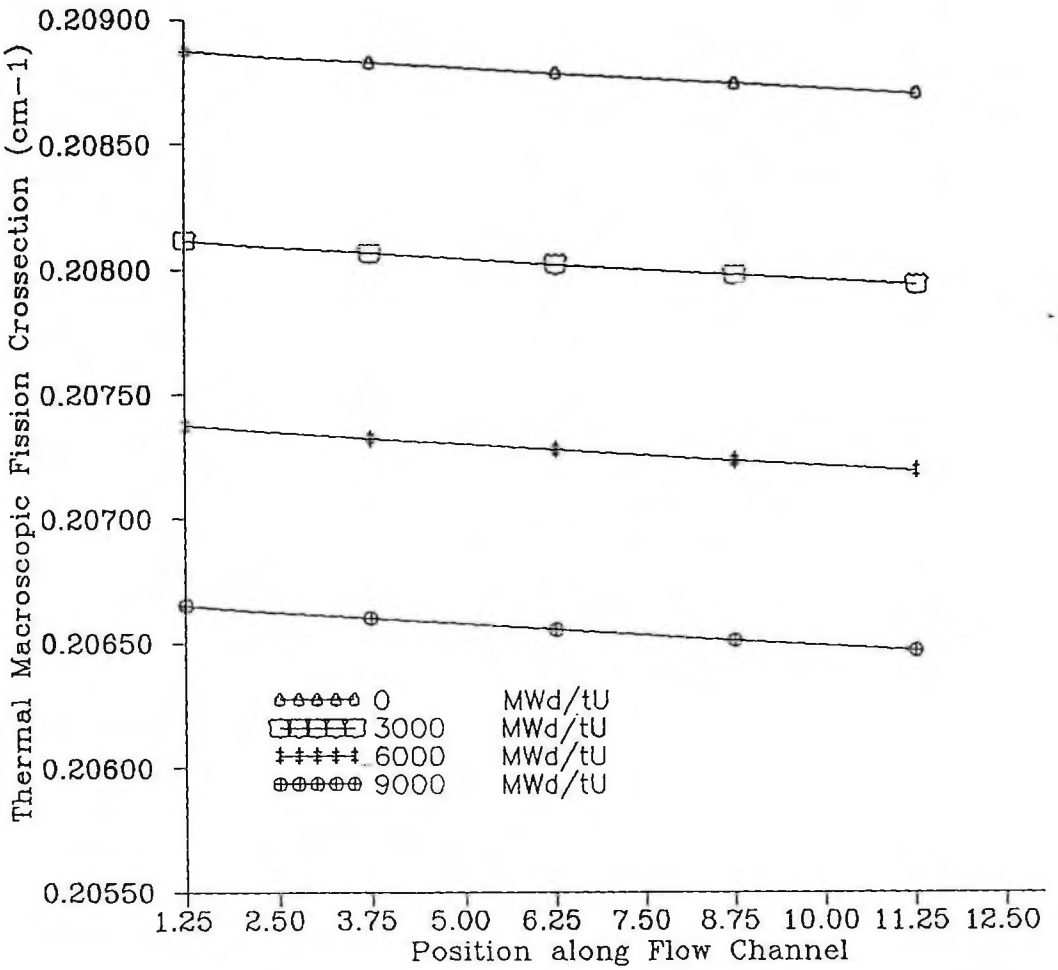

Fig 3.17: Thermal Macroscopic Fission Crossection vrs Position of Flow Channel

The correction term due to Xe-135 computed using the operating characteristics of the MNSR in Eq.(3.9) was found to be very small in comparison with axial and burnup effects on the thermal absorption cross-section value. In order to check the accuracy of the polynomial representation of the group constants calculated by the present method, the calculated forms of the BMCs $\Sigma_1^{xg}(cal)$ were compared with the accurate values obtained using the WIMSPC code and designated $\Sigma_1^{xg}(acc)$.

The accuracy is indicated by the relative error:

$$error = \frac{\Sigma_1^{xg}(cal) - \Sigma_1^{xg}(acc)}{\Sigma_1^{xg}(acc)} \qquad (3.36)$$

The values of the maximum errors found to be below 1% are listed in Table. 3.1

Group Constant	D_1	D_2	Σ_{a1}	Σ_{a2}	$\nu\Sigma_{f1}$	$\nu\Sigma_{f2}$	$\Sigma_{s1\to2}$
Maximum Error	0.022	0.141	0.073	0.032	0.207	0.010	0.013

Table 3.1: Maximum Error in Paramaterized Group Constants

In conclusion, a two group data base has been created using a simplified model. The error analysis depicts an accurate data base for neutronic calculations. The data could be used to solve a 2-D transport or diffusion code for fast and thermal neutron fluxes produced at any point in the reactor. The predicted values are to be compared with those obtained from experiments as a further confirmation of the present analysis.

METHOD OF SOLUTION OF TWO-GROUP DIFFUSION EQUATION

The KWABEN code is a finite difference method based computer code which solves a 2-D (r,z) neutron diffusion equation for two-energy groups (fast and thermal). The KWABEN code is written for IBM PC AT to form part of a proposed computer package **MEPE** for the analysis of the MNSR. It can however exist in isolation from the MEPE package and could also be applicable to other water moderated reactors subject to the conditions that:

(1) the reactor has cylindrical geometry

(2) the program is supplied with appropriate two-energy data base consisting of group constants in radial, axial (r,z) dimensions.

A major assumption in the utilization of the MEPE code is that the nuclear properties such as macroscopic cross-sections are dependent only on the homogeneous zones of the reactor core and the energy group under consideration. The code comprises the main program KWABEN and other libraries such as **BMC.LIB** which contains cross-sections obtained at the middle of the core and with corrections due to the effect of burnup. Corrections were also introduced to the BMCs to account for temperature changes along the axis of the flow channel. These are listed in the **AXIS.INP** file.

In the present work, the mathematical model, numerical methods and techniques used in the code are presented. The model was applied to the criticality parameters and group average fluxes for the various homogeneous zones.

4.1 Mathematical model

The diffusion equation for a 2-D (r,z) region is written for any one group g in the form [6]

$$D_g(r,z)\nabla^2\phi_g(r,z) + \Sigma_{tg}(r,z)\phi_g = S_g(r,z) \qquad (4.1)$$

where

D_g = diffusion coefficient for energy group g

ϕ_g = group neutron flux

Σ_{tg} = total macroscopic neutron cross-section for group g

S_g = source term for group g

Eq.(4.1) is a neutron balance equation where losses on the left hand side (LHS) are balanced by neutron gains on the right hand side (RHS). For a 2-D plane, cylindrical and spherical geometries, the leakage or advection term $D_g(r,z)\nabla^2\phi_g(r,z)$ is written as:

$$D_g(r,z)\nabla^2\phi_g(r,z) = -\left\{\frac{1}{r^\alpha}\frac{\partial}{\partial r}r^\alpha D_g(r,z)\frac{\partial}{\partial r}\phi_g(r,z) + \frac{\partial}{\partial z}D_g(r,z)\frac{\partial}{\partial z}\phi_g(r,z)\right\} \tag{4.2}$$

where

$$\alpha = \begin{cases} 0 & \text{plane (rectangular) region} \\ 1 & \text{cylindrical geometry} \\ 2 & \text{spherical geometry} \end{cases}$$

The diffusion constant in group g at position (r,z) is $D_g(r,z)$. The total cross-section for group g is expressed in the form

$$\Sigma_{tg}(r,z) = D_g(r,z)B_g^2(r,z) + \Sigma_{ag}(r,z) + \Sigma_{rg}(r,z) \tag{4.3}$$

where

B_g^2 = transverse buckling for group g

Σ_{ag} = macroscopic absorption cross-section for group g

Σ_{rg} = macroscopic removal cross-section for energy group g

The source term in group g is similarly expressed in the form

$$S_g(r,z) = \frac{\chi_g(r,z)}{\lambda}\sum_{g'=1}^{G} \nu_g \Sigma_{fg}(r,z)\phi_{g'}(r,z) + \sum_{\substack{g'=1 \\ g'\neq g}}^{G} \Sigma_{sg'\to g}(r,z)\phi_g(r,z) \tag{4.4}$$

where

χ_g = fraction of fission neutrons in group g

ν_g = average number of neutrons per fission in group g

λ = eigenvalue related to the effective multiplication factor (k_{eff})

Σ_{fg} = macroscopic fission cross-section in group g

$\Sigma_{sg'\to g}$ = macroscopic scattering cross-section from g' to g

Dropping the group subscript g, Eq.(4.1) is re-written as

$$\frac{1}{r^\alpha}\frac{\partial}{\partial r}r^\alpha D(r,z)\frac{\partial}{\partial r}\phi(r,z) + \frac{\partial}{\partial z}D(r,z)\frac{\partial}{\partial z}\phi(r,z) - \Sigma_t(r,z)\phi(r,z) = -S(r,z) \tag{4.5}$$

which may be parametrically expressed in the form

$$\frac{1}{r^{\alpha}}\frac{\partial}{\partial r}J + \frac{\partial}{\partial z}Y = \Sigma_t\phi - S \qquad (4.6)$$

where the parameters J and Y are defined as

$$J = r^{\alpha}D\frac{\partial\phi}{\partial r} \qquad (4.7)$$

$$Y = D\frac{\partial\phi}{\partial z} \qquad (4.8)$$

It is assumed in this analysis that discontinuities in the nuclear properties of D, Σ and S lie on basic interpolation points (r_i, z_j) as illustrated below in Fig 4.1.

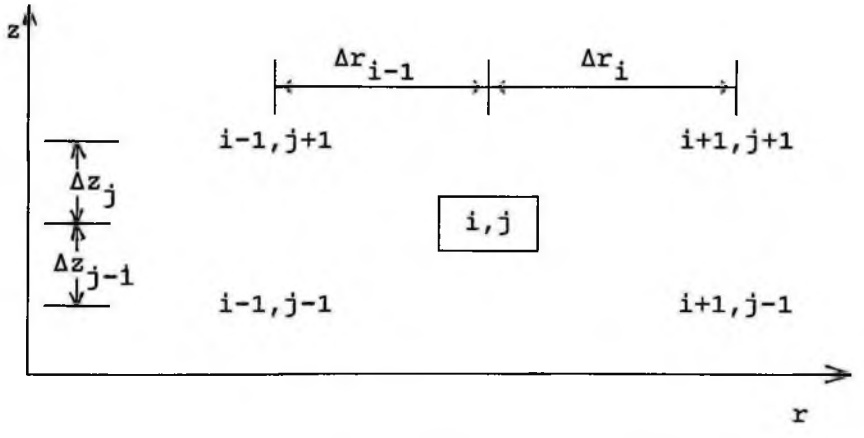

Fig 4.1: A mesh layout in r,z geometry

One way of formulating a finite difference equation is by numerical integration of Eq.(4.6), the group diffusion equation over an interval on a spatial mesh. It is worth defining some terms which will be helpful in performing the numerical integration. Consider the schematic of the spatial mesh with central grid point (i,j) and four adjacent grid points (i-1,j), (i+1,j), (i,j-1) and (i,j+1) in Fig 4.2 below.

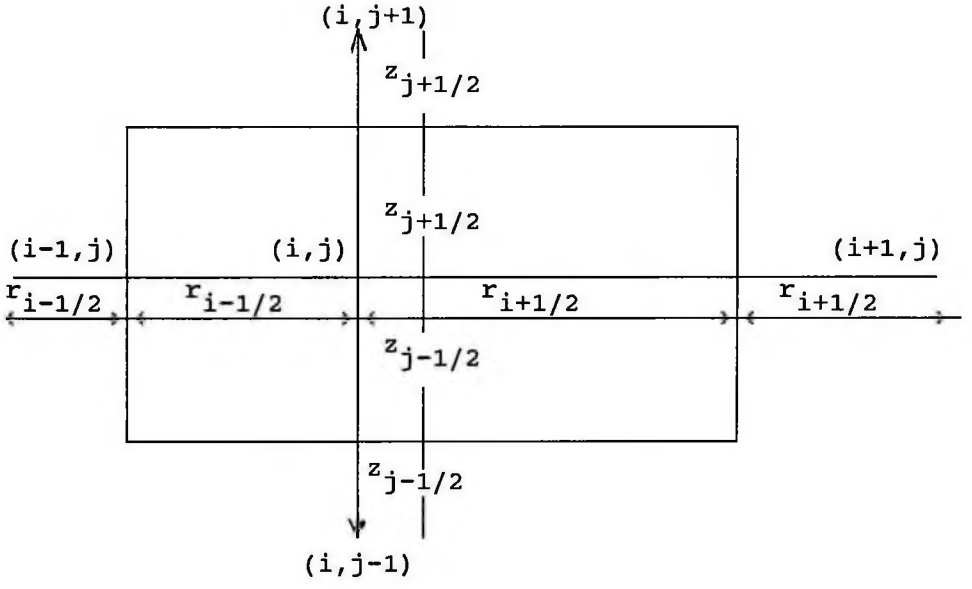

Fig 4.2: Coordinate System around mesh point (i,j)

The rectangular boxes around the central mesh point (i,j) are defined by the intersecting lines over four rectangles. The spacing however, need not be uniform. The intervals are defined as follows:

$$r_{i+1/2} = \frac{1}{2}\left(r_{i+1} + r_i\right) \tag{4.9a}$$

$$r_{i-1/2} = \frac{1}{2}\left(r_i + r_{i-1}\right) \tag{4.9b}$$

$$z_{j+1/2} = \frac{1}{2}\left(z_{j+1} + z_j\right) \tag{4.9c}$$

$$z_{j-1/2} = \frac{1}{2}\left(z_j + z_{j-1}\right) \tag{4.9d}$$

$$\Delta r_{i+1/2} = r_{i+1} - r_i \tag{4.9e}$$

$$\Delta r_{i-1/2} = r_i - r_{i-1} \tag{4.9f}$$

$$\Delta z_{j+1/2} = z_{j+1} - z_j \tag{4.9g}$$

$$\Delta z_{j-1/2} = z_j - z_{j-1} \tag{49h}$$

The nuclear properties are defined to correspond to the various regions of the reactor core and assumed to remain constant within a mesh interval. For example, the group diffusion coefficient at

various mesh points is given as

$$D^g_{i-1/2,j} = \frac{1}{2}\left(D^g_{i,j} + D^g_{i-1,j}\right) \tag{4.10a}$$

$$D^g_{i+1/2,j} = \frac{1}{2}\left(D^g_{i+1,j} + D^g_{i,j}\right) \tag{4.10b}$$

$$D^g_{i,j-1/1} = \frac{1}{2}\left(D^g_{i,j} + D^g_{i,j-1}\right) \tag{4.10c}$$

$$D^g_{i,j+1/2} = \frac{1}{2}\left(D^g_{i,j+1} + D^g_{i,j}\right) \tag{4.10d}$$

With the box drawn around the arbitrary point, the diffusion equation is integrated over the box to obtain the fluxes and the parameters are evaluated at the mesh points. Multiplyiing Eq.(4.6) by r^{α} and integrating over the mesh intervals

$$r_{i-1/2} < r_i < r_{i+1/2} \quad \text{and} \quad z_{j-1/2} < z_j < z_{j+1/2},$$

yields the expression

$$\int_{z_{j-1/2}}^{z_{j+1/2}} \left(J_{i+1/2} - J_{i-1/2}\right)dz + \int_{r_{i-1/2}}^{r_{i+1/2}} \left(Y_{j+1/2} - Y_{j-1/2}\right)r^{\alpha}dr$$

$$= \int_{r_{i-1/2}}^{r_{i+1/2}} \int_{z_{j-1/2}}^{z_{j+1/2}} \left(\Sigma_t\phi - S\right)r^{\alpha}drdz \qquad (4.11)$$

which in accordance with the above assumption, can be written as

$$\int_{z_{j-1/2}}^{z_{j+1/2}} \left(J_{i+1/2} - J_{i-1/2}\right)dz = \left(J_{i+1/2,j} - J_{i-1/2,j}\right)\Delta z_j \qquad (4.12)$$

$$\int_{r_{i-1/2}}^{r_{i+1/2}} \left(Y_{j+1/2} - Y_{j-1/2}\right)r^{\alpha}dr = \left(Y_{i,j+1/2} - Y_{i,j-1/2}\right)r_i^{\alpha}\,\Delta r_i \qquad (4.13)$$

and

$$\int_{r_{i-1/2}}^{r_{i+1/2}} \int_{z_{j-1/2}}^{z_{j+1/2}} \left(\Sigma_t \phi - S\right) r^{\alpha} dr dz = \left(\Sigma_t \Delta r \Delta z\right)_{i,j} \phi_{i,j}\, r_i^{\alpha} - \left(S \Delta r \Delta z\right)_{i,j} r_i^{\alpha} \qquad (4.14)$$

By using Eqs.(4.12) to (4.14), Eq.(4.11) reduces to the simplified form

$$\left(J_{i+1/2,j} - J_{i-1/2,j}\right)\Delta z_j + \left(Y_{i,j+1/2} - Y_{i,j-1/2}\right) r_i^{\alpha} \Delta r_i$$

$$- \left(\Sigma_t \Delta r \Delta z\right)_{i,j} \phi_{i,j} r_i^{\alpha} = - \left(S \Delta r \Delta z\right)_{i,j} r_i^{\alpha} \qquad (4.15)$$

Integration of Eq.(4.7) over the intervals $r_i < r < r_{i+1/2}$; $z_{j-1/2} < z < z_{j+1/2}$ eliminates J whilst an integration of Eq.(4.8) performed over the limits $r_{i-1/2} < r < r_{i+1/2}$; $z_j < z < z_{j+1/2}$ eliminates Y. The simplified expressions for the parameters J and Y are then arrived at as

$$J: \quad \phi_{i+1,j} - \phi_{i,j} = \left(\frac{\Delta z}{D}\right)_{i+1/2,j} \left(\frac{\Delta r_{i+1/2}}{\Delta z_j}\right) \frac{J_{i+1/2}}{r^{\alpha}_{i+1/2}} \tag{4.16}$$

$$Y: \quad \phi_{i,j+1} - \phi_{i,j} = \left(\frac{\Delta r}{D}\right)_{i,j+1/2} \left(\frac{\Delta z_{j+1/2}}{\Delta r_i}\right) Y_{i,j+1/2} \tag{4.17}$$

It follows immediately from Eqs.(4.16) and (4.17) that

$$J_{i+1/2,j} = r^{\alpha}_{i+1/2} \frac{\Delta z_j}{\Delta r_{i+1/2}} \frac{\phi_{i+1,j} - \phi_{i,j}}{\left(\frac{\Delta z}{D}\right)_{i,j+1/2}} \tag{4.18}$$

$$Y_{i,j+1/2} = \frac{\Delta r_i}{\Delta z_{j+1/2}} \frac{\phi_{i,j+1} - \phi_{i,j}}{\left(\frac{\Delta r}{D}\right)_{i,j+1/2}} \tag{4.19}$$

respectively. Similar equations can be written for

$$J_{i-1/2,j} = r^{\alpha}_{i-1/2} \frac{\Delta z_j}{\Delta r_{i-1/2}} \frac{\phi_{i,j} - \phi_{i-1,j}}{\left(\frac{\Delta z}{D}\right)_{i-1/2,j}} \tag{4.20}$$

and

$$Y_{i,j-1/2} = \frac{\Delta r_i}{\Delta z_{j-1/2}} \frac{\phi_{i,j} - \phi_{i,j-1}}{\left(\frac{\Delta r}{D}\right)_{i,j-1/2}} \tag{4.21}$$

Substituting Eqs.(4.18) - (4.21) into Eq.(4.15) we obtain the relation

$$\psi(\phi_{i,j}) + \alpha \frac{\Delta r_{i+1/2}}{2r_i} \gamma(\phi_{i,j}) - \eta_{i,j}\phi_{i,j} = - F_{i,j} \tag{4.22}$$

where

$$\psi(\phi_{i,j}) = \beta_{i-1/2,j}\phi_{i-1,j} + \beta_{i+1/2,j}\phi_{i+1,j} + \beta_{i,j-1/2}\phi_{i,j-1}$$

$$+ \beta_{i,j+1/2}\phi_{i,j+1} \tag{4.23}$$

$$\gamma(\phi_{i,j}) = \beta_{i+1/2,j}\phi_{i+1,j} - \frac{\Delta r_{i-1/2}}{\Delta r_{i+1/2}} \beta_{i-1/2,j}\phi_{i-1,j} \tag{4.24}$$

$$\eta_{i,j} = \beta_{i-1/2,j} + \beta_{i+1/2,j} + \beta_{i,j-1/2}\,\beta_{i,j+1/2}$$

$$+ \alpha\frac{\Delta r_{i+1/2}}{2r_i}\left(\beta_{i+1/2,j} - \frac{\Delta r_{i-1/2}}{\Delta r_{i+1/2}}\beta_{i-1/2,j}\right) + \left(\sum \Delta r \Delta z\right)_{i,j} \qquad (4.25)$$

and

$$F_{i,j} = \left(S\Delta r\Delta z\right)_{i,j} \qquad (4.26)$$

The parameters appearing in Eq.(4.23) - (4.25) are expressed as follows:

$$\beta_{i-1/2,j} = \frac{\Delta z_j^2}{\Delta r_{i-1/2}\left(\frac{\Delta z}{D}\right)_{i-1/2,j}} \quad ; \quad \beta_{i+1/2,j} = \frac{\Delta z_j^2}{\Delta r_{i+1/2}\left(\frac{\Delta z}{D}\right)_{i+1/2,j}}$$

$$\beta_{i,j-1/2} = \frac{\Delta r_i^2}{\Delta z_{j-1/2}\left(\frac{\Delta r}{D}\right)_{i,j-1/2}} \quad ; \quad \beta_{i,j+1/2} = \frac{\Delta r_i^2}{\Delta z_{j+1/2}\left(\frac{\Delta r}{D}\right)_{i,j+1/2}} \qquad (4.27)$$

Further simplification of Eq.(4.22) gives the five point finite difference equation for any energy group g of the form

$$a_{i,j}\phi_{i+1,j} + b_{i,j}\phi_{i-1,j} + c_{i,j}\phi_{i,j+1} + d_{i,j}\phi_{i,j-1} + e_{i,j}\phi_{i,j} = f_{i,j} \qquad (i = 1,2,\ldots,n) \quad (j = 1,2,\ldots,m) \qquad (4.28)$$

where the coefficients are defined as

$$a_{i,j} = \beta_{i+1/2,j}\left(1 + \alpha\frac{\Delta r_{i+1/2}}{2r_i}\right) \qquad (4.29a)$$

$$b_{i,j} = \beta_{i-1/2,j}\left(1 - \alpha\frac{\Delta r_{i+1/2}\,\Delta r_{i-1/2}}{2r_i\,\Delta r_{i+1/2}}\right) \qquad (4.29b)$$

$$c_{i,j} = \beta_{i,j+1} \qquad (4.29c)$$

$$d_{i,j} = \beta_{i,j-1} \qquad (4.29d)$$

$$e_{i,j} = -\left\{\beta_{i+1/2,j} + \beta_{i-1/2,j} + \beta_{i,j+1/2} + \beta_{i,j-1/2}\right.$$

$$\left. + \alpha\frac{\Delta i_{i+1/2}}{2r}\left(\beta_{i+1/2,j} - \frac{\Delta r_{i-1/2}}{\Delta r_{i+1/2}}\beta_{i-1/2,j}\right) + \left(\sum \Delta r \Delta z\right)_{i,j}\right\} \tag{4.29e}$$

$$f_{i,j} = -F_{i,j} = -\left(S\Delta r\Delta z\right)_{i,j} \tag{4.29f}$$

A mesh system was imagined to cover the whole 2-D space of the core. In addition it was assumed that all the coefficients of Eq.(4.28) are constant in each mesh interval. The quantity f is proportional to the source term S and has different values for various energies under consideration. The source term S appearing in Eq.(4.29f) is determined from fission and scattering processes. It was also assumed that the birth of neutrons occurs at fast energies only and neutrons from lower energies do not scatter to higher energies. This is often referred to as "no upscattering". Furthermore in-group scattering is not allowed. The source term can thus be expressed in the form

$$S_{g'} = \begin{cases} \frac{1}{\lambda} \sum_{g'=1}^{G} \chi_{g'} \left(\nu\Sigma_f\right)_{g'} \phi_{g'} & g'=1 \text{ (fast group)} \\ \\ \sum_{\substack{g'=1 \\ g' \neq g}}^{G} \left(\Sigma_{sg'g} \phi_{g'}\right) & g' < 2 \text{ (thermal group)} \end{cases} \qquad (4.30)$$

The resulting matrix for any point (r_i, z_j) is written in matrix form as

$$A_g \phi_g = \frac{1}{\lambda} B_g + \sum_{\substack{g'=1 \\ g' \neq g}}^{G} C_{sg'g} \phi_{g'} \qquad (4.31)$$

where

$$B_g = \sum_{g'=1}^{G} \chi_{g'} \left(\nu\Sigma_f\right)_{g'} \phi_{g'} \quad , \qquad C_{gg'} = \Sigma_{sg'g}$$

As mentioned earlier in Chapter Two, the present analysis is limited to two-group theory which is the simplest form of multi-group theory to avoid complexity and computational cost. The two-group approximation is often used to illustrate a variety of fuel management concepts [20] which is the main objective in the development of this code. The scattering for the source term for the fast group (g'=1) is neglected in line with our assumption of no upscattering. The source of neutrons for the thermal group (g'=2) is from downscattering of neutrons from fast to thermal energies. For the two-group model, Eq.(4.30) simplifies to

$$S_{g'} = \begin{cases} \frac{1}{\lambda}\left(\chi_1\left(\nu\Sigma_f\right)_1\phi_1 + \chi_2\left(\nu\Sigma_f\right)_2\phi_2\right), & g=1 \\ \Sigma_{sg'g}\phi_{1'}, & g=2 \end{cases} \qquad (4.32)$$

The finite difference approximation to the matrix Eq.(4.31) is written according to two-group theory in the matrix form as

$$\left.\begin{aligned} \mathbf{A}_1\phi_1 &= \frac{1}{\lambda}\left(\mathbf{F}_1\phi_1 + \mathbf{F}_2\phi_2\right) && g=1 \\ \mathbf{A}_2\phi_2 &= \mathbf{H}\phi_1 && g=2 \end{aligned}\right\} \qquad (4.33)$$

where ϕ_1 and ϕ_2 are the fluxes for the fast and thermal neutrons respectively. A_1 and A_2 are matrices representing the finite difference operators and F_1, F_2 and H represent the quantities $\chi_1\left(\nu\Sigma_f\right)_1$, $\chi_2\left(\nu\Sigma_f\right)_2$ and $\Sigma_{s1\to2}$ respectively. The boundary conditions required to satisfy Eq.(4.28) are

$$\left.\begin{aligned} J_{1/2,j} &= 0 \ ; & Y_{i,1/2} &= 0 \\ \phi(r_i,H_e) &= 0 & \phi(R_e,z_j) &= 0 \end{aligned}\right\} \qquad (4.34)$$

where it assumed that the centres of the first interpolation intervals Δr and Δz are at r=0 and z=0 and H_e, R_e represent the respective extrapolated height and radius of the core. The finite difference equation for the 2-D cylindrical symmetric region as written in Eq.(4.26) is solved for $\phi_{i,j}$ values to satisfy the following boundary conditions:

For r-axis:

$$\phi_{0,j} = \phi_{1,j} \ ; \ \phi_{n+1,j} = 0 \qquad (j= 1,2,\ldots,n) \qquad (4.35)$$

For z-axis:

$$\phi_{i,0} = \phi_{i,1} \quad ; \quad \phi_{i,m+1} = 0 \qquad (i,1,2,\ldots,m) \qquad (4.36)$$

The first of each of these above equations are symmetry conditions to the r- and z- axes respectively. The second set are boundary conditions resulting from the fact that the solution vanishes at the external boundary. Using the boundary conditions for Eq.(4.28) yields

$$b_{1,j} = 0, \quad d_{i,1} = 0, \quad a_{n,j} = 0, \quad c_{i,m} = 0 \qquad (4.37)$$

A discussion of the numerical solution of the matrix equation [Eq.(4.33)] is presented in the next section.

4.2 METHOD OF SOLUTION

Two kinds of iterative (inner and outer) schemes are involved in the numerical solution to Eq.(4.33). The matrices A_1 and A_2 are pentadiagonal and direct inversions of them are not practicable.

The Chebyshev polynomial method is used to solve the equation and this is referred to as outer iteration. Each outer iteration requires a solution for the LHS of Eq.(4.33) whenever the right sides are given. This problem is reduced to the solution of the equation written in the form

$$A_g \phi_g = E_g \tag{4.38}$$

where

$$E_g = \frac{1}{\lambda} B_g + \sum_{\substack{g'=1 \\ g' \neq g}}^{G} C_{g'g} \phi_{g'} \tag{4.39}$$

The outer iteration scheme determines the value of the eigenvalue λ. The iterative scheme to solve the inhomogeneous problem is called inner iteration. For this work, the method of successive

approximation (SOR) was used. The solution gives the fluxes for fast and thermal groups of energy. The flow chart of the schemes for solving the 2-D, two-group neutron diffusion equation code KWABEN is illustrated in Fig 4.3.

A discussion of the numerical techniques for the inner iteration scheme for the subroutine SOR [21] is first presented. This will be followed by a discussion on the outer iteration scheme based on the Chebyshev polynomial method.

4.2.1 Inner Iteration - Successive-Over-Relaxation(SOR) Method

The SOR method as mentioned in the preceding section was used to solve the five point finite difference equation [Eq.(4.28)] written without the energy group subscript g in the matrix form

$$A\phi = E \tag{4.40}$$

We can conveniently express the matrix A as

$$A = L + D + U \tag{4.41}$$

where **D** is the diagonal part of **A**, **L** and **U** are the lower and upper diagonals of matrix **A**. respectively.

The Gauss-Seidel method corresponds to the matrix decomposition

$$\left(\mathbf{L} + \mathbf{D}\right)\phi^{(r)} = -\mathbf{U}\phi^{(r-1)} + \mathbf{E} \tag{4.42}$$

The SOR method, which provides a practical algorithm enabling an overcorrection to the value $\phi^{(r)}$ to be made at the r^{th} stage of the Gauss-Seidel iteration is now applied. By addition and subtraction of $\phi^{(r)}$ on the RHS of Eq.(4.42), the equation becomes

$$\phi^{(r)} = \phi^{(r-1)} - \left(\mathbf{L} + \mathbf{D}\right)^{-1}\left[\left(\mathbf{L} + \mathbf{D} + \mathbf{U}\right)\phi^{(r-1)} - \mathbf{E}\right] \tag{4.43}$$

Designating the term in square brackets on the RHS of Eq.(4.43) as $\xi^{(r-1)}$ and calling it the residual vector, Eq.(4.43) reduces to

$$\phi^{(r)} = \phi^{(r-1)} - \left(\mathbf{L} + \mathbf{D}\right)^{-1}\xi^{(r-1)} \tag{4.44}$$

The overcorrection to the value of $\phi^{(r)}$ is

$$\phi^{(r)} = \phi^{(r-1)} - \omega\left(L + D\right)^{-1}\xi^{(r-1)} \qquad (4.45)$$

where ω is called the acceleration parameter.

The problem of prime importance associated with the SOR method is the determination of a suitable value of ω. Essentially, an optimum value ω_b of ω is required which will minimize the spectral radius of the SOR iteration matrix and consequently maximize the rate of convergence of the method. The theory of its determination is placed on firm grounds by Varga [22]. The following observations were made:

(a) the method is convergent only for $0 < \omega < 2$.
If $0 < \omega < 1$, then there is under-relaxation.

(b) under certain mathematical restrictions generally satisfied by matrices from finite differencing, only over-relaxation ($0 < \omega < 2$) can give faster convergence than the Gauss-Seidel method.

(c) the optimum value of ω for maximum convergence rate is given by the relationship [21]

$$\omega_b = \frac{2}{1+\sqrt{1+\rho^2}} \tag{4.46}$$

where ρ is the spectral radius. The boundary conditions as given in Eq.(4.34) is for a homogeneous Neumann boundary condition on an nxm grid (for which $\Delta r = \Delta z$). The spectral radius can be expressed in the form

$$\rho = \frac{\cos\left(\frac{\pi}{n}\right)+\left(\frac{\Delta r}{\Delta z}\right)^2\cos\left(\frac{\pi}{m}\right)}{1+\left(\frac{\Delta r}{\Delta z}\right)^2} \tag{4.47}$$

Solving Eq.(4.28) for $\phi_{i,j}$. yields the expression

$$\phi^*_{i,j} = \frac{1}{e_{i,j}}\left[f_{i,j} - a_{i,j}\phi_{i+1,j} - b_{i,j}\phi_{i-1,j} - c_{i,j}\phi_{i,j+1} - d_{i,j}\phi_{i,j-1}\right] \tag{4.48}$$

The new weighted value $\phi^{new}_{i,j}$ is

$$\phi^{new}_{i,j} = \omega\phi^*_{i,j} + \left(1-\omega_b\right)\phi^{old}_{i,j} \tag{4.49}$$

The residual at any stage becomes

$$\xi_{i,j} = a_{i,j}\phi_{i+1,j} + b_{i,j}\phi_{i-1,j} + c_{i,j}\phi_{i,j+1} + d_{i,j}\phi_{i,j-1}$$

$$+ e_{i,j}\phi_{i,j} - f_{i,j} \qquad (4.50)$$

The SOR algorithm presented in Eq.(4.44) or Eq.(4.49) is

$$\phi_{i,j}^{new} = \phi_{i,j}^{old} - \omega_b \frac{\xi_{i,j}}{e_{i,j}} \qquad (4.51)$$

This formulation can now be programmed and the norm of the residual vector $\xi_{i,j}$ is used as a criterion for terminating the iteration. The KWABEN code invoked the subroutine SOR and required ω_b of value 1.5. Convergence was achieved for a maximum of fifty-five iterations.

4.2.2 Outer Iteration - Chebyshev Polynomial Method

This section describes the method used for accelerating iterative convergence of eigenvalue problems. The Chebyshev polynomial method is used to obtain the best linear combination when there is no knowledge of higher eigenvalues. The description presented below attempts to explain the techniques applied in the subroutine CHEBY which forms part of the computational flow chart of Fig 4.3.

The outer iteration procedure to calculate λ using Eq.(4.33) can be expressed in the matrix notation

$$\begin{bmatrix} \phi_1^{(t)} \\ \phi_2^{(t)} \end{bmatrix} = \frac{1}{\lambda^{(t-1)}} \begin{bmatrix} A_1 & 0 \\ -H & A_2 \end{bmatrix} \begin{bmatrix} F_1 & F_2 \\ 0 & A_2 \end{bmatrix} \begin{bmatrix} \phi_1^{(t-1)} \\ \phi_2^{(t-1)} \end{bmatrix} \qquad (4.52)$$

Defining

$$Y = F_1\phi_1 + F_2\phi_2 \qquad (4.53)$$

ϕ_1 and ϕ_2 may then be expressed respectively as

$$\phi_1 = \frac{1}{\lambda} A_1^{-1} y \tag{4.54}$$

$$\phi_2 = \frac{1}{\lambda} A_2^{-1} H A_1^{-1} y \tag{4.55}$$

Substitution of Eqs.(4.54) and (4.55) into Eq.(4.53) gives

$$y = \frac{1}{\lambda} Sy \tag{4.56}$$

where

$$S = F_1 A_1^{-1} + F_2 A_2^{-1} H A_1^{-1} \tag{4.57}$$

The iterative solution given by Eq.(4.52) may be written as

$$y^{(t)} = k^{(t)} Sy^{(t+1)} \tag{4.58}$$

where

$$k^{(t)} = \frac{1}{\lambda^{(t)}} \tag{4.59}$$

The effective multiplication factor $k^{(t)}$ is calculated using the expression

$$k^{(t)} = \frac{< w, Sy^{(t-1)} >}{< w, y^{(t-1)} >} \qquad (4.60)$$

where w is the weighting factor and its selection is arbitrary.

The Chebyshev polynomial method is now applied to accelerate the iterative convergence [Eq.(4.58)] for the eventual determination of k .The basic technique applied in most convergent acceleration methods is to replace the vector $\phi^{(t)}$ with some linear combination of $\phi^{(t)}$ and the previous iterates $\phi^{(t-1)}$, $\phi^{(t-2)}$, etc. If $\phi^{(t)}$ is replaced with a linear combination of only two previous iterates, then the scheme can be written as

$$S\phi^{(t)} = k^{(t)}\phi^{*(t-1)} \qquad (4.61)$$

and

$$\phi^{(t+1)} = \left(1 + \theta^{(t)}\right)\phi^{(t+1)} - \theta^{(t)}\phi^{(t)} \qquad (4.62)$$

In particular, it is desired to choose the optimum set of θs to maximize the rate of convergence of the iterative process. Combining Eqs.(4.61) and (4.62) gives

$$\phi^{(t+1)} = \left[\left(1 + \theta^{(t)} \right) \frac{S}{k^{(t)}} - \theta^{(t)} I \right] \tag{4.63}$$

where I is the unit matrix. Eq.(4.63) may be simply re-written as

$$\phi^{(t+1)} = R_t \phi^{(t)} \tag{4.64}$$

The equation below can be deduced from Eq.(4.64) as

$$\phi^{(t+1)} = R_t R_{t-1} \cdots R_0 \phi^{(0)} \tag{4.65}$$

where $\phi^{(0)}$ is the initial guess for ϕ. The eigenvalues of the matrix S is denoted by $\sigma_m < \sigma_{m-1} < \ldots < \sigma_1$ with the assumption that the values of the matrix are real and positive. If the eigenvectors associated with σ_q are represented by μ_q and they form a complete set for the vector space of U, then the initial flux guess can be represented in terms of these eigenvectors as

$$\phi^{(0)} = \sum_{q=1}^{m} c_q \beta_q \tag{4.66}$$

Writing

$$R_j \beta_q = \left[\frac{1 + \theta^{(j)}}{k^{(j)}} \right] S\beta_q - \theta^{(j)} \beta_q \tag{4.67}$$

and substituting Eq.(4.66) into Eq.(4.67) gives

$$\phi^{(n)} = \prod_{j=0}^{n-1} R_j \sum_{q=1}^{m} c_q \beta_q \tag{4.68}$$

or

$$\phi^{(n)} = \sum_{q=1}^{m} c_q \prod_{j=0}^{n-1} \left[\frac{1 + \theta^{(j)}}{k^{(j)}} \sigma_q - \theta^{(j)} \right] \tag{4.69}$$

An attempt to converge on the largest eigenvalue σ_1, and its associated eigenvector β_1 now has to be made. Eq.(4.69) can be rewritten in the form

$$\phi^{(n)} = \prod_{j=0}^{n-1}\left(\frac{1+\theta^{(j)}}{k^{(j)}}\sigma_1 - \theta^{(j)}\right)\left\{c_1\beta_1 + \sum_{q=2}^{m} c_q \prod_{j=0}^{n-1}\left(\frac{c_q - \frac{k^{(j)}\theta^{(j)}}{1+\theta^{(j)}}}{\sigma_1 - \frac{k^{(j)}\theta^{(j)}}{1+\theta^{(j)}}}\right)\beta_q\right\} \tag{4.70}$$

$$= w_n\left[c_1\beta_1 + \sum_{q=2}^{m} c_k z_n\left(\theta,\sigma_q\right)\beta_q\right] \tag{4.71}$$

where

$$w_n = \prod_{j=0}^{n-1}\left(\frac{1+\theta^{(j)}}{k^{(j)}}\sigma_1 - \theta^{(j)}\right) \tag{4.72}$$

and

$$z_n(\theta,\sigma_q) = \prod_{j=0}^{n-1} \left(\frac{\sigma_q - \dfrac{k^{(j)}\theta^{(j)}}{1+\theta^{(j)}}}{\sigma_1 - \dfrac{k^{(j)}\theta^{(j)}}{1+\theta^{(j)}}} \right) \qquad (4.73)$$

Indeed, Eq.(4.71) provides a criterion for the determination of an optimum set of extrapolated parameters $\theta^{(j)}$. The objective now is to determine $\theta^{(j)}$ so that the maximum rate of convergence is achieved. This is accomplished by choosing $\theta^{(j)}$ so that the expression in the bracket of Eq.(4.71) is minimized. A selection of $\theta^{(j)}$ means the function w_n is constant and consequently absorbed into c_1. This leaves the function $z_n(\theta,\sigma_q)$ to be minimized. By minimizing $z_n(\theta,\sigma_q)$, q = 2,3,..,m, in effect also minimizes the contributions of all other eigenvectors β_q, q = 2,3,...,m, with respect to the desired β_1.

The function $z_n(\theta,\sigma_q)$ is a polynomial of degree n in σ_q. Hence we can write

$$z_n(\theta,\sigma_q) = 1 \qquad (4.74)$$

Our task is to make $|z_n(\theta,\sigma_q|$ as small as possible such that

$$\max_{q} \left| z_n(\theta,\sigma_q) \right| \leq \max_{\sigma_m \leq \sigma \leq \sigma_2} \left| z_n(\theta,\sigma_q) \right| . \qquad (4.75)$$

It is more convenient to transfer σ to μ [22] as

$$\mu = \frac{2\sigma}{\sigma_2 - \sigma_m} - \frac{\sigma_2 + \sigma_m}{\sigma_2 - \sigma_m} \qquad (4.76)$$

Eq.(4.76) transforms the interval $[\sigma_m,\sigma_2]$ into $[-1,1]$. Defining

$$v_n(\theta,\mu) = z_n(\theta,\sigma) \qquad (4.77)$$

a polynomial is sought which minimizes

$$\max_{-1 \leq \mu \leq 1} \left| v_n(\theta,\mu) \right| \qquad (4.78)$$

subject to $v_n(\theta,\mu) = 1$

According to the theorem of Flanders and Shortley [23], among all polynomials of degree m in μ having the value +1 at $\mu>1$, there is only one value with the minimum absolute throughout the

interval [-1,1], namely the polynomial

$$w_n(\mu) = \frac{T_m(\mu)}{T_m(\mu_1)} \tag{4.79}$$

where $T_m(\mu)$ is the mth order Chebyshev polynomial obtained by expanding in powers of μ given as

$$T_m(\mu) = \cos(m\cos^{-1}\mu) \tag{4.80}$$

In order to make

$$v_n(\theta,\mu) = \frac{T_m(\mu)}{T_m(\mu_1)} \tag{4.81}$$

the zeros of each polynomial have to be equated since they both have similar values at $\mu = \mu_1$. Using Eq.(4.80) the zeros of $T_m(\mu)$ are

$$\mu_l = \frac{\cos(2l+1)\pi}{2n}, \qquad l = 0,\ldots,n-1 \tag{4.82}$$

Clearly the zeros of $v_n(\theta,\mu)$ are those of $z_n(\theta,\sigma)$ which can be translated using Eq.(4.76) to give the expression

$$\mu_l = \frac{2}{\sigma_2 - \sigma_m}\left[\frac{k^{(l)}\theta^{(l)}}{1+\theta^{(l)}}\right] - \frac{\sigma_2 + \sigma_m}{\sigma_2 - \sigma_m} \qquad l = 1,\ldots n-1 \qquad (4.83)$$

Equating Eq.(4.82) to Eq.(4.83) gives

$$\theta^{l}_{(n)} = \frac{1 + \left[\frac{\sigma_2 - \sigma_m}{\sigma_2 + \sigma_m}\right]\cos\left[\frac{(2l+1)\pi}{2n}\right]}{\frac{2k^{(l)}}{(\sigma_2 + \sigma_m)} - 1 - \left[\frac{\sigma_2 - \sigma_m}{\sigma_2 + \sigma_m}\right]\cos\left[\frac{(2l+1)\pi}{2n}\right]} \qquad (4.84)$$

for $l = 0,1,\ldots,n-1$. The sequence of θs provides the best possible result as discussed earlier. In order to apply the result of Eq.(4.84), it is essential that the values of the eigenvalues σ_2 and σ_m be known in advance. However, these are not known and more approximations are required. The first and most important assumption is that the smallest eigenvalue σ_m which was previously assumed to be positive, may be ignored in comparison to σ_2. Therefore Eq.(4.84) simplifies to the form

$$\theta_{(n)}^{(l)} = \frac{1 + \cos\left[\frac{(2l+1)\pi}{2n}\right]}{\frac{2k^{(l)}}{\sigma_2} - 1 - \cos\left[\frac{(2l+1)\pi}{2n}\right]} \qquad (4.85)$$

An estimate for either σ_2 or the ratio $k^{(l)}/\sigma_2$ will have to be made. In particular, since at iteration l, $k^{(l)}$ is the best estimate for σ_1, the largest eigenvalue, this means that the ratio σ_1/σ_2 is actually being sought. Defining

$$\bar{\sigma} = \max_{i=1} \left|\frac{\sigma_i}{\sigma_1}\right| = \frac{\sigma_2}{\sigma_1} \qquad (4.86)$$

$\theta^{(l)}$ can now be computed from

$$\theta_{(n)}^{(l)} = \frac{\bar{\sigma}\, c_l(n)}{2 - \bar{\sigma} c_l(n)} \qquad (4.47)$$

where

$$c_l(n) = 1 + \cos\frac{2l+1}{2n} \qquad (4.88)$$

The parameter $\bar{\sigma}$ in Eq.(4.86) is called the dominance ratio since it provides an idea of the separation between the largest eigenvalue and the second largest. Details of the theory for obtaining initial and updated estimates for $\bar{\sigma}$ are available in ref [23].

The quantity $1/T_n(\mu_1)$ in Eq.(4.81) is the maximum of $|h_n(\mu)|$ in the interval [-1,1] and it is a measure of the reduction of the coefficients of all eigenvectors with eigenvalues in the range σ_m to σ_2, relative to β_1 as represented in Eq.(4.71). Using Eq.(4.76), the equation below is obtained.

$$\mu_1 = \mu(\sigma_1) = \frac{2\sigma_1}{\sigma_2 - \sigma_m} - \frac{\sigma_2 + \sigma_m}{\sigma_2 - \sigma_m} \tag{4.89}$$

By following the same assumption leading to Eq.(4.85) that σ_m may be neglected in comparison to σ_2, Eq.(4.89) is simplified to

$$\mu_1 = \frac{2\sigma_1}{\sigma_2} - 1 \tag{4.90}$$

Consider now the quantity

$$\frac{\varepsilon(l)}{T_n \frac{2}{\bar{\sigma}} - 1} \tag{4.91}$$

where

$$\varepsilon(l) = \frac{\bar{k}(l) - \underline{k}(l)}{k(l)}$$

to determine what degree of the Chebyshev polynomial will most likely reduce the eigenvalue or $\varepsilon(l)$ to an acceptable value. This means n is required such that

$$\frac{\varepsilon(l)}{T_n \frac{2}{\sigma} - 1} < \varepsilon_1 \qquad (4.92)$$

where ε_1 is the input convergence criterion.

In practice, a cycle of n iterations using a sequence of θs given by Eq.(4.87) will have to be performed for $l = 0,1,\ldots,n-1$. In case convergence has not been achieved, a new set of n is found based on the inequality in Eq.(4.92) and another cycle of n iterations is followed. This procedure is repeated until the iteration converges to the criterion

$$\frac{\left| \phi_n^{i(l)} - \phi_n{}^{i(l)} \right|}{\phi_n^{i(l)}} \qquad \begin{matrix} i = 1,2,\ldots, I \\ n = 1,2,\ldots, N \end{matrix} \qquad (4.93)$$

for two successive iterations. Fig 4.3 illustrates the computational flow chart for the subprogram CHEBY.

4.3 NORMALIZATION OF SOURCES AND FLUXES

The subroutine ACTS is written to form part of the KWABEN code to compute and print the average flux in each homogeneous zone of the reactor.The average of the region *l* and the group g is defined by

$$\bar{\phi}_{g,l} = \frac{\int_0^{R_l} \phi_g(r)\, dV_l^{\alpha}}{\int_0^{R_l} dV_l^{\alpha}} \qquad (4.94)$$

where dV_l^{α} is the volume elements expressed in the form

$$dV_l^{\alpha} = \begin{cases} 1 & \alpha = 0 \text{ (slab)} \\ 2\pi r_l & \alpha = 1 \text{ (cylinder)} \\ 4\pi r_l & \alpha = 2 \text{ (sphere)} \end{cases} \qquad (4.95)$$

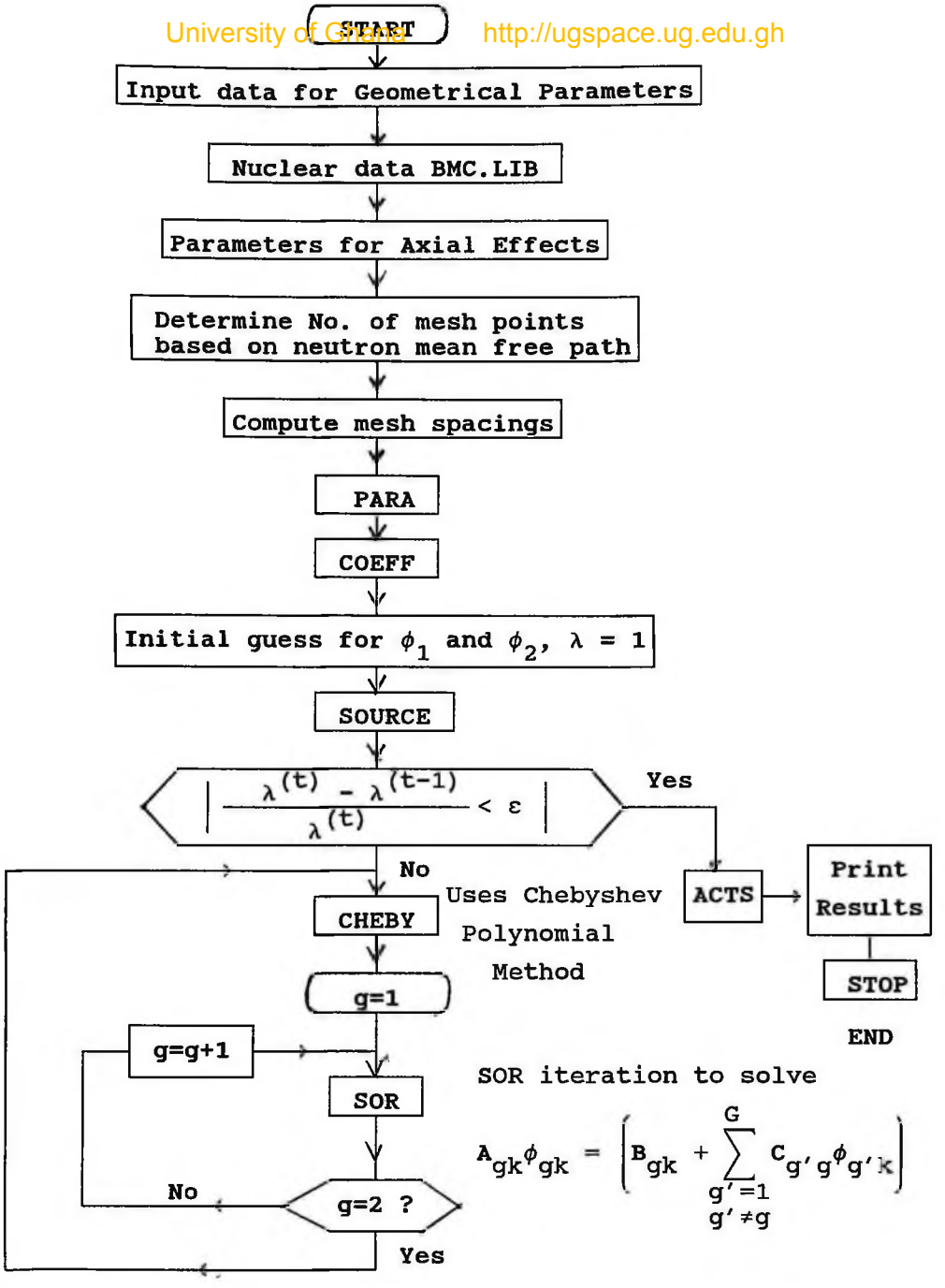

Fig 4.3: Computational Flow Chart for KWABEN.

Designating

$$y(r) = \sum_{g=1}^{G} \nu_g \Sigma_{fg}(r) \phi_g(r)$$

the normalized source is then defined by the expression

$$s(r) = \frac{y(r)}{\int_0^{R_l} y(r) dV_l^{\alpha}} \qquad (4.96)$$

The integral term for any zone l can now be approximated. The denominator of Eq.(4.96) is

$$\int_{r_{1,l}}^{r_{2,l}} y(r) dV_l^{\alpha} = c_{\alpha} \int_{r_{1,l}}^{r_{2,l}} r_l^{\alpha} y(r) dr \qquad (4.97)$$

$$= c_{\alpha} \left[\frac{h}{2!} \left(r_1^{\alpha} y_1 + r_2^{\alpha} y_2 \right) + \frac{h}{3!} \alpha \left(r_1^{\alpha-1} y_1 - r_2^{\alpha-1} y_2 \right) + \frac{h}{4!} \alpha(\alpha-1) \left(r_1^{\alpha-2} y_1 - r_2^{\alpha-2} y_2 \right) \right.$$

where

$$Y_j = y(r_k) \text{ and } r_{2,l} = r_{1,l} + h \tag{4.98}$$

The evaluation of Eq.(4.98) provides the normalized sources for individual rings of the reactor. The neutron flux shall now be normalized to a given level. The total power produced within the core of the reactor is defined as

$$p_\phi = \zeta \int_{V_R} \sum_{g=1}^{G} \phi_g(r) \Sigma_{fg'}(r) dV_l^\alpha \tag{4.99}$$

where $\zeta = 3.2 \times 10^{-11}$ Watts-s per fission and V_R is the volume of the reactor. The integrals of the flux in each ring of the reactor can be related to the average flux of the region. Thus

$$p_\phi = \zeta \sum_{g=1}^{G} \sum_{l=1}^{L} \Sigma_{fg,l} \, \bar{\phi}_{g,l} \, \Delta V_l^\alpha \tag{4.100}$$

where ΔV_l^α, the volume element corresponding to the geometry of the reactor is defined as

$$\Delta V_l^{\alpha} = \begin{cases} \left(r_{l+1} - r_l\right) HL & \text{for } \alpha = 0 \text{ (slab)} \\ \pi\left(r_{l+1}^2 - r_l^2\right) H & \text{for } \alpha = 1 \text{ (cylinder)} \\ \frac{4}{3}\pi\left(r_{l+1}^3 - r_l^3\right) & \text{for } \alpha = 2 \text{ (sphere)} \end{cases}$$

H and L are the transverse dimensions of the slab. H is the height of the cylinder. Assuming the solution of the matrix Eq.(4.38) provides values for the fluxes $\bar{\phi}_{g,k}$, a constant ψ must be obtained such that

$$\bar{\phi}_{g,k} = \psi \bar{\phi}_{g,k} \tag{4.101}$$

yields the desired power level

$$\psi = \frac{P}{\zeta \sum_{g=1}^{G} \sum_{l=1}^{L} \phi_{g,l} \Delta V_l^{\alpha} \Sigma_{fg,l}} = \frac{P}{P_{\phi}} \tag{4.102}$$

The subroutine ACTS which computes the normalized sources and fluxes for all regions is shown in Fig 4.3.

4.4 INPUT DESCRIPTION

Besides the geometry and material composition, the following two-group data are important to start the reactor calculations:

(i) the macroscopic group constants, bucklings, fractions and number of neutrons produced per fission for every homogeneous zone of the reactor. These cross-sections were obtained at a selected reference level (middle of the core). These are contained in the **BMC.LIB** file.

(ii) corrections due to axial effects of the temperatures in the fuel, cladding and coolant, and fluid density variations. These terms are listed in **AXIS.INP**.

The description of the files are as follows:

(a) File **BMC.LIB**

The specification of the geometry and conditions required for the solution of the two-group, 2-D neutron diffusion equation are given in the first part of the input data. In the second part are written the two-group macroscopic cross-section data for all thirteen zones along the radius of the core obtained at the reference position (middle of the core) for nominal power at 27kW. The third part consists of the coefficients of the polynomial

equation depicting the changes of the macroscopic cross-sections due to fuel burnup. The WIMSPC code, a PC version of the lattice code WIMS was used to generate two-group macroscopic constants $\left(D_1,,\ D_2,\ \Sigma_{a1},\ \Sigma_{a2},\ \nu_1\Sigma_{f1},\ \nu_2\Sigma_{f2}\right.$ and $\left.\Sigma_{s1\to2}\right)$ for the prototype MNSR. Details of the method of preparation of input data were presented in Chapter Three.

All input data were written in the prescribed order and format as shown below:

Card No.	Format	Parameter	Mathematical symbol	Description
1	3i3	ig, ng, nrl	α, G, L	α = geometry parameter G = total energy group L = total number of radial zones
2	2f10.5	power,h_c	p, H	p = operating reactor power H = height of core(cm)
3	f11.5	tau	τ	burnup value (MWd/tU)
4	nrl(e10.3)	delr	$R_{l+1} - R_l$	interval between rings (cm)
5	,,	dcl0(kg,*l*)	$D_{g,l}$	diffusion constant for zone *l* (cm^{-1})

Card No.	Format	Parameter	Mathematical Symbol	Description
6	''	siga*l*0(kg,*l*)	$\Sigma_{ag,l}$	macroscopic absorption cross-section for zone *l* and group g (cm-1)
7	''	sigf*l*0(kh*l*)	$\nu_g\Sigma_{fg,l}$	macroscopic fission cross-section for zone *l* and group (cm-1)
8	''	sigs*l*0(kg,*l*)	$\Sigma_{sgg',l}$	macroscopic scattering cross-section for zone *l* and group g (cm-1)
9	''	sp*l*(kg,*l*)	$\Sigma_{pg,l}$	macroscopic poison cross-section for zone zone *l* and group g
10	''	bu*l*(kg,*l*)	$B_{g,l}$	transverse buckling for zone *l* and group g (cm^2)
11	''	chi*l*(kg,*l*)	$\chi_{g,l}$	neutron fission fraction for zone *l* aand group g
12	''	snu*l*(kg,*l*)	$\nu_{g,l}$	number of neutrons per fission

This is followed by the information on burnup. Data for the polynomial equation as shown below

$$b^{xg}(\tau) = \sum_{n=1}^{2} b_n^{xg}\tau^n = b_1^{xg}\tau + b_2^{xg}\tau^2 \qquad (4.103)$$

are read from **BMC.LIB** through a single DO loop:

```
      do * kg 1,ng
      read(*,*) db1(kg), abs1(kg), sfb1(kg), scb1(kg)
      read(*,*) db2(kg), abs2(kg), sfb2(kg), scb2(kg)
**    format(4e10.3)
*     continue
```

where db1(kg), abs1(kg), sfb1(kg) scb1(kg) are coefficients b_1 for the energy group g for diffusion constant, macroscopic absorption cross-section, fission and scattering respectively and b_2 are values for the various cross-sections in the same order.

(b) File **AXIS.INP**

This is the library file containing coefficients obtained for the polynomial equation representing axial effects caused by variations in coolant density, fuel temperatures along the axis of the flow channel from the reference position. The relevant equation derived as shown in Chapter Three is of the form

$$a_l^{xg}(z) = \sum_{n=0}^{2} a_{l,n}^{xg} z^n = a_{l,0}^{xg} + a_{l,1}^{xg} z + a_{l,2}^{xg} z^2 \qquad (4.104)$$

In this case, the coefficients $a_{l,0}^{xg}$, $a_{l,1}^{xg}$ and $a_{l,2}^{xg}$ are read for every zone l and energy group g following the order: diffusion constant, macroscopic absorption cross-section, fission and scattering. The data in the file are written on the next page in the following order:

Card No.	Format	Parameter	Mathematical Symbol	Description
1	nr*l*(e10.3)	ad0(kg,*l*)	$a^{xg}_{l,0}$	coefficients for diffusion constant for zone *l* and group g
2	"	ad1(kg,*l*)	$a^{xg}_{l,1}$	
3	"	ad2(kg,*l*)	$a^{xg}_{l,2}$	
4	"	ab0(kg,*l*)	$a^{xg}_{l,0}$	coefficients for macroscopic absorption cross-section for zone *l* and group g
5	"	ab1(kg,*l*)	$a^{xg}_{l,1}$	
6	"	ab2(kg,*l*)	$a^{xg}_{l,2}$	
7	"	af0(kg,*l*)	$a^{xg}_{l,0}$	coefficients for macroscopic fission cross-section for zone *l* and group g
8	"	af1(kg,*l*)	$a^{xg}_{l,1}$	
9	"	af2(kg,*l*)	$a^{xg}_{l,2}$	
10	"	as0(kg,*l*)	$a^{xg}_{l,0}$	coefficients for macroscopic scattering cross-section zone *l* and group g
11	"	as1(kg,*l*)	$a^{xg}_{l,1}$	
12	"	as2(kg,*l*)	$a^{xg}_{l,2}$	

4.5 OUTPUT DESCRIPTION

The output of the program KWABEN is contained in the KWABEN-OUT file written on UNIT 3. The code first prints the name of the code "KWABEN" and the establishment of the authors and a summary of the input data including the macroscopic cross-sections at the reference position along the radius of the core. The next part of the output is for each stage of the iteration: the iteration number and the eigenvalue λ.

After the convergence of the outer iterations, the converged value of k_{eff} is printed. The normalized fluxes of each mesh point for the two-energy groups (fast and thermal) at the specified power level are also printed. Finally, the normalized flux values for each homogeneous zone and each group are printed.

4.6 RESULTS AND DISCUSSION

In general, the development of computer codes for reactor analysis is an interesting, albeit difficult and time costly exercise. Computer codes such as KWABEN which are intended for the purposes of multigroup, two-dimensional reactor physics calculations and analysis demand a lot of time and effort. Considering this fact and coupled with the time constraint set for the presentation of this thesis, the KWABEN diffusion code could not be

fully developed to its final stage at the time of submitting this thesis. However, the code in its present form could be used in the prediction of fast and thermal fluxes along the radius of the reactor core. The computational flow chart for the KWABEN code is shown in Fig 4.3. Illustrated in Fig 4.4 is the computational model used for the present analysis. After its completion, it is expected that it will solve the two-group neutron fluxes in both radial and axial directions of the core. The known fluxes will then be used to generate the eigenvalues leading to the condition of criticality for the core.

The code could also be used to study the effect of nuclides on the multiplication factor and for the determination of the worth of the top Be shim plates added to compensate for fuel depletion. Preliminary calculations however, were carried out with the code and the computed zone average fluxes at 20 kW in the radial directions are listed below in Tables 4.1 and 4.2 for both fast and thermal groups. The plot of the fluxes can be seen in Fig 4.5. The average thermal flux in the region of the annular reflector where the inner irradiation sites are located was determined to be 7.777000E+10^{11}n/cm^2-s which compares favourably with the value of 7.688000E+10^{11}n/cm^2-s reported in ref [24].

As stated earlier, the development of the code is still in progress and the final form will be helpful in verifying experimental measurements such as relative flux distribution in the axial direction, effective multiplication factor and the worth of the Be shims in the Al tray.

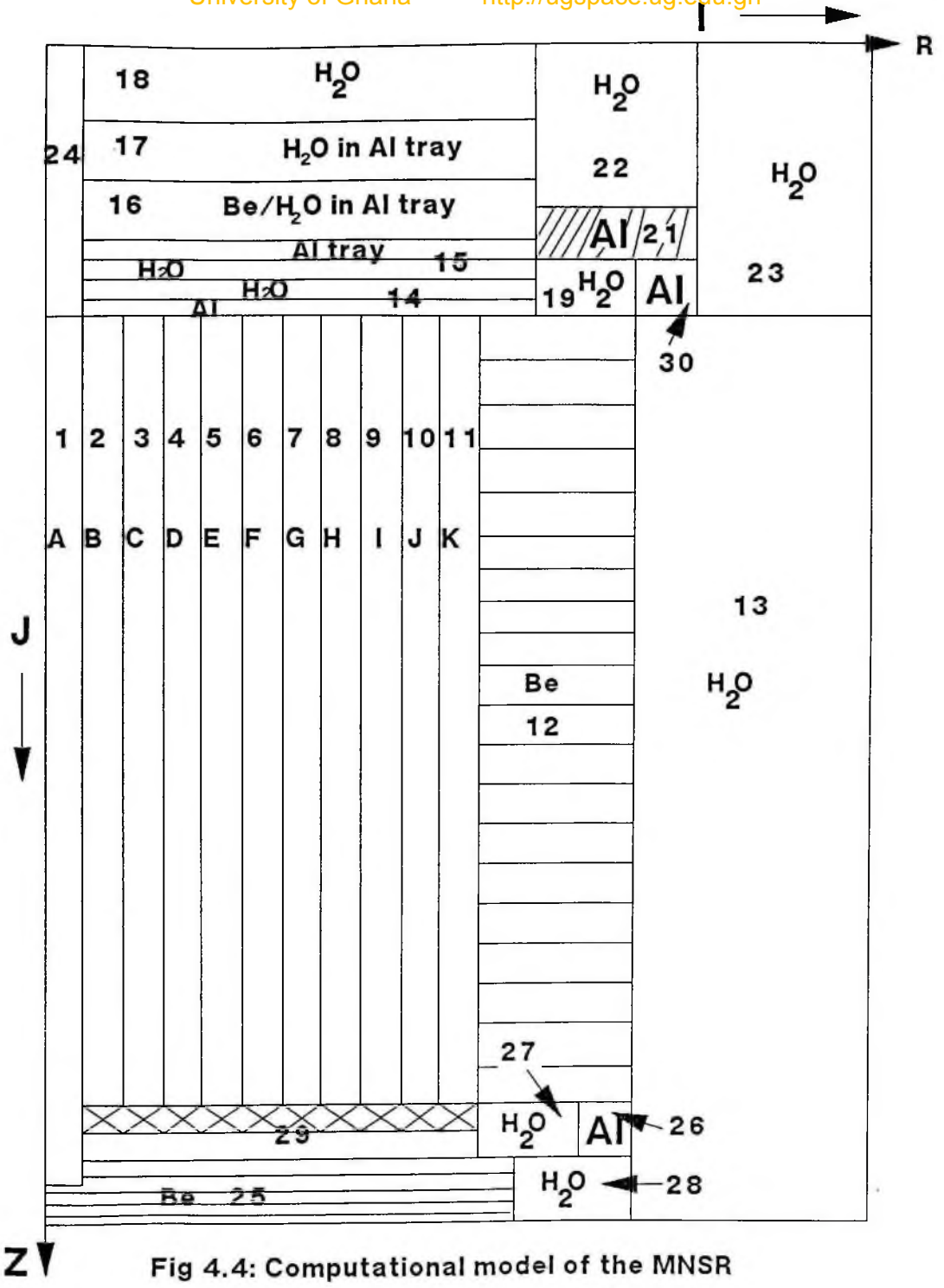

Fig 4.4: Computational model of the MNSR

Energy Group No	Zone No	Radius (cm)	Neutron Flux (n/cm^2 -s)
1	1	5.893000E-01	2.196517E+12
1	2	1.585300E+00	8.208591E+11
1	3	2.581300E+00	3.126535E+11
1	4	3.577300E+00	1.411125E+11
1	5	4.573300E+00	7.312678E+10
1	6	5.569300E+00	4.586392E+10
1	7	6.565300E+00	2.925973E+10
1	8	7.561299E+00	1.585588E+10
1	9	8.557300E+00	8.542776E+09
1	10	9.553300E+00	7.018482E+09
1	11	10.349300E+00	5.501925E+09
1	12	20.549300E+00	4.242780E+08
1	13	34.799300E+00	6.134543E+00

Table 4.1: Computed zone average fluxes at 20kW for radial direction (fast group)

Energy Group No	Zone No	Radius (cm)	Neutron Flux (n/cm^2-s)
2	1	5.893000E-01	2.086245E+11
2	2	1.585300E+00	9.858476E+10
2	3	2.581300E+00	5.163733E+10
2	4	3.577300E+00	3.316888E+10
2	5	4.573300E+00	2.462278E+10
2	6	5.569300E+00	2.005640E+10
2	7	6.565300E+00	1.740958E+10
2	8	7.561299E+00	1.650480E+10
2	9	8.557300E+00	1.542763E+10
2	10	9.553300E+00	1.435605E+10
2	11	10.349300E+00	1.315503E+10
2	12	20.549300E+00	7.777000E+11
2	13	34.799300E+00	7.661966E+10

Table 4.2: Computed zone average fluxes at 20kW for radial direction (thermal group)

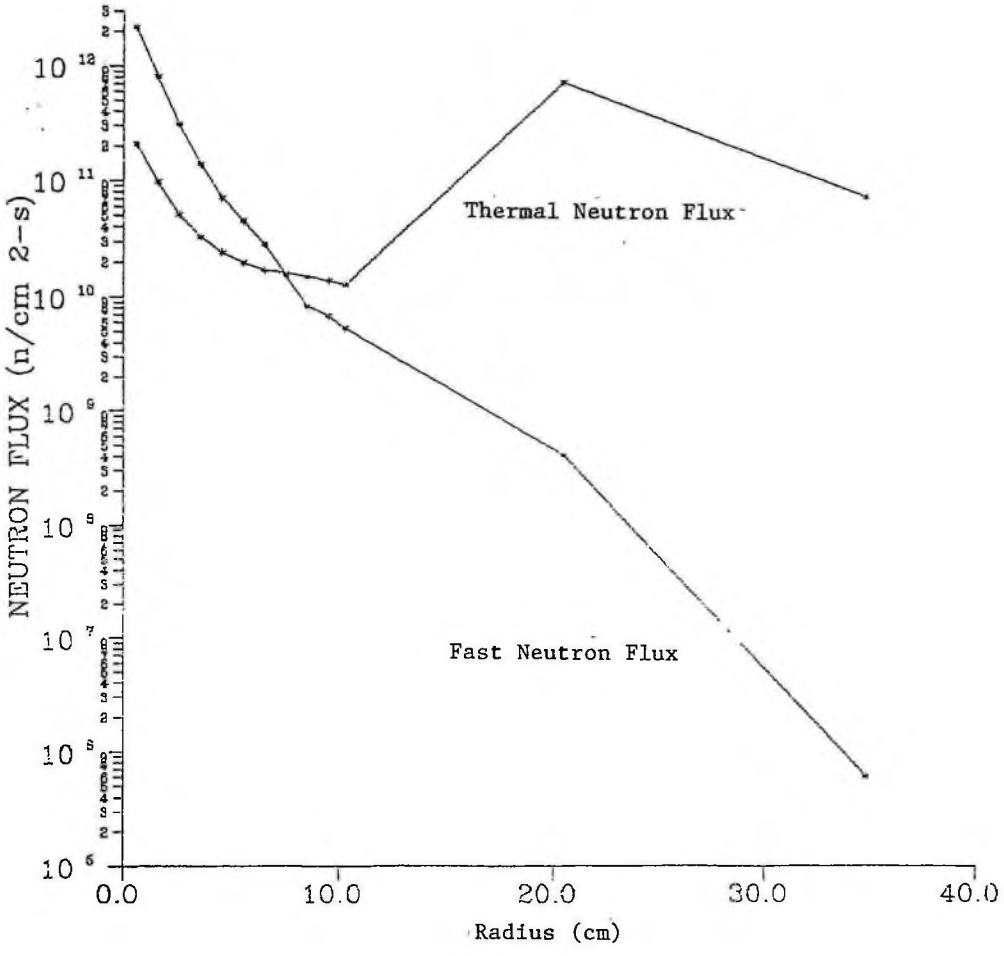

Fig 4.5: Neutron Flux Variation Along Radial Direction

CHAPTER FIVE

CONCLUSIONS AND RECOMMENDATIONS

The literature on the fundamental principles of nuclear reactor theory, numerical methods used for solving the diffusion equation as related to nuclear reactor systems was reviewed in Chapter Two. Geometrical features of the Miniature Neutron Source Reactor were also presented in this chapter. The results of this study were given in Chapters Three and Four. It will suffice to present a short summary here of the main findings.

For neutronic calculations for the reactor, a two-dimensional two-group data base was created. An appropriate computational model was developed taking into account all known parameters such as fuel burnup, U-238 temperature, Xe effect, etc, which influence group constants. The model was used to determine group constants that are in good agreement with those calculated using the WIMS lattice code. A diffusion code KWABEN, based on the finite difference scheme is being developed to solve the two-dimensional neutron diffusion equation for fast and thermal neutron fluxes for any point in the reactor system. The numerical methods and techniques applied in KWABEN are discussed.

The KWABEN diffusion code in its present form is capable of predicting fast and thermal neutron fluxes along the radial direction of the core. However, due to the relatively short time

available to this research work and coupled with the fact that the development of complete computer codes for nuclear reactor analysis are often tedious and time consuming, the code could not be fully completed within the alloted time.

It is recommended that further work be done towards the completion of the KWABEN code. It would be of great interest to test the final form of the code for the following:

(1) Solution of the two-group neutron fluxes in both radial and axial directions for absolute and relative fluxes within any region of the reactor.

(2) Determination of eigenvalues and effective multiplication factor for the critical system.

(3) Calculation of the worth of the thickness of the top Be shim reflector in the Al tray used for compensation of the loss of U-235 during fuel depletion.

```
1.002E+00 1.469E+00 1.572E+00 1.635E+00 1.667E+00 1.674E+00 1.688E+00
1.643E+00 1.639E+00 1.562E+00 1.333E+00 6.220E-01 3.075E-01 0.000E+00 D
9.571E-02 1.533E-01 1.655E-01 1.750E-01 1.804E-01 1.811E-01 1.888E-01
1.801E-01 1.963E-01 1.855E-01 1.575E-01 4.093E-01 9.569E-02 0.000E+00 D
4.797E-03 2.029E-02 2.083E-02 2.115E-02 2.114E-02 2.076E-02 2.219E-02
2.141E-02 2.246E-02 2.666E-02 2.114E-02-8.204E-05 1.495E-02 0.000E+00 Sa
2.906E-02 1.305E-01 1.518E-01 1.685E-01 1.779E-01 1.790E-01 1.925E-01
1.774E-01 1.752E-01 1.868E-01 1.158E-01 2.017E-03 2.907E-02 0.000E+00 Sa
3.298E-02 3.298E-02 3.503E-02 3.626E-02 3.657E-02 3.595E-02 3.883E-02
3.700E-02 3.860E-02 4.644E-02 3.310E-02 0.000E-00 0.000E-00 0.000E-00 S1
2.089E-02 2.089E-01 2.527E-01 2.871E-01 3.065E-02 3.087E-01 3.365E-01
3.054E-01 3.000E-01 3.249E-01 1.780E-01 0.000E+00 0.000E+00 0.000E+00 S1
5.449E-04 5.358E-03 8.579E-03 1.156E-02 1.427E-02 1.672E-02 1.942E-02
2.388E-02 2.720E-02 3.592E-02 5.777E-02 1.450E-02 1.598E-01 0.000E+00 Sc
0.000E+00 0.000E+00 0.000E+00 0.000E+00 0.000E+00 0.000E+00 0.000E+00
0.000E+00 0.000E+00 0.000E+00 0.000E+00 0.000E+00 0.000E+00 0.000E+00 Sc
0.000E+00 0.000E+00 0.000E+00 0.000E+00 0.000E+00 0.000E+00 0.000E+00
0.000E+00 0.000E+00 0.000E+00 0.000E+00 0.000E+00 0.000E+00 0.000E+00 Sp
0.000E+00 0.000E+00 0.000E+00 0.000E+00 0.000E+00 0.000E+00 0.000E+00
0.000E+00 0.000E+00 0.000E+00 0.000E+00 0.000E+00 0.000E+00 0.000E+00 Sp
1.139E-02 1.139E-02 1.139E-02 1.139E-02 1.139E-02 1.139E-02 1.139E-02
1.139E-02 1.139E-02 1.139E-02 1.139E-02 1.139E-02 1.139E-02 1.139E-02 B1
1.117E-02 1.117E-02 1.117E-02 1.117E-02 1.117E-02 1.117E-02 1.117E-02
1.117E-02 1.117E-02 1.117E-02 1.117E-02 1.117E-02 1.117E-02 1.117E-02 B2
1.000E+00 1.000E+00 1.000E+00 1.000E+00 1.000E+00 1.000E+00 1.000E+00
1.000E+00 1.000E+00 1.000E+00 1.000E+00 1.000E+00 1.000E+00 0.000E+00 K1
0.000E+00 0.000E+00 0.000E+00 0.000E+00 0.000E+00 0.000E+00 0.000E+00
0.000E+00 0.000E+00 0.000E+00 0.000E+00 0.000E+00 0.000E+00 0.000E+00 K2
2.450E+00 2.450E+00 2.450E+00 2.450E+00 2.450E+00 2.450E+00 2.450E+00
2.450E+00 2.450E+00 2.450E+00 2.450E+00 2.450E+00 2.450E+00 0.000E+00 B1
2.400E+00 2.400E+00 2.400E+00 2.400E+00 2.400E+00 2.400E+00 2.400E+00
2.400E+00 2.400E+00 2.400E+00 2.400E+00 2.400E+00 2.400E+00 0.000E+00 B2
2.032E-08 7.089E-08-1.446E-06-3.341E-07
-2.800E-12-1.400E-11 3.193E-11 3.540E-11
1.008E-07-4.836E-07-1.227E-06 0.000E+00
3.618E-12-1.560E-11 5.004E-12 0.000E+00
```

The BMC.LIB File

```
534e-05-2.214e-05-2.000e-05-1.464e-05-1.464e-05-9.999e-06-1.143e-05
857e-06-7.856e-06-4.285e-06 3.571e-06 9.786e-06-5.821e-06 0.000e-00 ad0D
000e-01-1.750e-06-1.750e-06-1.607e-06-1.750e-06-1.571e-06-1.536e-06
571e-06-1.536e-06-1.429e-06-1.714e-06-7.143e-08-1.882e-06 0.000e-00 ad0D
566e-02-3.466e-03-8.177e-03-1.007e-02-1.042e-02-1.070e-02-1.140e-02
106e-02-1.194e-02-1.165e-02-6.089e-03-4.451e-03 5.389e-03 0.000e-00 ad1D
522e-03 2.333e-03 2.373e-03 2.411e-03 2.416e-03 2.445e-03 2.481e-03
445e-03 2.521e-03 2.469e-03 2.335e-03 3.471e-04 2.043e-03 0.000e-00 ad1D
439e-02-4.000e-03 5.714e-03 9.429e-03 8.286e-03 1.029e-02 1.029e-02
572e-03 8.572e-03 8.000e-03-2.857e-03 6.000e-03-1.751e-02 0.000e+00 ad2D
896e-03-5.800e-03-5.800e-03-5.800e-03-5.686e-03-5.943e-03-5.971e-03
943e-03-5.971e-03-5.829e-03-5.943e-03-4.000e-04-5.831e-03 0.000e+00 ad2D
507e-07 1.107e-06 1.946e-06 9.786e-07 8.821e-07 7.571e-07 8.393e-07
571e-07 4.036e-07 1.500e-07-3.250e-07-7.839e-08 1.857e-07 0.000e-00 ab0S
214e-07 3.214e-07 2.500e-07 3.571e-07 5.000e-07 2.143e-07 2.857e-07
786e-07 3.536e-06 1.429e-07 2.143e-07-1.429e-09 5.179e-07 0.000e-07 ab0S
813e-04-9.420e-04-7.826e-04-5.302e-04-4.440e-04-3.922e-04-3.802e-04
914e-04-4.421e-04-6.751e-04-8.136e-04 2.537e-05-1.658e-03 0.000e-00 ab1S
383e-03-2.287e-03-2.496e-03-2.636e-03-2.689e-03-2.706e-03-2.835e-03
695e-03-2.672e-03-2.817e-03-2.115e-03-2.050e-05-1.396e-03 0.000e+00 ab1S
674e-04 1.286e-03 2.077e-03 7.143e-04 6.200e-04 5.714e-04 5.857e-04
057e-04 6.943e-04 1.011e-03 1.209e-03-3.283e-05 2.514e-03 0.000e+00 ab2S
646e-03 3.514e-03 3.914e-03 4.057e-03 3.943e-03 4.057e-03 4.229e-03
086e-03 3.800e-03 4.229e-03 3.371e-03 2.400e-05 2.660e-03 0.000E+00 ab2S
000e+00 1.679e-06 1.679e-06 1.579e-06 1.464e-06 1.282e-06 1.175e-06
964e-07 6.071e-07 1.786e-07-6.036e-07 0.000e+00 0.000e+00 0.000e+00 af0S
000e+00-3.214e-07-1.489e-12-1.071e-07 2.572e-28-1.786e-07-1.430e-07
923e-05-1.429e-07-1.071e-07-1.071e-07 0.000e+00 0.000e+00 0.000e+00 af0S
000e+00-1.320e-03-9.781e-03-7.628e-04-6.332e-04-5.491e-04-5.284e-04
399e-04-6.145e-04-1.006e-03-1.027e-03 0.000e+00 0.000e+00 0.000e+00 af1S
000e+00-2.113e-03-2.531e-03-2.851e-03-3.037e-03-3.055e-03-1.411e-03
326e-03-2.973e-03-3.269e-03-1.760e-03 0.000e+00 0.000e+00 0.000e+00 af1S
000e+00 1.686e-03 1.229e-03 9.771e-04 8.400e-04 7.686e-04 7.743e-04
257e-04 9.429e-04 1.446e-03 1.420e-03 0.000e+00 0.000e+00 0.000e+00 af2S
000e+00 2.543e-03 3.086e-03 3.400e-03 3.657e-03 3.686e-03-1.275e-02
508e-03 3.543e-03 3.971e-03 2.257e-03 0.000e+00 0.000e+00 0.000e+00 af2S
836e-08 3.055e-07 4.449e-07 5.286e-07 5.643e-07 5.411e-07 4.882e-07
761e-07 9.893e-08-4.536e-07-2.698e-06-1.618e-06-3.338e-06 0.000e+00 as0S
000e+00 0.000e+00 0.000e+00 0.000e+00 0.000e+00 0.000e+00 0.000e+00
000e+00 0.000e+00 0.000e+00 0.000e+00 0.000e+00 0.000e+00 0.000e+00 as0S
608e-04-1.196e-03-1.752e-03-2.222e-03-2.650e-03-3.057e-03-3.431e-03
305e-03-4.895e-03-6.518e-03-1.221e-02 1.435e-03-3.005e-02 0.000e+00 as1S
000e+00 0.000e+00 0.000e+00 0.000e+00 0.000e+00 0.000e+00 0.000e+00
000e+00 0.000e+00 0.000e+00 0.000e+00 0.000e+00 0.000e+00 0.000e+00 as1S
209e-04 1.510e-03 2.182e-03 2.745e-03 3.263e-03 3.759e-03 4.208e-03
281e-03 5.977e-03 7.919e-03 1.506e-02-1.828e-03 3.492e-02 0.000e+00 as2S
000e+00 0.000e+00 0.000e+00 0.000e+00 0.000e+00 0.000e+00 0.000e+00
000e+00 0.000e+00 0.000e+00 0.000e+00 0.000e+00 0.000e+00 0.000e+00 as2S
```

The AXIS.INP File

REFERENCES

[1]. Yang Yue Men. "Low Power Research Reactors Structural Design" IAEA Workshop on Low Power Research Reactors, China Institute of Atomic Energy, Beijing.(1990).

[2]. Li Yu Lun. " Safety Analysis Report on the MNSR". China Institute of Atomic Energy, Beijing.(1990).

[3]. Levine, S.H., " Basic Reactor Physics". ICTP Workshop on Reactor Physics Calculations for Application in Nuclear Technology. 12 Feb - 16 Mar, 1990, Trieste, Italy.

[4]. Lamarsh, J.R., " Introduction to Nuclear Reactor Theory". Addison-Wesley Publishing Company, Reading, Mass.(1966).

[5]. Alcouffe, R.E. and O'Dell, R.D., "Transport Calculations for Nuclear Reactors". Handbook of Nuclear Reactors Calculations. VOL 1. CRC Press Inc, Boca Raton, FL, USA.(1962).

[6]. Duderstadt, J.J. and Hamilton, L.J., " Nuclear Reactor Analysis". John Wiley and Sons, New York.(1976).

[7]. Nakamura, S., "Computational Methods in Engineering and Science With Applications to Fluid Dynamics and Nuclear Systems". John Wiley and Sons, New York.(1971).

[8]. Zienkiewicz, C.C., "The Finite Element Method in Engineering Sciences". M^{C} Graw Hill, New York.(1971).

[9]. Whiteman, J.R., " A bibliography for finite elements". Academic Press, New York.(1975).

[10]. Vondy, D.R., "Diffusion Theory". Handbook of Nuclear Reactor Calculations. VOL 1. CRC Press Inc, Boca Raton, USA. (1962).

[11]. Akaho, E.H.K., Boadu, H.O., "Core Thermohydraulic Analysis of the Miniature Neutron Source Reactor". GAEC Technical Report, GAEC-NNRI-RT-8.(1991).

[12]. Akaho, E.H.K., Anim-Sampong, S., "Two-group Macroscopic Data Base for the Prototype Miniature Neutron Source Reactor" GAEC Technical Report, GAEC-NNRI-RT-17.(1993).

[13]. Mele, I., and Ravnik, M., " TRIGAP - A Computer Program for Research Reactor Calculations". Josef Stefan Institute Report. IJS-DP-4238.(1985).

[14].Roth, M.J., MacDougall, J.D and Kemshell, P.B., "Preparation of Input Data for WIMS". AEEW-R538, Winfrith, England.(1967).

[15]. Fayers, F.J, et al., " LWR-WIMS: A Modular Computer Code for the Evaluation of Light Water Reactor Lattices - Part 1: Description of Methods" UKAEA Report AEEW-R785, Winfrith, England.(1972).

[16]. Huynh Dong Phoung, " WIMSPC - A PC version of WIMS-D/4 Adapted to AT-286/386 with Math-Coprocessor 80287/80387". (1990).

[17]. Halsall, M.J., " A summary of WIMS-D/4 Input Options". AEEW-M1327, Winfrith, England.(1980).

[18]. Akaho, E.H.K., Anim-Sampong, S., Maakuu, B.T. "Calculations for the Core Configurations of the Miniature Neutron Source Reactor". GAEC Technical Report. GAEC-NNRI-RT-13.(1992).

[19]. Zhu Gousheng, " Neutronic Physical experimrnts on Low Power Research Reactors". IAEA Workshop on Low Power Research Reactors, China Institute of Atomic Energy, Beijing.(1990).

[20]. Graves, H.W. Jr, "Nuclear Fuel Management" John Wiley & Sons Inc.(1979).

[21]. Varga, R.S. " On estimating Rates of Convergence in Multigroup Diffusion Problems, WAPD-TM-41, Bettis Atomic Power Laboratory, Pittsburgh, Pa. (1957).

[22]. Varga, R.S., " Matrix Iterative Analysis, Prentice-Hall, London.(1962).

[23]. Flanders, D.L and Shortley, G., " Numerical Determination of Fundamental Modes" Journal of Appl.Physics 21, 1326.(1950).

[24]. Guo Chenzhan and Gao Yongchun, " Safety Analysis Report for the Miniature Neutron Source Reactor (MNSR)", China Institute of Atomic Energy, Beijing.(1993).